# LANOSTEROL IS A SURVIVAL FACTOR FOR DOPAMINERGIC NEURONS

LYNETTE LIM
(B.Sc)

A THESIS SUBMITTED

FOR THE DEGREE OF DOCTOR OF PHILOSOPHY

DEPARTMENT OF BIOLOGICAL SCIENCES

NATIONAL UNIVERSITY OF SINGAPORE

(2011)

## Summary

Parkinson's disease (PD) is a neurodegenerative disorder, marked by the selective degeneration of dopaminergic neurons in the nigrostriatal pathway. Several lines of evidence indicate that mitochondrial dysfunction contributes to its etiology. Other studies have suggested that alterations in sterol homeostasis correlate with increased risk for PD. Whether these observations are functionally related is, however, unknown. In this study, I used a toxin-induced mouse model of PD and measured levels of nine sterol intermediates. I found that lanosterol is significantly (~50%) and specifically reduced in the nigrostriatal regions of MPTP-treated mice, indicative of altered lanosterol metabolism during PD pathogenesis. Remarkably, exogenous addition of lanosterol rescued dopaminergic neurons from MPP+-induced cell death in culture. Furthermore, there is a marked redistribution of lanosterol synthase (LSS) from the endoplasmic reticulum (ER) to mitochondria in dopaminergic neurons exposed to MPP+, suggesting of that lanosterol might exert its survival effect by regulating mitochondria function. Consistent with this model, I find that lanosterol induces mild depolarization of mitochondria and promotes autophagy. Collectively, these results highlight a novel sterol-based neuroprotective mechanism with direct relevance to PD.

## List of tables and figures

## List of symbols

| Abbreviations | Definitions |
| --- | --- |
| AA | Aracodonic acid |
| APCI | Atmospheric pressure chemical ionization |
| ATP | Adenosine triphosphate |
| AV | Autophagosome vacuoles |
| CCCP | m-chlorophenylhydrazone |
| CCD | Charge-coupled device |
| cdk5 | Cyclin dependent kinase 5 |
| CoQ | Coenzyme Q/ Ubiquinone |
| DAT | Dopamine transporter |
| DHA | Docodehaxnoic acid |
| DIV | Days in vitro |
| DJ-1 | (PARK7) Parkinson disease 7 |
| DNA | Deoxyribonucleic acid |
| ECL | Enchance chemi-luminescence |
| ER | Endoplasmic reticulon |
| FBS | Fetal bovine serum |
| FDU | fluorodeoxyuridine |
| GC-MS | Gas chromatography- mass spectrometry |
| GDNF | Glia derived neurotrophic factor |
| GSK-3$\beta$ | Glycogen synthase kinase 3 beta |
| HMG-CoA | 3-hydroxy-3-methyl-glutaryl-Coenzyme A reductase |
| HPLC | High pressure liquid chromatography |
| JC-1 | 5,5',6,6'-tetrachloro-1,1',3,3'-tetraethylbenzimidazolocarbocyanine iodide |
| KDEL | ER retention sequence (lys-asp-glu-leu) |
| KEGG | Kyoto Encyclopedia of Genes and Genomes |
| LC3 | Microtubule-associated protein light chain 3 |
| LDL-C | low-density lipoprotein cholesterol |
| LRRK2 | Leucine-rich repeat kinase 2 |
| LSS | Lanosterol synthase |
| MPP+ | 1-methyl-4-phenylpyridinium |
| MPTP | 1-methyl-4-phenyl-1,2,3,6-tetrahydropyridine |
| MRM | Multiple reaction monitoring |
| P0-P2 | Postnatal day0 to day2 |
| p35 | cdk5 activator protein with 35kDa |
| PBS | Phosphate buffer saline |
| PC | Phosphatidylcholine |
| PD | Parkinson's Disease |
| PINK1 | PTEN-induced putative kinase 1 |
| PUFA | Polyunsaturated fatty acids |
| SEM | Standard error of mean |
| SNpc | Substantia Nigras par compacta |
| SNpc | Substantia nigras par compacta |
| SREBP2 | Sterol regulatory element binding protein 2 |
| TH | Tyrosine hydroxylase |

| | |
|---|---|
| TOMM20 | Translocases of outer mitochondria membrane 20 |
| TUJ1 | Neurons-specific class III beta tubulin |
| UCP | Uncoupling protein |
| VTA | Ventral Tegmental Areas |
| $\Delta\Psi$ | Mitochondria membrane potential |

## <u>Acknowledgements</u>

I would like to thank all members from the lab of Markus Wenk for helpful suggestions and advice throughout this thesis work. In particular, the former and current members: Robin, Lukas, Federico, and Madhu- thank you for your support, friendship, coffee breaks, and sense of humor.

A special acknowledgement to the collaborators:

i) Serge Przedborski and members of his lab, particularly Vernice Jackson-Lewis. Thank you for being welcoming to me as a visitor in the lab and teaching me many indispensable techniques in neurobiology.

ii) Marc Fivaz and his lab members: Loo Chin, Liz, Vivian, Kai Wee and Elisabeth for being so friendly to me as a visitor using the live imaging system.

Finally, this work is only possible with the support and guidance of my supervisor, Markus who has fostered my independence, accepted and encouraged my ideas, and always allowed me to disagree with him.

## **Introduction**

Parkinson's Disease (PD) is a movement disorder marked by selective degeneration of dopaminergic neurons in the nigrostriatum pathway (Dauer and Przedborski, 2003). It affects about 1% of the population over 60 years old and 4% of people over 80 years old. Named after the clinician who first described the disease in 1817, James Parkinson, this is currently the second most common age-related neurodegenerative disorder (Elbaz and Moisan, 2008).

The clinical characterization of the disease, started about half a century ago, is extremely accurate. Among experienced clinicians, PD is diagnosed with a 98.5% accuracy (de Lau and Breteler, 2006), compared to about 83% for Alzheimer's disease (Lim et al., 1999). Most patients with PD exhibit numerous deficits in movement with obvious symptoms such as: rigidity or stiffness of limbs and/or neck, tremor, bradykinesia, and reduction of movement. Other less apparent symptoms include depression, dementia or confusion, uncontrolled drooling, speech impairment, swallowing difficulty, and constipation.

The main clinical features of PD are caused by the selective loss of dopaminergic neurons in the nigrostriatal pathway, which is also a hallmark of the disease. However, it is important to note that neuronal cell deaths are also detected in other regions of the brain such as cerebellum and cortex (Braak et al., 2003). Clearly, the most severely affected region is the nigrostriatal pathway (Fig 1), which regulates fine voluntary movements. Thus, the main motor deficits in PD patients are most likely attributed to this pathway, while

the other less common and non-motor symptoms such as confusion and dementia are most likely due to impairments in other brain regions.

In a healthy nigrostriatal circuit (Fig 1A), dopaminergic neurons from the substantia nigra par compacta (SNpc) send both excitatory and inhibitory signals to two types of GABAergic neurons in the striatum, which have either receptor of D1 (dopamine receptor subtype 1) or D2 (dopamine receptor subtype 2) respectively. GABAergic neurons with D1 receptors form the direct pathway, whereas neurons with D2 receptors form the indirect pathway. These two pathways link the striatum to the cortex via the thalamus and subthalmic nucleus. In PD, the loss of dopaminergic input from the SNpc typically leads to overactivity in the indirect output and underactivity of the direct output of the nigrostriatal circuit (Fig 1B). This results in a reduction of movement due to reduced glutamergic output from the thalamus to the motor cortex.

The overactive indirect pathway and the underactive direct pathway have long been proposed to be the cause of motor deficits in Parkinsonism (Bergman et al., 1990). As such, a number of deep-brain stimulation and surgical procedures are aimed at reducing this indirect pathway. However, until recently, there has been no direct experimental evidence to suggest that this is the case. Consistent with the classical model proposed, in 2010, a seminal paper by Anotol Kreitzer's group in collaboration with Karl Deisseroth (one of the pioneers of optogenetic techniques), demonstrated that the activation of GABAergic neurons from the striatum with D1 receptor

(direct pathway) reduce freezing and increase locomotion in a mouse model for PD (Kravitz et al., 2010).

*Figure 1: The nigrostriatal circuit in healthy and disease state*
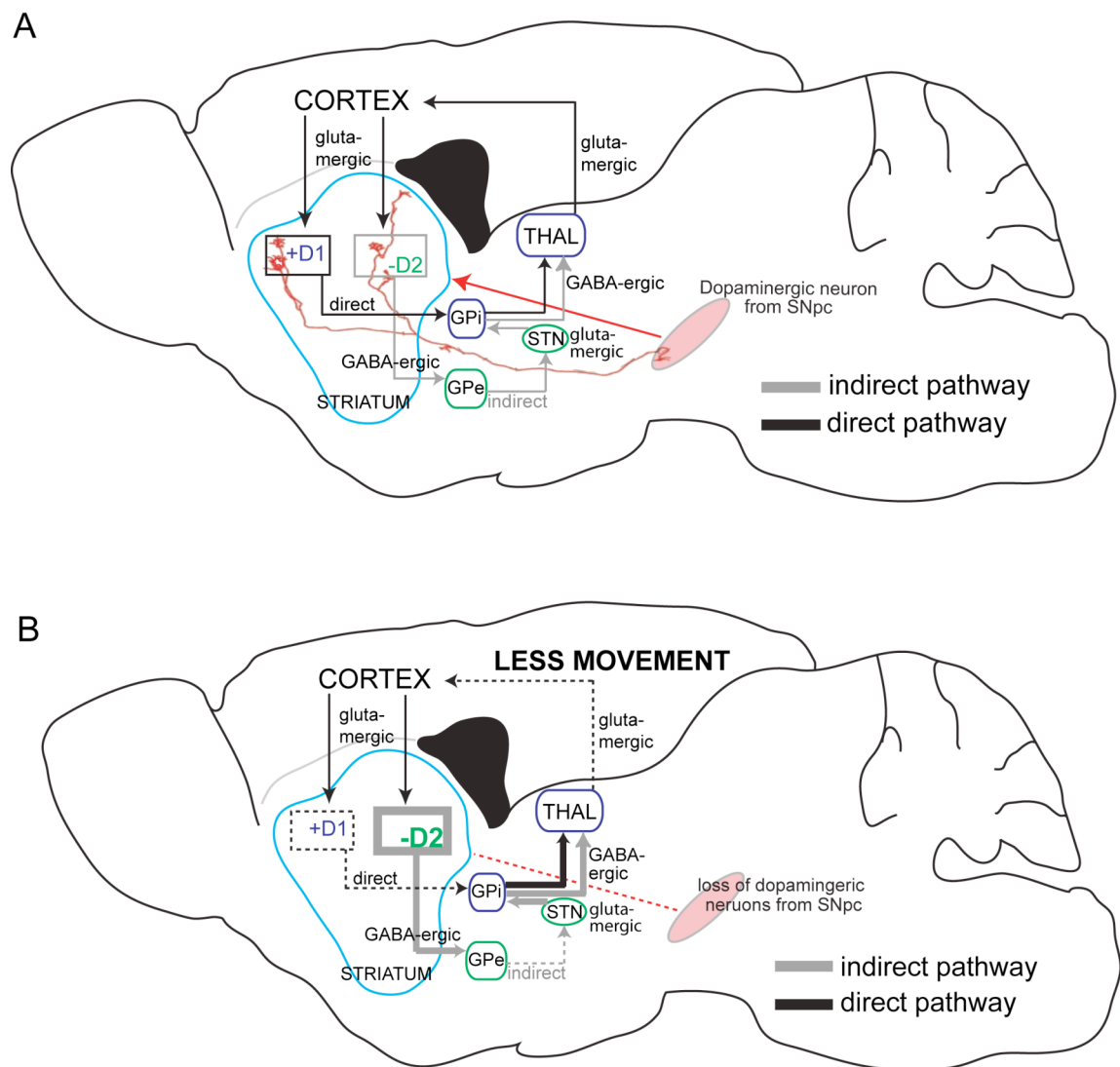


Figure 1: Graphical drawing of sagittal plane of a rodent brain, left represents anterior and right represents posterior. (A) In a healthy state, dopaminergic neurons in the substantial nigra par compacta (SNpc) send excitatory and inhibitory signals to two classes of GABAergic neurons of the caudate putamen (striatum), consisting of D1 and D2 receptors respectively. In the direct pathway, D1 GABAergic neurons synapse onto GABAergic neurons of the globus pallidus internal segment (GPi). GPi GABAergic neurons synapse onto gluatmergic neurons of the thalamus (THAL), sending signal to the motor cortex. In the indirect pathway, D2 GABAergic neurons synapse onto GABAergic neurons of the globus pallidus external segment (GPe). GPe GABAergic neurons synapse onto glutamergic neurons of the subthalmic nucleus (STN). From STN, glutamergic neurons synapse onto GPi GABAerigc neurons. The balance between this direct and indirect pathway results in fine motor coordination such as speech. (B) In PD, upon the loss of dopaminergic neurons, D1 (direct) pathway is less active wheras D2 (indirect) is hyperactive. The final result is an over-inhibition of thalamic neurons, reducing glutamergic synapses from the thalamus to motor cortex. Movement deficits are thus in patients with defects in the nigrostriatal circuit.

From the genetic level, in 1997, the first gene mutation identified to cause an inherited form of PD was alpha-synuclein (PARK1/4). Since then, numerous genes, such as PINK1 (PARK6), LRRK2 (PARK8), DJ1 (PARK7), Parkin (PARK5), and other loci (list in Table 1), have been identified to be involved in familial PD (Schapira, 2008). These disease-associated mutations represent only 5-10% of all PD cases; the remaining 90-95% have currently unknown causes (Lesage and Brice, 2009). Though genetic causes of Parkinsonism represent the minority of total incidences, they have been important to the PD field in deciphering the events of pathogenesis.

For example, taking advantage of the disease-related mutations, there are now many transgenic model organisms including mice (see Table 1), worm, yeast, and flies. All of these models have been instrumental in uncovering the molecular and cellular events that lead to cell death. Despite the importance of transgenic models, it is important to note that none of the genetic models expressing familial PD mutations are well established and could recapitulate the hallmark of PD such as the selective loss of dopaminergic neurons. The notable exceptions, such as overexpression of α-synuclein and Lrrk2, are highly controversial. For example, in the case of α-synuclein, overexpression of wild type human form of α-synuclein also induces a selective loss of dopaminergic neurons, suggesting that the observed phenotype is an overexpression artefact. For Lrrk2, while the R1441G transgene induces selective loss of dopaminergic neurons in the SNpc, the R1441C does not (Li et al., 2009). In a recent paper, mice overexpressing the G2019S mutation of Lrrk2 showed a selective loss of dopaminergic neurons in

the SNpc. However, the authors were extremely cautious of the results, since this is unique to a specific mouse line as the same mutation in a different line did not recapitulate this (Ramonet et al., 2011).

In the same line of thinking, other groups have taken a different approach trying to elucidate the selective vulnerability of dopaminergic neurons. It is well known that in PD, dopaminergic neurons have degenerated in the SNpc while the adjacent dopaminergic neuron of the VTA remain. Thus by comparing gene-array expression profiles in dopaminergic neurons in these two regions, one could theoretically find pathways or genes unique to dopaminergic neurons of the SNpc. In a few array studies, the results suggested that different expression of transcription factors may explain the selective vulnerability of dopaminergic neurons (Chung et al., 2005; Greene et al., 2005; Yao et al., 2005). However, it is also not clear how these array data fit with the known PD- linked mutations or what risk factors could cause such differences in expression of these identified transcription factors.

The current consensus is that PD is a multifactorial disease, whereby both extrinsic factors, such as exposure to environmental toxins, and intrinsic factors, such as genetic background, are important for pathogenesis (Ross and Smith, 2007). More importantly, there is a growing list of components associated with PD's etiology such as: oxidative stress, ER protein misfolding, mitochondria dysfunction, transcription factors changes, epigenetic changes, calcium toxicity, and cholesterol misregulation. It is not known if all of the above are related or independent factors for the disease's progression. Among

this list, the evidence implicating the involvement of impaired mitochondrial functions in PD appears to be the most substantial.

As mentioned, the genetic linkage represent only 5-10% of all PD occurrences (Lesage and Brice, 2009). Yet, in this list of rare genetic PD cases, many genes point towards mitochondrial dysfunction (see compiled list in Table 1, (Dauer and Przedborski, 2003; Elbaz and Moisan, 2008; Lesage and Brice, 2009; Ross and Smith, 2007; Schapira, 2008; Schon and Przedborski, 2011)). A number of these genes, such as PINK1, DJ-1, and HTRA2, localize to the mitochondria, and have been shown to control mitophagy during oxidative stress (Cookson, 2010). Another gene involved in PD, Parkin, interacts with Parkin-interacting substrates (PARIS), which in turn represses PGC-1$\alpha$ expression. Repression of PGC-1$\alpha$ reduces mitochondria bioenergetics (Shin et al., 2011). Parkin also interacts with PINK1, and together they play important roles in mitophagy (Matsuda et al., 2010; Narendra et al., 2008; Narendra et al., 2010). In patients with idiopathic PD, brain mitochondrial complex I catalytic activity is compromised (Keeney et al., 2006). Furthermore, a number of environmental toxins that directly affect mitochondrial function induce Parkinsonism. For example, in the French Indian island of Guadeloupe, a typical Parkinsonism has been closely associated with the regular consumption of soursop, a tropical plant containing the complex I inhibitor, annonacin (Schapira, 2008; Schapira, 2010). Perhaps the best example of toxin-induced PD is MPTP (or its active metabolite MPP+), which is the main contaminant found in the illegally manufactured opioid drugs. MPP+ selectively enters into dopaminergic neurons via the

dopamine transporter (DAT), inhibits complex I of the mitochondria, and recapitulates PD's clinical symptoms (Watanabe et al., 2005).

Because MPTP/MPP+ toxicity emulates PD symptoms, it has been widely used in animal and cellular models to study neuronal cell death and to screen for neuroprotective agents. Of the neuroprotective metabolites identified, many are found in mitochondria, including L-carnitine, creatine, and coenzyme Q10 (CoQ) (Virmani et al., 2005). Among these metabolites, CoQ is a class of lipid-based electron carrier found predominately in the mitochondria. In some cohorts of patients with PD, administering CoQ is beneficial, but its efficacy has yet to be determined (Muller et al., 2003; Shults et al., 2002; Spindler et al., 2009). In MPTP rodent and primate animal model, the supplement of CoQ is partially protective by inducing "mild" uncoupling in nigral neurons (Horvath et al., 2003). However, other than CoQ, no other classes of lipids have been shown to be important in modulating mitochondrial function and improving dopaminergic neuronal survival. Consistent with this model, uncoupling proteins (UCPs) are protective in the MPTP model of PD (Andrews et al., 2005; Conti et al., 2005), and their expression is down regulated in mice lacking DJ-1, a gene linked to early onset of PD (Guzman et al., 2010).

While the evidence implicating mitochondria in PD is substantial, the evidence showing the involvement of lipid misregulation is relatively weak. Even though about fifty percent of the brain's dry weight is lipid, neuroscientists still have a limited explanation for this observation (Piomelli et al., 2007). Perhaps the simplest explanation for a high lipid composition is due

to white matter, which is largely composed of myelin. However, emerging evidence now shows that beyond acting as insulators, lipids also play important regulatory roles in signalling (Piomelli et al., 2007). Due to the high diversity in structural, biochemical and biophysical properties of lipid molecules (see chapter 1, Fig 2), they participate in a range of brain function including development, synaptic vesicle cycle, axonal cargo trafficking, and even in disease pathogenesis (Buccoliero and Futerman, 2003; Di Paolo and De Camilli, 2006; Vance et al., 2006).

In the context of PD, there is some evidence for the involvement of lipids. In clinical studies, low-density lipoprotein cholesterol (LDL-C) has been associated with higher risk of PD (Huang et al., 2008; Huang et al., 2007), and higher serum levels of total cholesterol were associated with a significantly decreased risk of PD (de Lau et al., 2006). Yet, these might not reflect brain cholesterol levels as cholesterol in the brain is synthesized independently of the rest of the body. While oxidized cholesterol has been shown to accelerate α-synucleinopathy – the major component of Lewy bodies – (Koob et al., ; Liu et al., ; Rantham Prabhakara et al., 2008), these studies were done mostly *in vitro*. In the brains of post-mortem PD patients, elevated levels of polyunsaturated fatty acids (PUFA) were detected (Sharon et al., 2003), but this represents cortices rather than affected brain regions. Clinically, there have been some reports linking Gaucher disease (a defect in glucocerebrosidase activitiy) to Parkinsonism (Aharon-Peretz et al., 2004; Zimran et al., 2005). Yet, it is still unclear how lipid metabolism and mitochondria function relates to PD disease progression or dopaminergic

neuronal degeneration. Whether misregulation in lipid metabolism and mitochondria dysfunction collaborate together in the selective cell death of dopaminergic neuron, or whether they are simply two independent factors remains to be elucidated.

Despite the lack of strong evidence for the involvement of lipids in PD, some findings mentioned above have been translated into treatments, though they are not entirely successful. The lipid-based therapies currently being evaluated in clinical trials for PD include polyunsaturated fatty acids (PUFA), such as fish-oils or docodehexanoic acid (DHA), and statins – classes of sterol lowering drugs. Fish oil appears to ameliorate depressive symptoms that are common among PD patients (da Silva et al., 2008), but the mechanism of action is unclear. Sterol-lowering drugs results have been conflicting as some studies reported a protective effect while many others see no effects, rendering no definite conclusion to be made (see review (Becker and Meier, 2009).

This work begins with the goal to (i) screen for lipid levels in brain that can contribute to the pathogenesis of PD, (ii) modify the lipids levels of dopaminergic neurons to assess their survival, and (iii) identify the mechanism of action of lipids metabolites in promoting cellular survival. This thesis is divided into various chapters that detail the different types of experimental procedures and results. I will now give a brief summary of each chapter.

Chapter 1: *In silico* analysis of the classes of lipids that could be particularly important to dopaminergic neurons. This *in silico* screen led to the identification of sterol metabolism as a candidate pathway. Upon measuring

nine precursors of cholesterol in the brains of mice treated with MPTP, a drug inhibiting complex I of the mitochondria respiratory chain and mimicking PD, levels of lanosterol, the first cyclic sterol, were found to be significantly reduced (chapter 1).

Chapter 2: To elucidate the role of lanosterol, I developed a modified method of culturing primary dopaminergic neurons. Upon establishing this method, I found that in ventral midbrain cultures, exogenous lanosterol rescues dopaminergic neurons from MPP+-induced cell death. In hippocampal cultures, lanosterol, along with cholesterol, induces neurite outgrowth. Lanosterol was identified as a survival factor in primary dopaminergic neuronal cultures.

Chapter 3: To determine if other metabolites alter upon addition of sterols, I performed GC-MS analysis on cultured neurons. Cell treated with lanosterol have marked increased levels of lanosterol, while other sterols appeared unchanged. Furthermore, ubiquinone levels did not change in neuronal cultures treated with sterols.

Chapter 4: To decipher the mechanism of lanosterol's survival effect, I evaluated a number of survival pathways that have been reported to change in PD or animal model of PD. Furthermore, I also checked the levels and the localization of lanosterol synthase (LSS) in dopaminergic neurons. Upon

toxin-induced stress, we observed that LSS redistributed from ER to mitochondria.

Chapter 5: To understand the role of LSS translocation from ER to mitochondria, I evaluated the role of lanosterol in modulating mitochondrial functions. I developed a live-imaging technique to monitor mitochondrial membrane potential. In this assay, I found that lanosterol induces "mild" uncoupling of the mitochondria, a mechanism that has been shown to be neuroprotective in several PD and neurodegeneration models. Finally, autophagy was increased upon lanosterol treatment. Collectively, these results point to lanosterol as a modulator of neuronal mitochondrial physiology and identify its unique role in the context of PD pathogenesis.

*Table 1: Genes and loci linked to Parkinson's disease*

| | Mode of inheritance | avg age of onset | locus/ gene/ protein | cellular localization | Mitochondrial association | Mouse model & evidence of nigrostriatal compromises | refs |
|---|---|---|---|---|---|---|---|
| PARK1/4 | dominant | 40s | α-synuclein | presynaptic terminal | interactions with cardiolipin | Knockout has fewer dock synaptic vesicles; overexpression of disease associated mutant A53T, A53P, or WT showed selective loss of dopaminergic neurons. | (Dauer and Przedborski, 2003; Larsen et al., 2009; Lo Bianco et al., 2002) |
| PARK2 | recessive | 20s | Parkin | cytosol | mitophagy | Knockout does not display nigrostriatal degeneration; truncated mutation driven by DAT promoter has loss of dopaminergic neurons at 16 months. | (Frank-Cannon et al., 2008; Lu et al., 2009) |
| PARK3 | dominant | 60s | 2p13 | | | | |
| PARK5 | dominant | 50s | UCHL1 | cytosol | ? | Knockout has axonopathy but no selective loss of dopaminergic neurons. | (Dauer and Przedborski, 2003) |
| PARK6 | recessive | 30s | PINK1 | mito | mitophagy | conditional RNAi has no loss of dopaminergic neuron. | (Zhou et al., 2007) |
| PARK7 | recessive | 30s | DJ-1 | cytosol/mito | mitophagy & oxidative stress | Disease associated mutant has accumulation of mitochondria; knockout has defects in calcium signaling and increased oxidative stress. | (Dauer and Przedborski, 2003; Guzman et al., 2010) |
| PARK8 | dominant | variable | LRRK2 | cytosol | associates with mito outer membrane | R1441G transgenic has loss of dopaminergic neurons; but R1441C has no loss of dopaminergic neurons; G2019S transgenic has specific loss of dopaminergic neurons but this is line dependent. | (Li et al., 2009; Ramonet et al., 2011) |
| PARK9 | recessive | variable | ATP13A2 | membrane | ? | No model yet. | |
| PARK10 | recessive | variable | 1p32 | | | | |
| PARK11 | dominant | variable | GIGYF2 | ER/ Golgi | enhances mito ERK1/2 activation | GIgYF2 (+/-) has motor dysfunction. | (Giovannone et al., 2009) |
| PARK12 | ? | ? | Xq21-q25 | | | | |
| PARK13 | ? | ? | HTRA2 | mito | apoptosis | Abnormality of lower motor neuron function, also mutated in motor neuron disease. | (Jones et al., 1993) |
| PARK14 | ? | ? | PLA2G6 | ER | associates with MAM | Point mutation (loss of function) has severe motor dysfunction, model of infantile neuroaxonal dystrophy | (Wada et al., 2009) |
| PARK15 | recessive | ? | FBXO7 | nucleus | ? | No model yet | (Zhao et al., 2011) |
| PARK16 | ? | ? | 1q32 | | | | |

## Chapter 1: Identification of a lipid metabolic pathway with potential relevance for dopaminergic neurons

*Introduction: Rational for in silico analyses*

One of the most puzzling questions in PD is why do dopaminergic neurons in the nigrostriatum pathway selectively degenerate? This hallmark feature of the disease has prompted various groups to conduct array studies comparing gene profiles of dopaminergic neurons in the SNpc to the ventral tegmental area (VTA). Yet, none of these array studies have conclusively mapped out a pathway that could explain the vulnerability of dopaminergic neurons.

Instead of comparing genetic profile changes of dopaminergic neurons in these two regions of the brain, we sought to look at groups of genes or pathways that are differentially expressed among various classes of neurons. We reasoned that such genes would be the key to explain the selective vulnerability of dopaminergic neurons observed in PD. In line with our logic, we employed the data generated from a study by Sugino et al., (2006). This array study took on an impressive and comprehensive task to molecularly characterize twelve major neuronal classes in the adult mouse forebrain. Their goal was to provide a molecular taxonomy for various subtypes of neurons. Sugino and colleagues also pointed out in their results that there is a large heterogeneity in gene expression among neurons. These differentially expressed genes (within the 12 populations of neurons investigated) fall into processes associated with cell-cell communication, synaptic vesicle dynamics, lipid binding, and lipid metabolism (Sugino et al., 2006).

Since different classes of neurons differ in their lipid metabolism genes, it is conceivable that vulnerabilities of dopaminegic neurons could be attributed to their lipid metabolic pathways. While lipids have been traditionally downplayed as membrane structural blocks and energy storage molecules, their functional importance is slowly gaining more attention. Furthermore, since lipids are highly diverse classes of molecules (Fahy et al., 2007), they are multifunctional in nature. Biologically, their roles include serving as signalling molecules and essential co-factors, governing functions as diverse as endo and extocytosis, survival, growth factor responses, and even apoptosis (Buccoliero and Futerman, 2003; Di Paolo and De Camilli, 2006; Vance et al., 2006). It is thus conceivable that part of the vulnerability of dopaminergic neurons lies in their unique lipid metabolic needs.

In line with this hypothesis, genes involved in PD, despite their functions, should also be highly differentially expressed among various classes of neurons. As a first proof of principle to this hypothesis, we gathered a list of genes reported to be involved in familial forms of PD (Table 2) and checked if they are differentially expressed among the twelve classes of neurons from the microarray data of Sugino et al., (2006). Out of the 19 genes in this list, fourteen (~73%) were highly differentially expressed (p-values, Table 2).

However, it is important to note that none of these 12 classes of neurons used in this array study are dopaminergic. Thus, a second proof of concept consists of assessing if genes differentially expressed between dopaminergic neurons from the SNpc and VTA. These genes should also be

differentially expressed genes according to the Sugino et al. paper. To our knowledge, three groups have compared gene expression of dopaminergic neurons in SNpc and compared to dopaminergic neurons in the VTA (Chung et al., 2005; Greene et al., 2005; Yao et al., 2005). Greene et al (2005), found 141 transcripts to be differentially expressed in rats. Chung et al., (2005), used mice and listed 125 transcripts with 2 fold differences in expression between the 2 types of dopaminergic neurons with 9 unknown genes. The results from Yao et al. (2005) were difficult to interpret due to some contamination with glia markers. Between the other two studies, Greene et al. and Chung et al., 116 transcripts overlapped. Thus, we cross-referenced these 116 transcripts to Sugino et al. (2006) study, and found that 103/116 (88%) carried a p-value of <0.001 (Data not shown).

*Table 2: A list of genes implicated in PD and corresponding p-values*

| Gene symbol | Name | *p-value |
|---|---|---|
| Snca | alpha-synuclein | 2.11E-17 |
| Lrrk2 | leucine-rich repeat kinase 2 | 1.72E-12 |
| Sncg | synuclein, gamma | 2.67E-12 |
| Mapt | microtubule-associated protein tau | 6.13E-11 |
| Ube2g2 | ubiquitin-conjugating enzyme E2G 2 | 6.12E-09 |
| Park7 | Parkinson disease (autosomal recessive, early onset) 7/ DJ-1 | 6.12E-09 |
| Sncaip | alpha-synuclein interacting protein | 2.78E-06 |
| Uchl1 | ubiquitin carboxy-terminal hydrolase L1 | 7.17E-06 |
| Comt | catechol-O-methyltransferase | 1.28E-05 |
| Sncb | synuclein, beta | 2.02E-05 |
| [#]Th | tyrosine hydroxylase | 2.41E-05 |
| Gpr37 | G protein-coupled receptor 37 | 6.04E-05 |
| Pink1 | PTEN induced putative kinase 1 | 2.93E-04 |
| Ube2l3 | ubiquitin-conjugating enzyme E2L 3 | 4.57E-04 |
| Ube2j2 | ubiquitin-conjugating enzyme E2, J2 homolog (yeast) | 7.54E-03 |
| Ubb | ubiquitin B | 1.71E-02 |
| Park2 | parkin (E3 ligase) | 2.29E-02 |
| Ube2l6 | ubiquitin-conjugating enzyme E2L 6 | 2.30E-02 |
| Ube1x | ubiquitin-activating enzyme E1, Chr X | 1.67E-01 |

*Material and Methods: In silico establishment of two-criteria system and MPTP mouse model*

### In silico analyses

I began to screen for lipid metabolic pathways. Lipids, as mentioned, are diverse molecules and can be loosely grouped into three categories: glycerolphospholipids (phosphatidylinositol- PI, phosphatidylethanolamine-PE, phosphatidylcholine-PC), sphingolipids (ceramide, sphingomyelin), and sterols (cholesterol) (Fig 2). Since lipid metabolism pathways involve many enzymes and are extensive and interconnected, it would be both laborious and inefficient to screen every pathway in a neuronal culture system. It is thus

crucial to focus on certain regions of particular pathways. Our first aim was to find the lipid metabolic pathway important and specific to dopamingeric neurons. To begin, I thus devised an *in silico* screening method building on existing informatics data, consisting of two simple levels of criteria.

**Criterion 1:**

Is the expression pattern of this lipid metabolic gene very different among all neurons? I define "very different" by a p-value <0.001 by Sugino et al. (2006) array data. If so, I would proceed to criterion 2.

**Criterion 2:**

Is the gene from criterion 1 preferentially expressed in the SNpc? For that, I checked *in situ* expression of that particular gene from the adult mouse brain section database provided by the Allen Brain Institute (Lein et al., 2007). *In situ* expression of tyrosine hydroxylase (TH) was used as a reference for dopaminergic neurons. As expected, TH is selectively expressed in the SNpc and VTA of the midbrain (Fig 3, left panel).

Using this as a reference for dopaminergic neurons in the brain, I look at the lipid metabolic enzymes that have fulfilled our first criterion. For example, Hmgcr, an enzyme involved in the biosynthesis of cholesterol (Fig 4) is expressed at high level in the hippocampus as well as in the SNpc and VTA as compared to the other regions of the brain (Fig 3, top right panel). On the other hand, phosphatidylinositol-4-phosphate 5-kinase type II alpha (pip5k2a) is concentrated in the hippocampus but displays diffuse expression in other parts of the brain (Fig 3, bottom right panel).

*Figure 2: Major classes of lipids and their structures found in mammalian brain*

A. Phosphatidylinositol(4,5)bisphosphate (PI(4,5)P2)
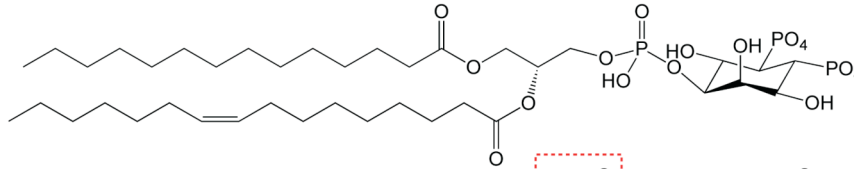
B. Phosphatidylethanolamine
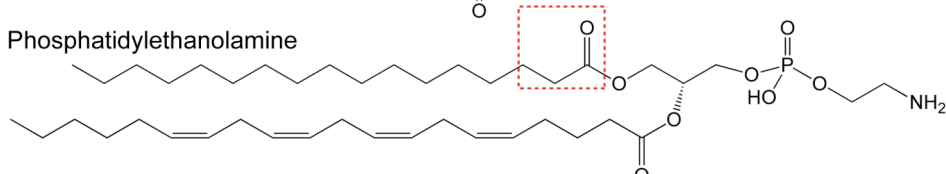
C. Ethanolamine plasmalogen
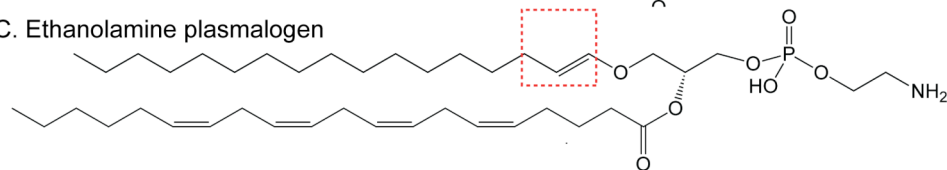
D. Phosphatidylserine
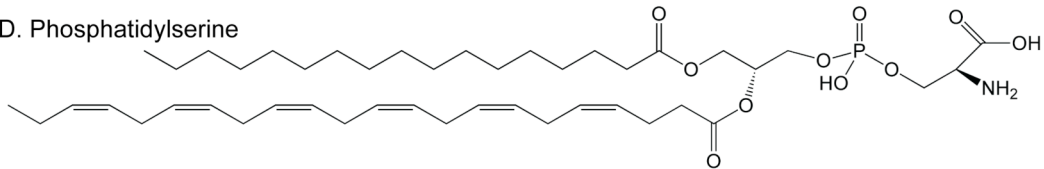
E. Phosphatidylcholine
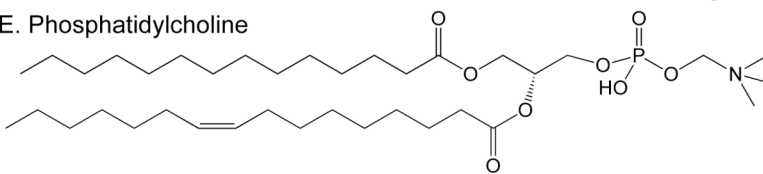
F. Cholesterol
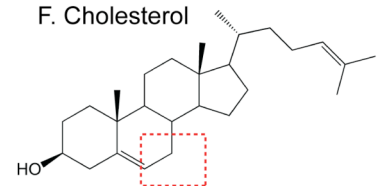
H. Ceramide
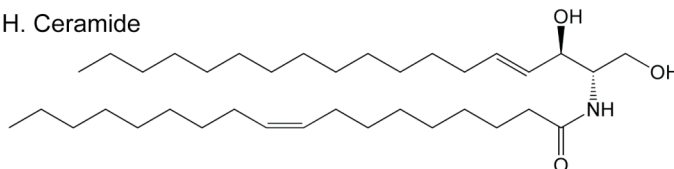
G. Oxysterol
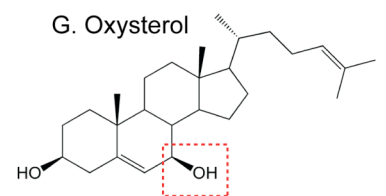
I. Sphingomyelin (SM)
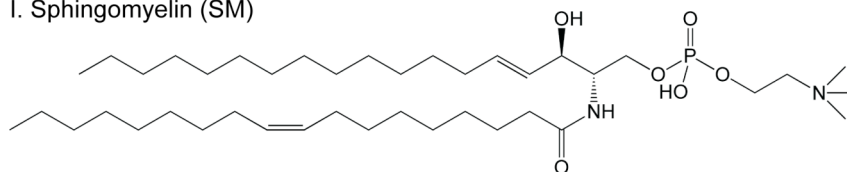
J. Sulfatide
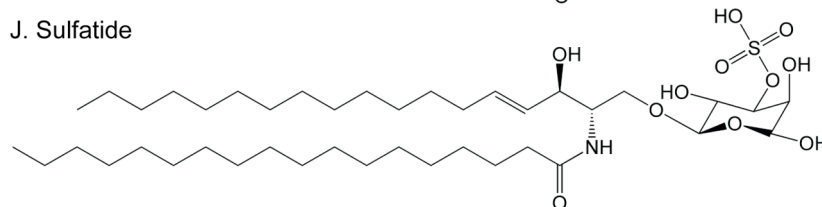
Figure legend

Note difference in oxidation

Figure 2: Structures of lipids found in the brain. (A) The headgroup of phosphatidylinositol-4,5-bisphoshate [PI(4,5)P$_2$] binds to various neuronal protein including adaptor and accessory factors of the clathrin coat. Metabolites from PI(4,5)P$_2$ (e.g. Ins(1,4,5)P$_3$ and DAG) function in neuronal signaling. (B, C) Glycerophosphatidylethanolamine - PE (B) with ester linked fatty acyls (B) and plasmalogens (C) are found in high levels in the brain. Ethanolamine plasmalogen has an ether linkage. A major fatty acyl brain PE is arachidonic acid (AA, 20:4), with double bond starting at the omega-6 position.  AA is the precursor to signal molecules such as prostaglandins. (D) Phosphatidylserine –PS -  is an abundant phospholipid in neuronal and synaptic vesicle membranes. Its headgroup binds to C2 domains of many proteins (e.g. synaptotagmin). The major fatty acyl chain in PS is docohexeanoic acid (DHA) (22:6), with double bonds starting at the omega-3 position (shown here). (E) Phosphatidylcholine – PC - is a very abundant lipids in many cells including neurons. Metabolism of PC at the headgroup via phospholipase D (PLD) leads to phosphatidic acid, a potent signaling phospholipid, which activates lipid kinases. (F, G) Cholesterol (F) and an oxidized derivative (oxysterol, G) can influence membrane structure and fluidity. The oxysterol shown has an additional hydroxyl group at the C7 ring position. (H, I, J) Ceramide (H) forms the backbone for a large class of chemically diverse sphingolipids. Sphingomyelin (I), a ceramide which carries a choline headgroup. More complex glycosphingolipids are extremely abundant in brain and myelin. Sulfatide (J) is a complex glycosphingolipid that has a sulfate group on the 3-OH position of the galactose.

*Figure 3: In situ expression of Hmgcr and Pip5K2a in ventral midbrain*
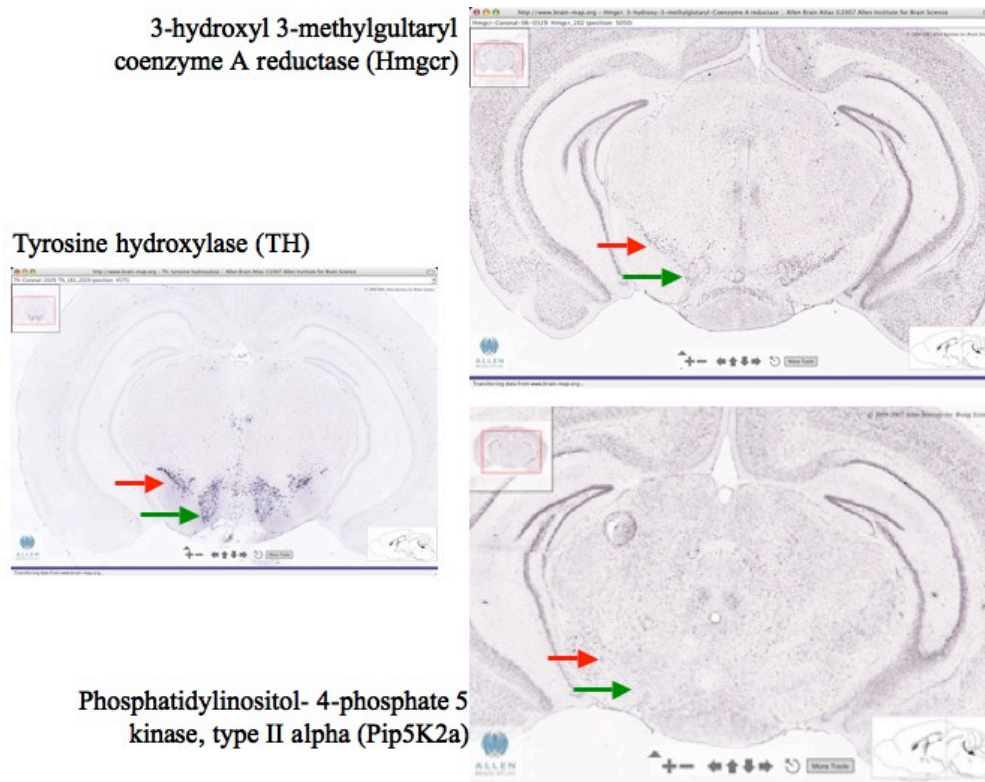


Figure 3: Images from Allen Brain Atlas ([www.brain-maps.org](www.brain-maps.org)) Lein et al., (2007). Green and red arrows indicate the VTA and SNpc respectively.

## PD animal model: 1-methyl-4-phenyl-1,2,3,6-tetrahydropyridines (MPTP) injections

All procedures performed in rodents were in accordance with IACUC guidelines. MPTP injections were performed according to previously published methods, following the acute schedule (Jackson-Lewis et al., 1995). Briefly, C57B6 mice were given four i.p. doses of either 18 mg/kg of MPTP (Sigma-Aldrich) or saline (control) every 2 h. Mice were decapitated 48 hours after the last dose, and the ventral midbrain and striatum were dissected and snap-frozen for subsequent lipid extraction and GC-MS analysis. Previously published data using the same protocol showed that at this timepoint about 35% of dopaminergic neurons have degenerated (Jackson-Lewis et al., 1995).

### Lipid standards

Lanosterol, cholesterol, 1,2-dimyristoyl-*sn*-glycero-3-phosphocholine (DMPC or PC), and desmosterol-$d_6$ (all of highest purity, >99%) were purchased from Avanti Polar Lipids. Oxysterol standards α-cholestane, 7α-hydroxycholesterol, 7β-hydroxycholesterol, 7-dehydrocholesterol, 25-hydroxycholesterol, and 7-ketocholesterol were obtained from Sigma (St. Louis, MO, USA). 7α-Hydroxycholesterol-$d_7$, 7β-hydroxycholesterol-$d_7$, β-sitosterol-$d_7$, campesterol-$d_3$, lathosterol-$d_4$, and 7-ketocholesterol-$d_7$ were purchased from CDN Isotopes (Quebec, Canada). 27-hydoxycholesterol-$d_5$, 24-hydroxycholesterol, and 24-hydroxycholesterol-$d_7$ were purchased from Medical Isotopes (Pelham, AL, USA). Deuterated standards obtained were of >95% purity.

### Sample preparation for Gas Chromatography-Mass Spectrometry (GC-MS)

Sample preparation and GC-MS analyses were performed as previously published (Chia et al., 2008; He et al., 2006). Extraction of lipids from tissues was carried out using a modified version of the Bligh and Dyer method (Bligh and Dyer, 1959). Ventral midbrain (~20-25 mg) or striatum tissues (~15-20 mg) were homogenized directly in 600 µl of ice-cold chloroform: methanol (1:2). Another 300 µl of chloroform were added to the homogenate followed by 450 µl of 1 M KCl. The homogenates were centrifuged at 14,000 rpm for 5 minutes at 4°C, and the lower organic phase was carefully transferred to a new eppendof tube. All organic phases were pooled and dried under vacuum using a speedvac. Samples were stored in -80°C until derivatization and subsequent GC-MS analysis.

Dried lipid extracts were resuspended in chloroform:methanol (1:1) to a concentration of 0.1 mg tissue/µl solvent. A 20-µl sample of lipid extract was removed and completely dried in a glass vial. For each sample, we added a mixture of heavy isotopes: 40 ng of 7$\alpha$-hydroxycholesterol-$d_7$, 40 ng of 7$\beta$-hydroxycholesterol-$d_7$, 40 ng of 26(27)-hydroxycholesterol-$d_5$, 80 ng of 7-ketocholesterol-$d_7$, 0.2 µg of 5$\alpha$-cholestane, 0.2 µg of desmosterol-$d_6$, 0.2 µg of lathosterol-$d_4$, 0.2 µg of campesterol-$d_7$, and 0.2 µg of $\beta$-sitosterol-$d_7$ in 25 µl of ethanol. Standards and sample mixtures were dried under a stream of $N_2$ before adding the derivatizing agent (15 µl acetonitrile and 15 µl BSTFA + TMCS; Pierce Thermoscientific). The derivatized samples were analyzed with an Agilent 5975 inert XL mass selective detector. Selective ion monitoring was performed using the electron ionization mode at 70 eV (with the ion source maintained at 230°C and the quadrupole at 150°C) to monitor one target ion. Two qualifier ions were selected for the mass spectrum of each compound to optimize for sensitivity and specificity.

*Results: Identification of sterol biosynthetic pathway and lanosterol as potential metabolite of importance to dopaminergic neuronal survival.*

### In silico pathway analyses identify sterol biosynthetic pathway

Out of the 3 major lipid pathways, which lead to the generation of membrane lipids, we found that the greatest number and percentage of genes that fulfill <u>both</u> criteria are from the sterol biosynthetic pathway (Fig 4A). In this pathway, 52% (10/19) were positive for both criteria. By contrast, the sphingolipid and glycerophospholipid pathways had approximately 10% (3/29) and 17% (6/35) representation, respectively. Most interestingly, seven consecutive enzymes involved in the metabolic chain from squalene to zymosterol fulfill both criteria (Table 3, Fig 4B). Such consistent representation string of metabolic pathways was not observed for glycerophospholipids (data not shown) and sphingolipids  (Fig 5).

*Table 3: Genes in cholesterol biosynthesis (see pathway in Fig 4)*

| Gene symbol | Name | *p-value | ** Expression in SNpc |
|---|---|---|---|
| Fdft1 | farnesyl diphosphate farnesyl transferase 1 | 1.89E-11 | ++ |
| Tm7sf2 | transmembrane 7 superfamily member 2 | 2.44E-10 | ++ |
| Sqle | squalene epoxidase | 6.24E-08 | ++ |
| Pmvk | Phosphomevalonate kinase | 1.66E-07 | + |
| Sc4mol | sterol-C4-methyl oxidase-like | 2.26E-06 | ++ |
| Idi1 | isopentenyl-diphosphate delta isomerase | 5.86E-06 | - |
| Lss | lanosterol synthase | 1.08E-05 | + |
| Fdps | farnesyl diphosphate synthetase | 2.44E-05 | +++ |
| Ebp | phenylalkylamine Ca2+ antagonist (emopamil) binding protein | 8.27E-05 | - |
| Nsdhl | NAD(P) dependent steroid dehydrogenase-like | 1.99E-04 | ++ |
| Hmgcr | 3-hydroxy-3-methylglutaryl-Coenzyme A reductase | 2.66E-04 | +++ |
| Cyp51 | lanosterol demethylase/ cytochrome P450, family 51 | 3.33E-04 | ++ |
| Hsd17b7 | hydroxysteroid (17-beta) dehydrogenase 7 | 3.75E-04 | + |
| Mvk | mevalonate kinase | 1.03E-03 | n/a |
| Dhcr24 | 24-dehydrocholesterol reductase | 3.27E-03 | n/a |
| Ggps1 | geranylgeranyl diphosphate synthase 1 | 1.06E-02 | n/a |
| Sc5d | sterol-C5-desaturase (fungal ERG3, delta-5-desaturase) homolog (S. cerevisae) | 1.56E-02 | n/a |
| Cyp27b1 | cytochrome P450, family 27, subfamily b, polypeptide 1 | 1.80E-02 | n/a |
| Dhcr7 | 7-dehydrocholesterol reductase | 4.52E-02 | n/a |

*p-value from supplementary data of Sugino et al. (2006). We consider $p < 0.001$ as differentially expressed.

**Gene expression in SNpc scoring by in situ data from Lein et al., (2007)

(Scoring key "N/a" = Not analyzed, "-" not expressed or ubiquitously expressed, "+" moderately and preferentially expressed in SNpc, "++" expressed preferentially in SNpc; "+++" highly preferentially expressed in SNpc)

*Figure 4: In silico analyses of genes involved in lipid metabolism*
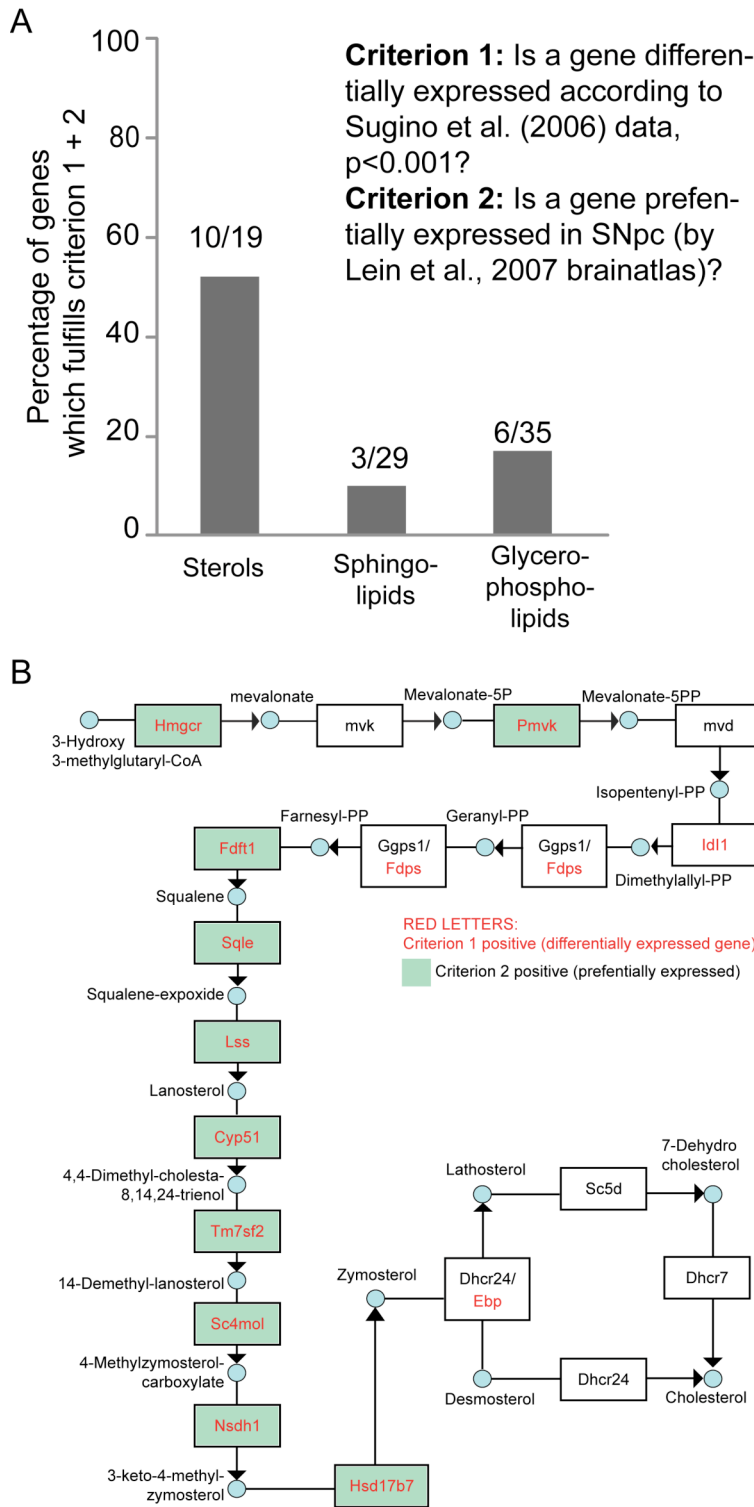


Figure 4: A two-criteria system was used to assess genes involved in biosynthesis and metabolism of the main classes of membranes lipids, i.e. sterols, sphingolipids, and glycerophospholipids. Criterion 1 assesses if a particular gene is differentially expressed among neurons (by p-value of <0.001) in the data set from Sugino et al. (2006). Criterion 2 assesses if a particular gene is preferentially expressed (in situ hybridization, Lein et al. (2007) (www.brain-maps.org) in the substantia nigra (SN). (A) Graph represents the percentage of genes from each lipid class that fulfills criterion 1 and 2. Numbers on top of each bar graph represent the number of genes that are positives for both criteria over the total number of genes assessed. (B) Graphical representation of cholesterol biosynthesis (modified from KEGG). Genes labeled in red letters scored positive for criterion 1. Genes with green background scored positive for criterion 2.

*Figure 5: Genes involved in sphingolipid biosynthesis were not differentially expressed among neurons or preferentially expressed in SNpc.*
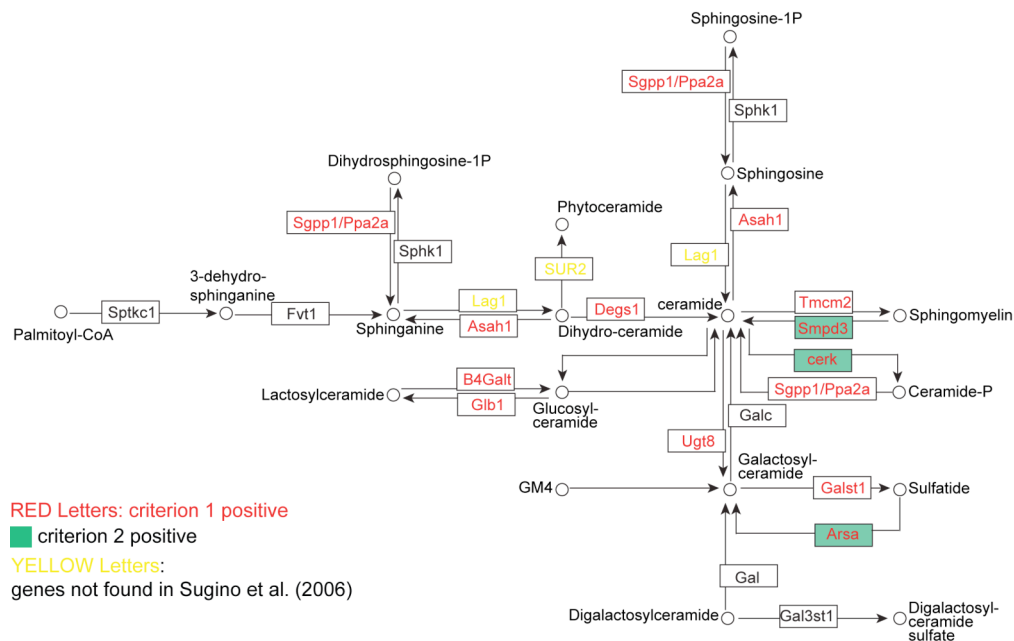


Figure 5: Graphical representation of the sphingolipid metabolic pathway (modified from KEGG). Genes shown in red letters scored positive for criterion 1 (see Fig 3). Genes shown with green background scored positive for criterion 2. Genes in yellow letters are genes not assessed because they were not included in Sugino et al. (2006). Only 3 out of 29 genes are positive for both criterion 1 and 2 (see also Fig 4A).

### Lanosterol level is significantly reduced in affected regions of PD animal models.

If one were to assume that sterol biosynthesis is important for dopaminergic neurons as the *in silico* analysis suggested, then brain sterol metabolites might also be altered upon pathogenesis of PD. To address this, we compared the levels of sterol metabolites in the two affected regions, striatum and ventral midbrain, of control versus a PD model. The PD model of choice is pharmacological treatment of animals with MPTP as it is the most widely used PD rodent model with a well-established and well-documented time course of pathogenesis (Jackson-Lewis et al., 1995; Jackson-Lewis and Przedborski, 2007). Using GC-MS, 9 sterol metabolites were measured. Out

of these, only lanosterol, the first cyclic sterol, was reduced by ~50% in the two affected brain areas (Fig 6), whereas, no other sterol metabolites differed significantly in levels.

*Figure 6: Lanosterol is specifically depleted in affected brain areas of mice treated with MPTP*
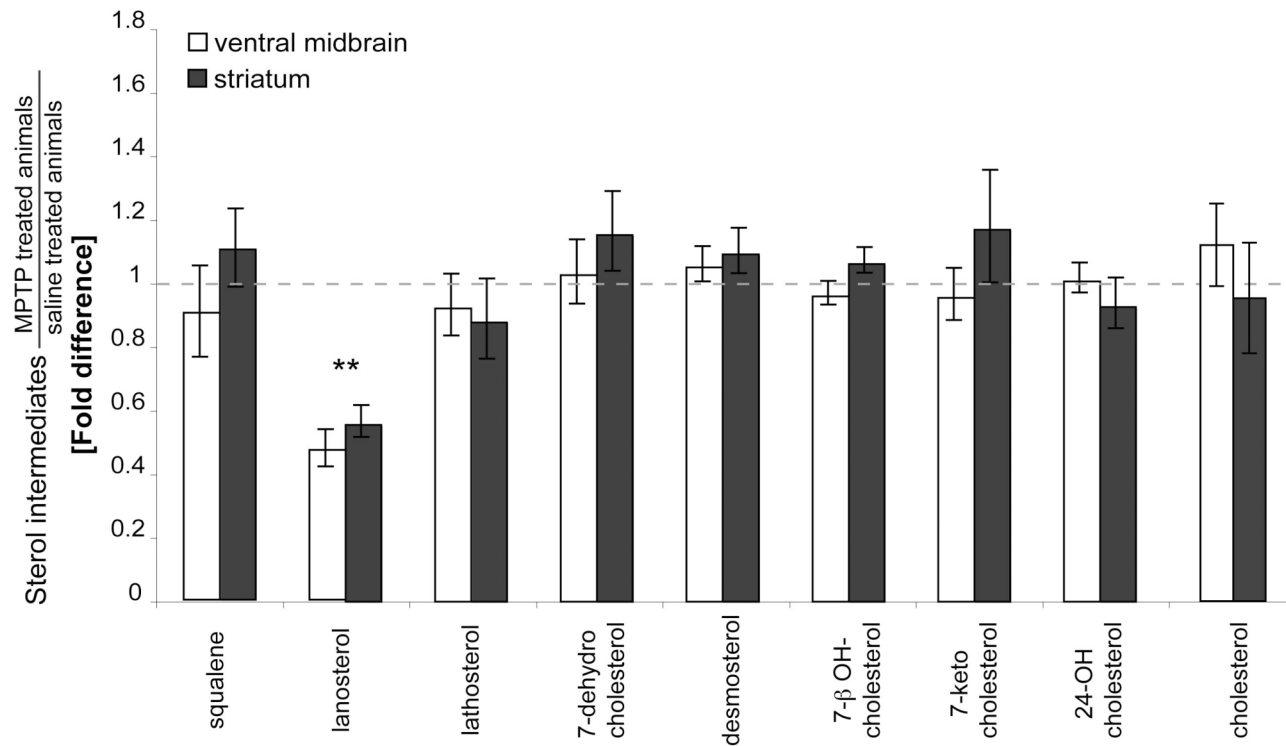


Figure 6: C576B6 mice were treated with either MPTP or saline. Ventral midbrain and striatum were dissected and lipids extracted for analysis of sterol intermediates by GC/MS. Average levels of sterol intermediates from MPTP treated animals (n=4) normalized by the average levels of saline treated (control) animals (n=6). Error bars represent standard error of mean (SEM). In both ventral midbrain and striatum, levels of lanosterol are reduced significantly in the MPTP treated animals. **p-value <0.01 (Mann Whitney U test).

While some previous studies compared levels of brain lipids in PD or MPTP animal models to controls, these were limited to the analysis of phospholipids and cortices were used rather than the affected areas (ventral midbrain and striatum), For example, Julien et al., (2006), measured fatty acids (docohexanoic acid, DHA and arachidonic acid, AA, see Fig 2 for structure) reasoning that nutritional intake could be easily modified to correct for changes in either DHA or AA. However, it is not clear if such lipid profiles are representative of the affected region as post-mortem cortices were used rather than ventral midbrain and striatum (Julien et al., 2006).

There are some reports linking sterol lipid metabolism to PD. An association study showed that serum cholesterol correlates with PD (Hu et al., 2008) and low levels of LDL-C may be associated with higher occurrence of PD (Huang et al., 2007). However, these remain surrogate observations as brain cholesterol is synthesized independently of the rest of the body (Dietschy, 2009; Han, 2004; Pfrieger, 2003).

In rats treated with 3-nitropropionic acid, lathosterol levels were lowered in the striatum but higher in serum (Teunissen et al., 2001). Recently, Nieweg et al. (2009) published data showing that lanosterol levels are much higher in neurons than in astrocytes or oligodendrocytes (Nieweg et al., 2009), suggesting that lanosterol could be an essential metabolite for neurons. To determine if lanosterol is a survival factor for dopaminergic neurons, we made use of primary postnatal ventral midbrain cultures treated with MPP+ or co-treated with various sterols (chapter 2).

**Chapter 2: Lanosterol rescues dopaminergic neurons from MPP+**

**toxicity in cultures**

*Introduction: Primary cultures of ventral midbrain neurons.*

   Primary dopaminergic neuronal culture is a technique commonly employed to study mechanism of cell death and/or to assess if certain compounds could act as survival factors. While there are many protocols, one of the most widely used in the field is the "Sulzer" protocol. Technically, dopaminergic neurons are more challenging to culture using postnatal animals but they give higher percentage of dopaminergic neurons (30-60% depending on area dissected) in contrast to the embryonic cultures (less than 0.5%). More importantly, by this stage, dopaminergic neurons in the midbrain have fully differentiated, which means that the observed improved survival is not due to induction of differentiation.

   There are a number of technical drawbacks to this system. Firstly, neurons are plated on an astrocytes feeder layer, a requirement for the survival of these neurons. Secondly, the number of neurons yield per neonatal animal is low, about 20,000 to 25,000 for rats and 10,000-12,000 for mice. Both of these drawbacks make it difficult to detect subtly biochemical changes. Furthermore, in this culture systems, dopaminergic neurons exposed to toxin such as MPP+, the active metabolite of MPTP, could die by many ways such as apoptosis, necrosis, or autophagy. Thus, to measure survival, it is laborious as one would need to count the total number of individual dopaminergic neurons instead of measuring apoptosis by commercial available kits. Finally, the postnatal cultures according to the Sulzer's lab protocol use a growth

medium that contains serum. Since we are adding lipids into the cultures, even small amounts of serum could mask the effects.

In this chapter, I modified the published and widely used Sulzer protocol for culturing postnatal ventral midbrain. Upon establishing a ventral midbrain cultures system that is viable and sensitive to MPP+, I demonstrated that exogenous addition of lanosterol rescues dopaminergic neurons from MPP+ toxicity. Furthermore, lanosterol, along with cholesterol can induce neurite outgrowth. Immunoblot analyses showed an increase expression of p35 in neurons treated with cholesterol and lanosterol. The mechanism of neurite outgrowth is thus likely via the p35 and subsequent activation of cdk5 as documented in other studies. Collectively, these results identify lanosterol as both a survival factor and inducer of neurite outgrowth.

*Material and Methods*

**Culturing of postnatal ventral midbrain neurons**

Ventral midbrain cultures were prepared according to previous published methods (Rayport et al., 1992) with slight modifications since the original method used serum in the medium, which is not suitable for lipid addition. In brief, ventral midbrains from postnatal day 0 to day 2 (P0-P2) rodents were dissected and digested in papain solution and plated on a glia feeder layer. Cells were cultured in serum-free media, neurobasal/B27 (Invitrogen), with additional supplementation of Superoxide Dismutase-1 (SOD1), apo-transferrin, and insulin (all from Sigma) to a final concentration of 5 μg/ml, 95 μg/ml, and 21 μg/ml respectively. After 1 hour, when cells are fully attached, 10 ng/ml of glial derived neurotrophic factor (GDNF, from Millipore) was added. To inhibit glial growth, a solution of FDU consisting of

16.5 µg/ml of Uridine and 6.7 µg/ml of 5-Fluorodeoxyuridine was added after 1 day of plating. Cells were cultured for 7 days (DIV7) before treatment with MPP+ or co-treatment with sterols/ lipids.

### Lipid and liposomes for cell cultures

Lanosterol, cholesterol, 1,2-dimyristoyl-*sn*-glycero-3-phosphocholine (DMPC or PC), and desmosterol-$d_6$ (all of highest purity, >99%) were purchased from Avanti Polar Lipids. Lanosterol, cholesterol, and PC were dissolved in chloroform:methanol (1:1). Cholesterol or lanosterol was mixed in equimolar proportion with PC and dried by vacuum in a Speedvac (Thermosavant). The lanosterol/PC or cholesterol/PC mixture was resuspended and sonicated in culture medium on the day of treatment to make a 0.5 mM stock liposome. Each type of stock liposome was used in the neuronal cultures within a day of preparation.

### Fluorescence microscopy and quantification of dopaminergic neuronal survival

Ventral midbrain cultures plated on 12 mm coverslips were treated for 24 hours with 10 µM of MPP+ and or co-treatment with 5 µM PC, 5 µM cholesterol, or 5 µM lanosterol. After aspirating the medium, cells were washed 3 times with 1 X PBS to remove all dead cells. Cells were then fixed with 4% paraformaldehyde for 20 minutes, followed by permeabilization and blocking using 5% FBS in 0.1% TritonX-100 for 30 minutes. Coverslips were then stained with anti-TH (secondary alex-fluor488 – green) and TUJ1 (secondary alexfluor555- red). Anti-mouse or rabbit alex-fluor488 or 555 dyes (1:1000) were purchased from Molecular Probes/ Invitrogen. Two types of cells were counted: TUJ1 positive and TH positive cells by using an Olympus fluorescence scope with Fluorescein and Rhodamine filter sets. Every neuron

on the entire 12 mm coverslip was assessed. Percentage of dopaminergic neurons for each condition was determined by number of TH+/TUJ1+. Typically, for control conditions, each coverslip consists of 2000-3000 TUJ1 positive and about 400-1200 are TH+. For each treatment, we assessed 4-6 coverslips in each independent experiment. The averages of 4-5 independent experiments were reported in the figures.

### Culturing hippocampal neurons

E18.5 hippocampal neurons were cultured according to previously described method in neurobasal/B27 (Kaech and Banker, 2006). Briefly, neurons were plated on a wax-dotted 15 mm coverslips coated with 1 mg/ml of poly-D-lysine (Sigma). Two hours after plating, when neurons have attached, the coverslips were flipped into a 12-well plate containing a glial feeder layer. For neurite outgrowth experiments, neurons were plated at extremely low density of 150 cells/mm$^2$. Various concentrations of cholesterol and lanosterol were added at this time of coverslip flipping. After 48 hours, neurons were either fixed for immunocytochemistry or both neurons and glia feeder lysed for protein extraction.

### Neurite outgrowth measurements

Hippocampal neurons were stained with an anti-Tau1 Ab (Chemicon) and imaged using a spinning disc confocal miscroscope. Total neurite (axon) length per cell was quantified for each condition using the neurite outgrowth segmentation algorithm (Metamorph v7.1).

***Western blot***

For western blot, cells in cultures were washed 3 times with 1X PBS after media was aspirated. Cells were then lysed in 100 µL of RIPA buffer (50 mM Tris-HCl, pH 7.4, 1% NP-40, 0.25% Na-deoxycholate, 150 mM NaCl, 1 mM EDTA) supplemented with a cocktail of protease inhibitors (Complete Mini-EDTA inhibitors, Roche Diagnostics). Approximately 20 µg of cell protein lysate were loaded in each well of a 10% polyacrylamide gel containing 0.1% SDS. Proteins were then transferred to nitrocellulose membrane. Membrane was immunoblotted with polyclonal antibodies rabbit-anti-cdk5 (C8) 1:500, and rabbit anti-p35 (C19) 1:1000, from Santa Cruz. Monoclonal mouse-anti-actin (1:10,000) was purchased from Sigma. Monoclonal mouse-anti-neuronal tubulin (TUJ1) (1:10,000) was purchased from Convance. Secondary antibodies anti-rabbit or mouse peroxidase conjugated (1:10,000) for western blots were purchased from Biorad. Immunoblot was visualized with ECL reagent from Pierce Thermoscientific.

***Statistical analyses***

Error bars represent standard errors of measurements (SEM) and p-values were calculated by Student's t-test.

***Results: Effects of sterol treatments of primary neurons.***

Primary ventral midbrains cultured in the modified medium survived well. Typically, there are about 25-30% of dopaminergic neurons as judged by TH+ staining (Fig 7). It is also important to note that the TH+ neurons are also selectively sensitive to MPP+ toxicity at the concentration of 10 µM (Fig 7A versus 7B), resulting in about 50% decrease of TH+ neurons ($p < 0.001$). However, the number of dopaminergic neuronal death did not increase

drastically with increasing dose of MPP+. At high MPP+ concentrations, there were also more "unselective" cell death (data not shown, personal observation). Therefore, I decided to use the lowest MPP+ concentration (10 µM) to test the survival effects of lanosterol.

After establishing the ventral midbrain cultures, we asked whether exogenous addition of lanosterol protects dopaminergic neurons against MPP+-induced cell death. Primary postnatal neuron cultures from ventral midbrain were treated with MPP+, and the survival of dopaminergic neurons was determined in the absence or presence of exogenously-added lanosterol. 48% of dopaminergic neurons survived upon treatment with MPP+ under these culture conditions (Fig 8A, 8C). Co-incubation of MPP+ with phosphatidylcholine (PC, vehicle control) or cholesterol did not improve survival of dopaminergic neurons (Fig 8B, 8C). In contrast, co-treatment of the cultures with MPP+ and lanosterol increased survival of dopaminergic neurons to 76% (Fig 8B, 8C). Thus, lanosterol rescues dopaminergic neurons from MPP+-induced cell death.

*Figure 7: Characterization of postnatal ventral midbrain cultures*
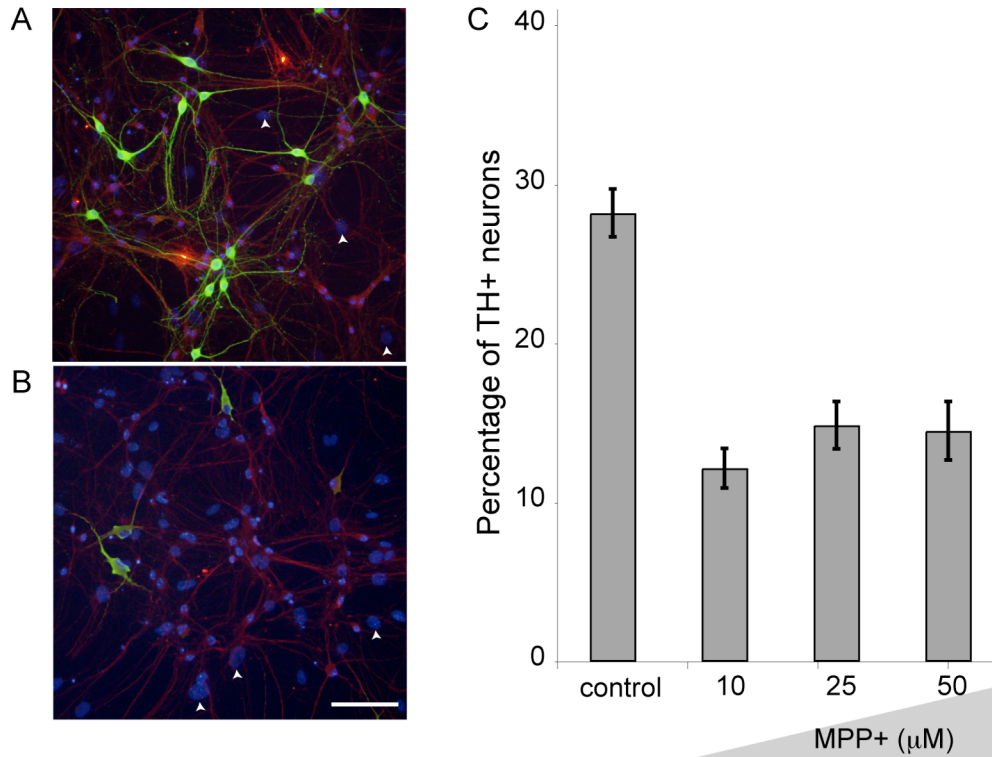


Figure 7: Ventral midbrain cultures (A) control (B) with 10µM of MPP+, stained with dopaminergic neuron marker – TH (green), neuronal marker TUJ1 (red) and nucleus dye DAPI (blue). White arrowheads show nucleus of astrocytes (feeder layer), which have bigger nucleus than neurons. Scale bar is 100µm. (C) Graphical representation of percentage of dopaminergic neurons (n = 3). Error bars represent +/- SEM.

*Figure 8: Lanosterol rescues dopaminergic neurons in MPP+-treated postnatal ventral midbrain cultures*
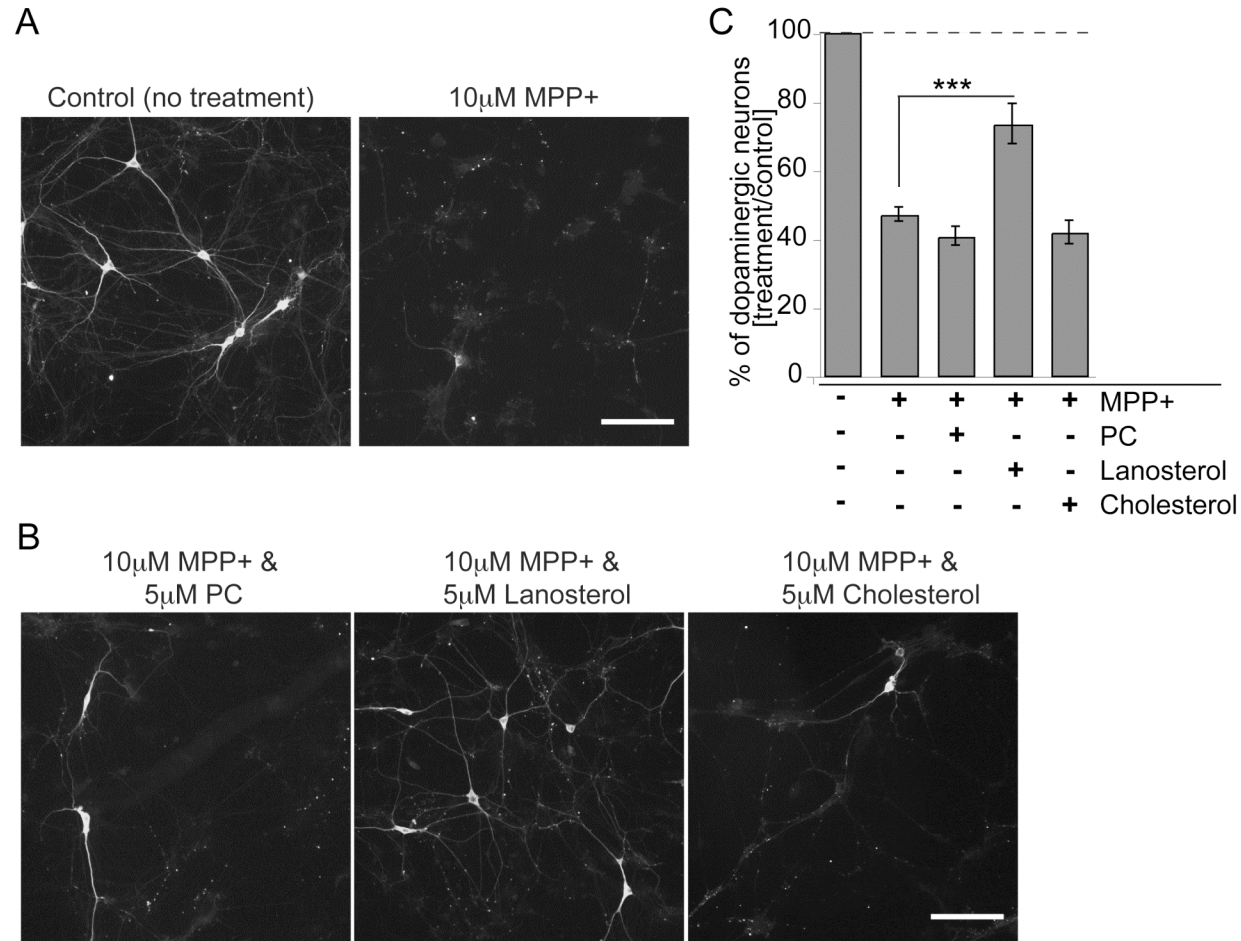


Figure 8: Fluorescence images of primary ventral midbrain cultures (DIV7) stained with anti–tyrosine hydroxylase (TH), a marker for dopaminergic neurons. (A) Control cells (no treatment) and cells treated with 10 µM MPP+; (B) co-treated cells for 24 h with 10 µM MPP+ and 5 µM of phosphatidylcholine (PC, left panel), lanosterol (middle panel), or cholesterol (right panel). Scale bars in A and B represent 200 µm. (C) Plot of fold changes of each treatment relative to control. Y-axis shows the average percentage of TH+ neurons from each treatment condition divided by the average percentage of TH+ neurons in control. Error bars represent SEM from four to five independent experiments. ***$p < 0.001$ between lanosterol/MPP+ and MPP+.

In addition to survival, dopaminergic neurons treated with lanosterol appear to have longer neurites. Since survival factors cause proliferation in dividing cells (Chaudhary and Hruska, 2001; Holmstrom et al., 2008) and may increase neurite length in neurons (Bonnet et al., 2004; Ma et al., 2009), it was thus important to establish if lanosterol increased neurite length.  From a technical perspective, it was difficult to measure neurites length of dopaminergic neurons accurately. This is because these neurons in cultures do not express their marker, TH, till after days in vitro 5 (DIV 5) (data not shown). By this stage, most neurites are far too long to trace accurately in a single field of view. Furthermore, postnatal dopaminergic neurons could only be grown in culture with direct contact with an astrocyte feeder. Thus, in order to investigate, biochemically, the effects in various cell types, I chose to use hippocamal neurons in co-culture "Banker style" cultures to assess neurite outgrowth, since their developmental stages are well documented (Kaech and Banker, 2006). In this hippocampal neuron-astrocytes co-cultures, neurons are plated on glass coverslips while astrocytes are grown on the culture dish. Coverslips with paraffin dots are inverted to face the monolayer glial cells allowing for free exchange of media and biochemical isolation of individual cell types.

Using an unbiased software-based quantification, I measured the neurite length two days after plating and showed that lanosterol significantly increased neurite length from an average length of 59 μm in the non-treated condition to 132 μm  (Fig 9A, 9B). This effect was also observed with cholesterol, demonstrating that both sterols have growth promoting properties. To determine if these two sterols activate known growth-promoting signaling

pathways, we biochemically assayed the expression level and activation state of Erk, Akt, Gsk-3β, and p35/cdk5. There were no dramatic differences in phospho-Akt or phospho-Gsk-3β(Ser9) levels (data not shown). Interestingly however, the addition of sterols induced an increase of p35 expression, the activator of cdk5, while expression levels of cdk5 itself remained unchanged (Fig 9C). This effect is neuron-specific as it was not observed in astrocytes. The expression of the neuron-specific microtubule-associated protein, TUJ1, is increased in sterol treated neurons. This is consistent with the neurite outgrowth assays (Fig 9), whereby longer neurites should have more microtubles. Therefore, lanosterol as well as cholesterol promote neurite outgrowth and induce increased expression of the activator of cdk5, p35.

*Figure 9: Lanosterol and cholesterol increase neurite outgrowth in hippocampal neurons.*

C
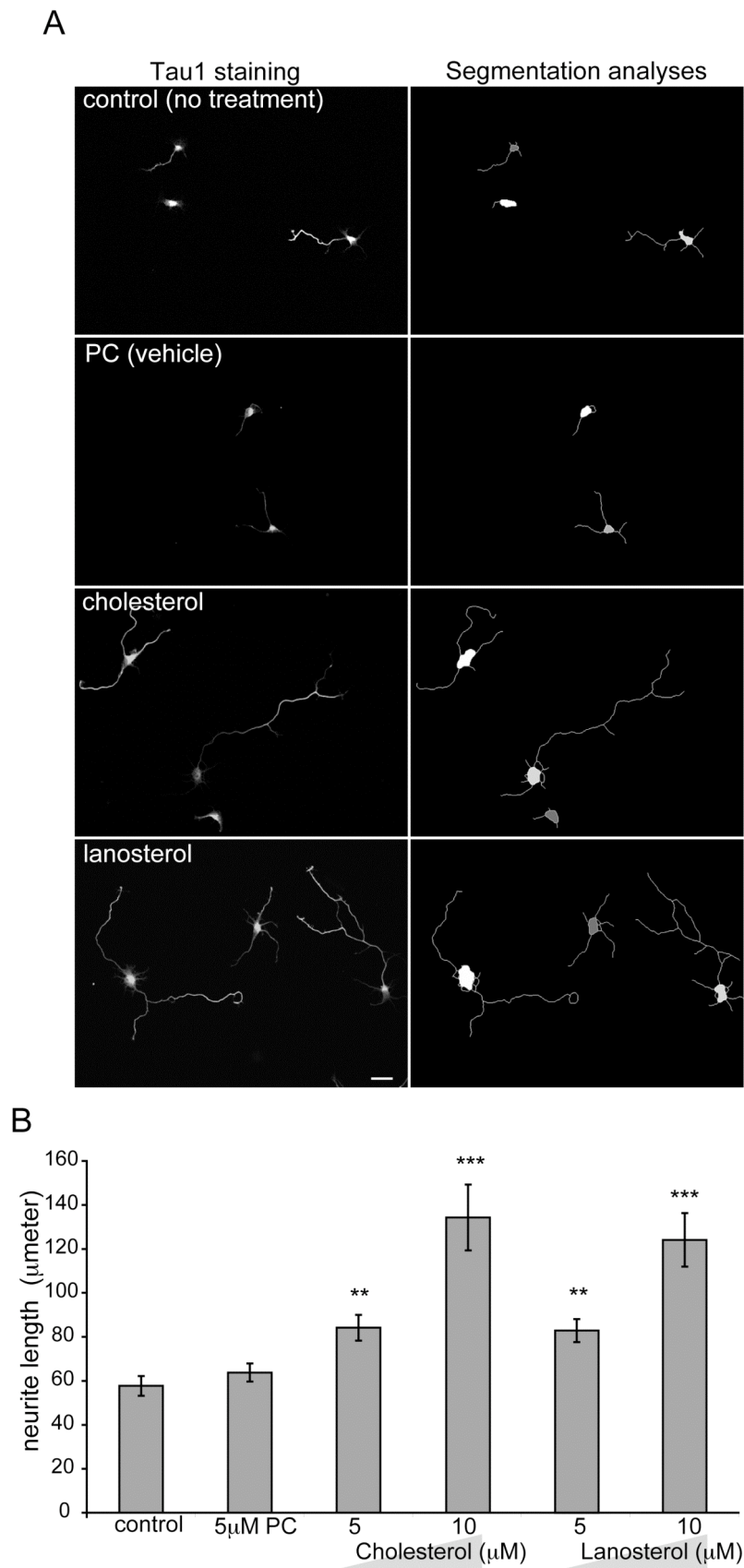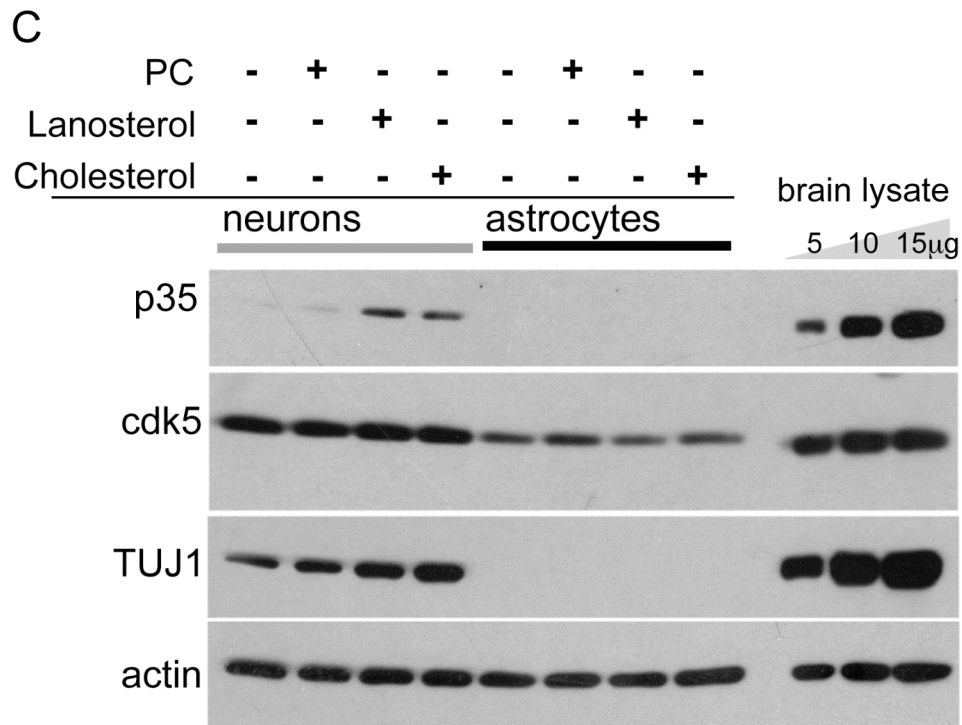


Figure 9: Tau1 staining and segmentation analysis of hippocampal neurons cultures. Scale bar represents 20μm. Lanosterol and cholesterol lead to extended neurites. (B) Total neurite length was assessed by segmentation software using Metamorph. 200-400 neurons were assessed per experiment. Error bars represent SEM of 3 independent experiments. **p<0.01 and ***p<0.001 between treatment conditions and control conditions were assessed by two tailed Student t-test. (C) Immunoblots of neurons and astrocytes (DIV 3) grown in "Banker style" co-cultures (see methods) and treated with various lipids for 48 hours. Antibodies used are anti-p35 (an activator of cyclin dependent kinase 5, cdk5), cdk5 (cyclin dependent kinase 5), TUJ1 (neuronal class III tublin). Lanosterol and cholesterol induce expression of p35 in neurons but not in astrocytes. Results shown are representative of 3 independent experiments.

Cholesterol biosynthesis has been previously shown to be essential to nerve regeneration in various models ranging from *in vivo* optic nerve crush (Heacock et al., 1984), to *in vitro* cultured rat sympathetic neurons (de Chaves et al., 1997). I demonstrate here that lanosterol and cholesterol enhance neurite outgrowth. Furthermore, I find that these sterols could also elevate the activity of intracellular kinases such as cdk5 via increased expression of p35. It has been reported and well-established that cdk5 is regulated by its activator p35 and could together induce neurite outgrowth in various models (Hahn et al., 2005; Namgung et al., 2004). In addition, a number of factors, such as

interferon gamma (Song et al., 2005), and Fas (Desbarats et al., 2003) could induce the increase in levels of p35. However, no lipid or sterol metabolite had been shown to increase p35 expression level. These results thus suggest a novel, sterol-dependent activation mechanism for p35/cdk5, which may promote neurite outgrowth.

Yet, this outgrowth mechanism via increase expression of p35 in neurons is unlikely to be the same to elicit the rescue effects seen in dopaminergic neurons. Firstly cholesterol, which also increases neurite outgrowth and expression of p35, fails to rescue dopaminergic neurons. Furthermore, in ventral midbrain cultures treated with lipids and MPP+, there were no significant changes in p35 levels (see chapter 4). To determine lanosterol's mechanism of rescue, I started to biochemically screen a number of pathways (chapter 3).

**Chapter 3: Biochemical analyses of metabolic pathways.**

*Introduction: Cross-talk of metabolic pathways*

Since sterol metabolites can be converted to other precursors by endogenous enzymes, it is important to determine if the addition of lanosterol would change other metabolites. Firstly, does addition of lanosterol change other sterols in the cholesterol biosynthetic pathway? Secondly, does lanosterol affect levels of other metabolites, which are reported as survival factors?

To answer the first question, I measured a number of metabolites in the sterol biosynthetic pathway. This would in part answer if addition of lanosterol alters other metabolites. In addition, another important metabolite to measure is ubiquinone or Coenzyme Q (CoQ), the lipid electron carrier that localizes mainly in the mitochondria. CoQ has a quinone chemical group and varying length of isoprenyl subunits. Thus, in the cell, there are cross talks between biosynthesis of sterols and CoQ since they both share isoprenyl as precursors (Fig 10). In the context of PD, CoQ has been shown to be beneficial to a subset of PD patients and is neuroprotectinve in the MPTP animal models (Beal et al., 1998; Cleren et al., 2008; Galpern and Cudkowicz, 2007; Muller et al., 2003; Yang et al., 2009).

*Figure 10: Cross-talk of sterol and  ubiquinone biosynthesis*
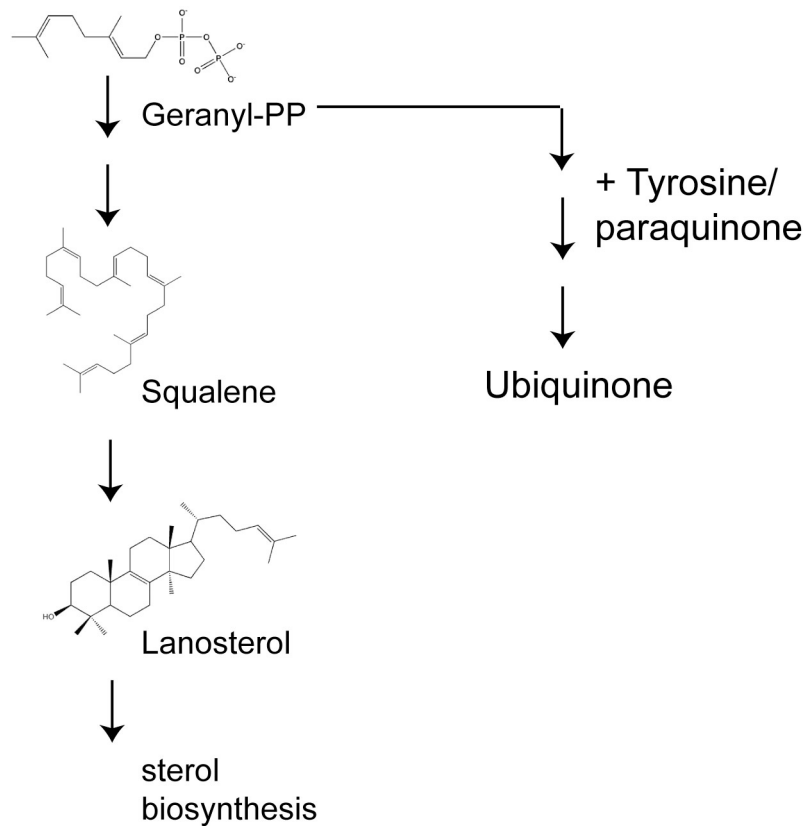


Figure 10: Simplified pathway of cross-talk between sterol and ubiquinone biosynthesis in mammalian cells. Both pathways use isoprenyl units as precursors

*Materials and Methods: Lipid extraction and measurements*

**Sample preparation for Gas Chromatography-Mass Spectrometry (GC-MS)**

Approximately 400,000 cells were used for each condition. After treatment, cells were washed 3 times with cold PBS and scraped with 400 μl ice-cold methanol and transferred to a 1.5-ml Eppendoff tube. Then, 200 μl of chloroform was added, followed by 1 minute of vortexing.  300 μl of 1 M KCl was added. The homogenates were centrifuged at 14,000rpm for 5 minutes at 4°C to separate the phases and the lower organic phase was carefully transferred to a new Eppendof tube. Aqueous phases were re-extracted twice with 300 μl of chloroform. All organic phases were pooled and dried under

vacuum using a Speedvac (Thermosavant) and stored in -80°C until derivatization and subsequent GC-MS analyses.

For each sample, I added a mixture of heavy isotopes, 20 ng of 7 alphahydroxycholesterol-$d_7$, 20 ng of 7 beta-hydroxycholesterol-$d_7$, 20 ng of 26 (27)-hydroxycholesterol-$d_5$, 40 ng of 7-ketocholesterol-$d_7$, 0.1 µg 5-alpha cholestane, 0.1 µg of desmosterol-$d_6$, 0.1 µg of lathosterol-d4, 0.1 µg of campesterol-$d_7$, and 0.1 µg of beta-sitosterol-$d_7$ in 25 µl of ethanol. Standards and sample mixture were dried under a stream of $N_2$ before the addition of a derivatizing agent, 15 µl acetonitrile and 15 µl BSTFA + TMCS (Pierce Thermoscientific). The derivatized samples were analyzed using Agilent 5975 inert XL mass selective detector. Selective ion monitoring was performed using electron ionization mode at 70 eV (with ion source maintained at 230°C and the quadrupole at 150°C) to monitor one target ion. Two qualifier ions were selected for each compound's mass spectrum to optimize sensitivity and specificity.

### *Measurement of Coenzyme Q*

For each condition, 3 to 4 million neurons (DIV 7) were treated with various lipids and incubated for 24 hours. Cells were washed twice with cold PBS and were scraped in 0.5 ml of cold PBS. Cells were centrifuge at 1000g to pellet and PBS was removed. To re-suspend the cell pellet, 100 µl of fresh PBS was added. 750 µl of hexane:ethanol (5:2 v/v) was added and vigorously vortexed for 1 minute. To extract coenzyme Q, 400 µl of the organic phase were collected and dried completely with $N_2$.

Agilent HPLC 1200 system (Agilent) coupled with an Applied Biosystems 3200 QTrap mass spectrometer (Applied Biosystems, Foster City, CA) was used for measurement of coenzyme Q8, Q9, Q10 and free cholesterol. Chromatographic separation was carried out using an Agilent Zorbax Eclipse XDB-C18 column (i.d. 4.6 × 150 mm). HPLC conditions were as follows: (1) chloroform:methanol 1:1 (v/v) as the mobile phase at a flow rate of 0.5 ml/min; (2) column temperature: 30°C; (3) injection volume: 10 μl. The LC-MS instrument was operated in the positive atmospheric pressure chemical ionization (APCI) mode with a vaporizer temperature of 500°C, and corona current of 3 μA. Coenzyme Q6 was used as an internal standard and monitored using MRM transition of 591.4→197.0. MRM transitions of 727.5→197.0, 795.5→197.0 and 863.6→197.0 were set up for analysis of coenzyme Q8, Q9 and Q10, respectively.

*Results: Metabolic changes upon sterol additions*

To determine if addition of lanosterol affects other sterol metabolites, I analyzed squalene, lanosterol, lathosterol, 7-dehydrocholesterol, desmosterol, cholesterol, 7-beta-hydroxylcholesterol, 7-keto-cholesterol, 24-hydroxylcholesterol in cell extracts by GC-MS. Cultures were treated with formulations of lanosterol or control lipids (cholesterol or PC). Cells were then washed and extracted for lipid analysis, which revealed two key findings: (1) a surprising capacity of the cells to accumulate lanosterol (Fig 11A, 11B); (2) among the precursors measured, lanosterol was the only metabolite that was significantly increased under any of the three treatment regimes.

It should be noted that in these experiments the postnatal dopaminergic neurons were grown in direct contact with glia cells. Thus, we cannot rule out the possibility that astrocytes rather than neurons took up lanosterol and mediate neuroprotection. To address this, we repeated the experiment with hippocampal neurons (rather than mid-brain derived neurons which are mixed cultures with approximately 30% dopaminergic neurons) cultured according to Banker's method (Kaech and Banker, 2006), which allows physical separation and extraction of individual cell types. We found that lanosterol levels increased in both neurons and astrocytes to a similar extent upon treatment with exogenous lanosterol (Fig 11C, 11D). While we cannot rule out a contribution of astrocytes in lanosterol-mediated neuroprotection, our result indicate that lanosterol levels are significantly elevated in neurons upon treatment, consistent with a direct role of lanosterol in promoting survival of dopaminergic neurons.

*Figure 11: Addition of lanosterol results in accumulation of lanosterol in both neurons and astrocytes*
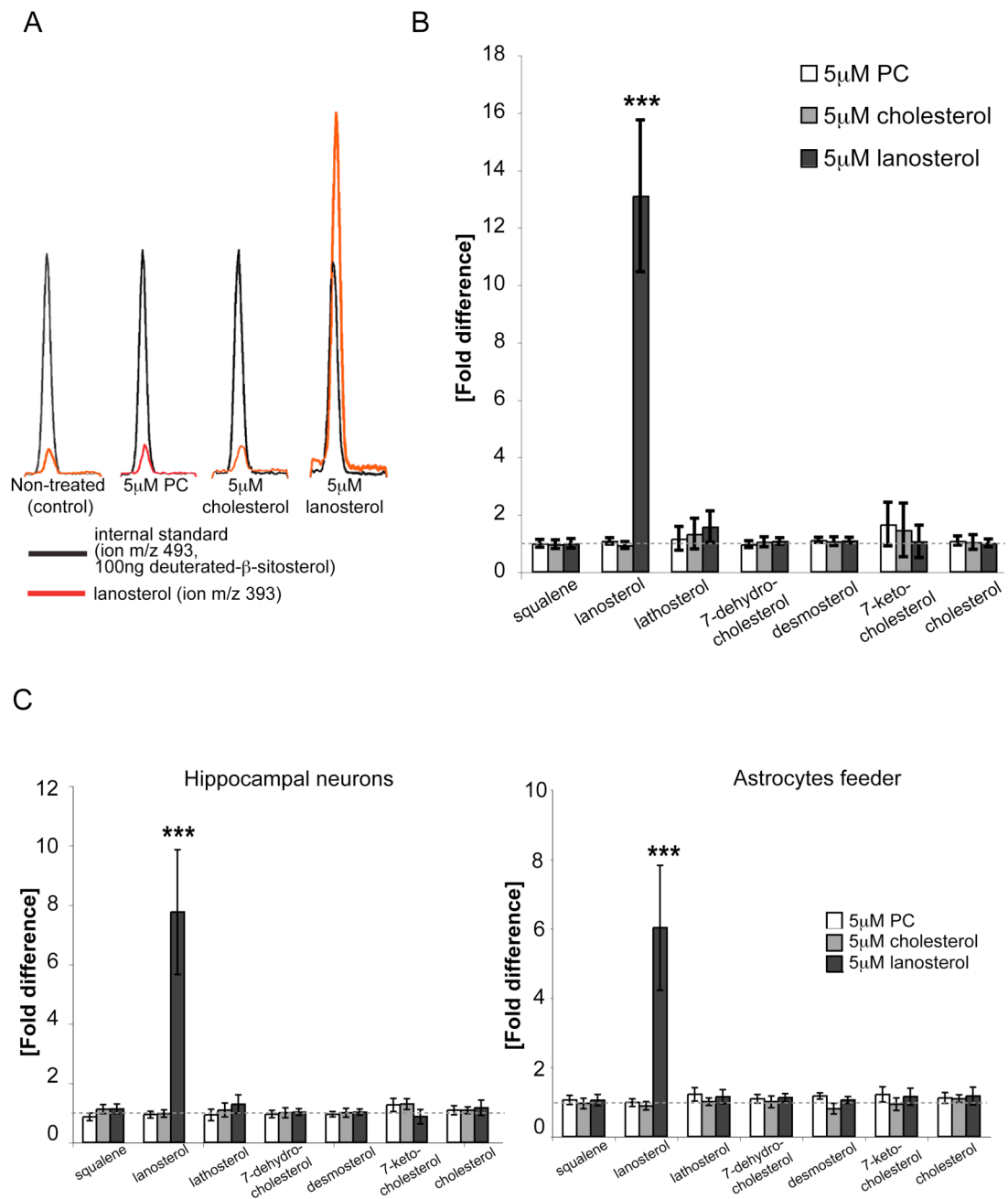


Figure 11: (A) GC-MS profiles of lanosterol ( m/z 393, red) and internal standard, deuterated ß-sitosterol, (m/z 493, black) of ventral midbrain cultures incubated (24h) with various lipid treatments. (B) Graphical representation of cellular levels of sterol intermediates with various treatments normalized to control (no treatment conditions) in ventral midbrain mixed cultures, (C) neurons only (right) and astrocytes only (left) in "Banker" style hippocampal cultures. Error bars represent SEM from 3 independent experiments. ***p-value <0.001 between lanosterol treated and control was calculated by Mann Whitney U test.

Since the addition of lanosterol causes an increase in lanosterol (Fig 10), this could in turn result in the increase of CoQ as the endogenous isoprene could be converted to ubiquinone instead of sterols. CoQ have been shown to improve survival of dopaminergic neurons in MPTP animal model and to benefit some PD patients in clinical trials (Beal et al., 1998; Cleren et al., 2008; Muller et al., 2003; Shults et al., 2002; Spindler et al., 2009). Therefore, it is possible that neurons with increased lanosterol could have altered CoQ levels. In mammalian cells, Q9 is the most abundant. Using LC/MS, Q9, along with two other lower abundant species of CoQ, corresponding to Q8 and Q10, were measured in hippocampal neurons treated PC, cholesterol, or lanosterol. However, there were no significant changes in all 3 species upon lanosterol treatment (Fig 12). It is thus unlikely that the survival effect seen by lanosterol addition is due to changes in ubiquinone levels.

*Figure 12: Addition of sterols does not change ubiquinone levels.*
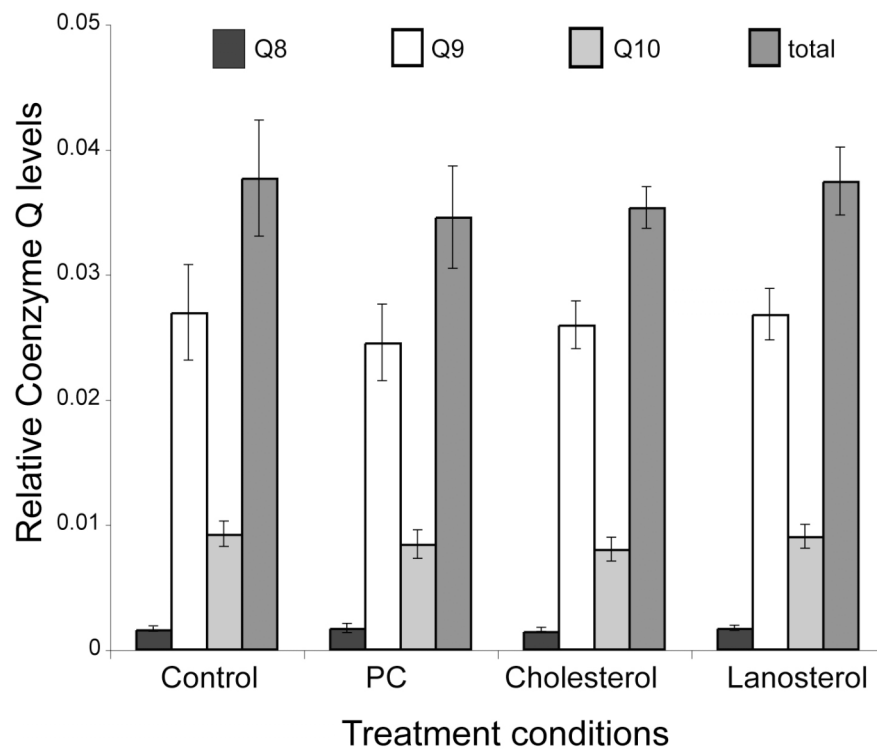


Figure 12: Coenzyme Q (CoQ) levels in neurons normalized to total cholesterol in cultures in various treatment conditions. Error bars represent SEM over 4 independent experiments.

**Chapter 4: Immunoblot and immunofluoresence analyses of surivival pathways**

*Introduction: Rational for assaying levels of SREBP2, Gsk-3β, p35/cdk5, and LSS*

In order to elucidate the mechanisms by which lanosterol may act as a survival factor, I probed a few pathways that have been shown in neuroprotection based upon the literature by immunoblot. For example, previous studies have shown that activation of the Sterol Regulatory Element Binding Protein 2 (SREBP2) is involved in exacerbating neuronal degeneration (Fernandez et al., 2009) and inhibition of SREBP2 attenuate cell death (Luthi-Carter et al., 2010). The GSK-3β pathway has been implicated in both Parkinson's and Alzheimer's disease, and inhibition of phosphorylation of ser9 in Gsk-3β appears to have beneficial effects (see recent review (Garcia-Gorostiaga et al., 2009). Based upon data in this thesis, the addition of lanosterol can induce neurite outgrowth and increase expression of p35 (chapter 2, Fig 9C). Thus, it is possible that p35/cdk5 could be a mechanism of neuroprotection. In addition, since I observed a reduction in lanosterol levels (chapter 1, Fig 6) in MPTP animal, it is likely that MPP+ results in mis-regulation of lanosterol synthase (LSS), the rate-limiting enzyme in lanosterol synthesis (Mori et al., 2007).

*Material and Methods:*

***Western blot analyses***

Ventral midbrain cultured cells were washed three times with PBS. Cells were lysed in 100 μL of RIPA buffer (50 mM Tris-HCl, pH 7.4, 1% NP-40, 0.25% Na-deoxycholate, 150 mM NaCl, 1 mM EDTA), supplemented with a cocktail of protease inhibitors (Complete Mini-EDTA inhibitors, Roche

Diagnostics). 20 μg of cell protein lysate were loaded in each well of a 10% polyacrylamide gel containing 0.1% SDS. After electrophoresis, proteins were transferred to nitrocellulose membrane and probed with the following antibodies: (i) rabbit anti-p35 (C19; 1:1000, Santa Cruz Biotechnology), (ii) rabbit anti–lanosterol synthase (1:1000, AVIA), (iii) rabbit anti–tyrosine hydroxylase (TH) (1:20,000, Covance), (iv) rabbit anti-SREBP2 (1:1000, Abcam), (v) rabbit anti-calnexin (1:2000, Abcam), (vi) rabbit anti-VDAC/porin (1:2000, Abcam), (vii) rabbit anti-pGSK-3$\alpha$/$\beta$ (ser21/9) 1:1000, Cell Signaling). Peroxidase-conjugated anti-rabbit or anti-mouse secondary antibodies (1:10,000) were purchased from Bio-Rad. Immunoblots were visualized with ECL reagent from Pierce Thermoscientific.

### *Confocal microscopy and co-localization studies*

Ventral midbrain cultures in control and MPP+ treated cells were stained with rabbit anti-LSS (1:100), monoclonal mouse anti-TOMM20 (1:1000, Abcam) or monoclonal mouse anti-KDEL (1:1500, Abcam), and sheep anti-TH (1:500, Abcam). The secondary antibodies, goat anti-mouse Alexa-fluor 555, goat anti-rabbit Alexa-fluor 488, and donkey anti-sheep Alexa-fluor 633, were obtained from Invitrogen. Cells were imaged with a laser-scanning confocal microscope (LSM510, Carl Zeiss) with excitation and emission filters meeting the secondary Alexa-fluor antibody dye specifications. Images were taken using a 63X objective. To quantify co-localization, we plotted the pixel intensities of LSS versus (vs) KDEL or TOMM20 from regions of interest (ROIs) drawn around single neurons (either TH positive or negative), and calculated the linear regression coefficient, $R^2$, for 16-22 individual ROI/neuron.

*Results: Lanosterol effects on various signaling pathways*

To explore the mechanisms underlying lanosterol-mediated neuroprotection, we investigated the effects of MPP+ and lanosterol on various signaling pathways previously implicated in cellular metabolism and neurodegeneration. First, we examined the expression level of sterol response element binding protein (SREBP2, Fig 13A), a transcription factor reported to exacerbate neuronal degeneration (Fernandez et al., 2009). We found that MPP+ induced a modest increase in SREBP2 levels, which was not rescued by lanosterol addition (Figure 13A, top panel). We also checked for levels of p35, the activator of cdk5, since the genetic ablation of p35/cdk5 confers neuroprotection in the MPTP model (Neystat et al., 2001). While we observed a decrease in p35 levels in MPP+-treated cells, addition of lanosterol did not restore p35 expression to control levels (Figure 13A, 2nd panel from top). Consistent with previous findings implicating Gsk-3β Ser9 phosphorylation in PD pathogenesis (Garcia-Gorostiaga et al., 2009), we found an increase of phospho-Gsk-3β levels in MPP+-treated cells. However, this increase was not affected by the addition of lanosterol (Figure 13A, 3rd panel from top).

Finally, we examined the levels of lanosterol synthase (LSS), the enzyme that catalyzes cyclization of oxidosqualene, the rate limiting step in lanosterol synthesis (Mori et al., 2007). The levels of LSS did not markedly change upon MPP+ addition (Figure 13A, 4th panel from top). Interestingly, however, we observed a different localization pattern of LSS in MPP+-treated dopaminergic neurons. LSS immunostaining appeared much more punctate after MPP+ treatment (Figure 13B), suggesting that drug-induced redistribution of LSS and lanosterol to a different intracellular compartment.

We thus proceeded to examine the subcellular localization of LSS in control

and MPP+ treated dopaminergic neurons.

*Figure 13: Analyses of SREBP2, Gsk-3β, p35/cdk5, and LSS in ventral midbrain treated with lipids and MPP+*
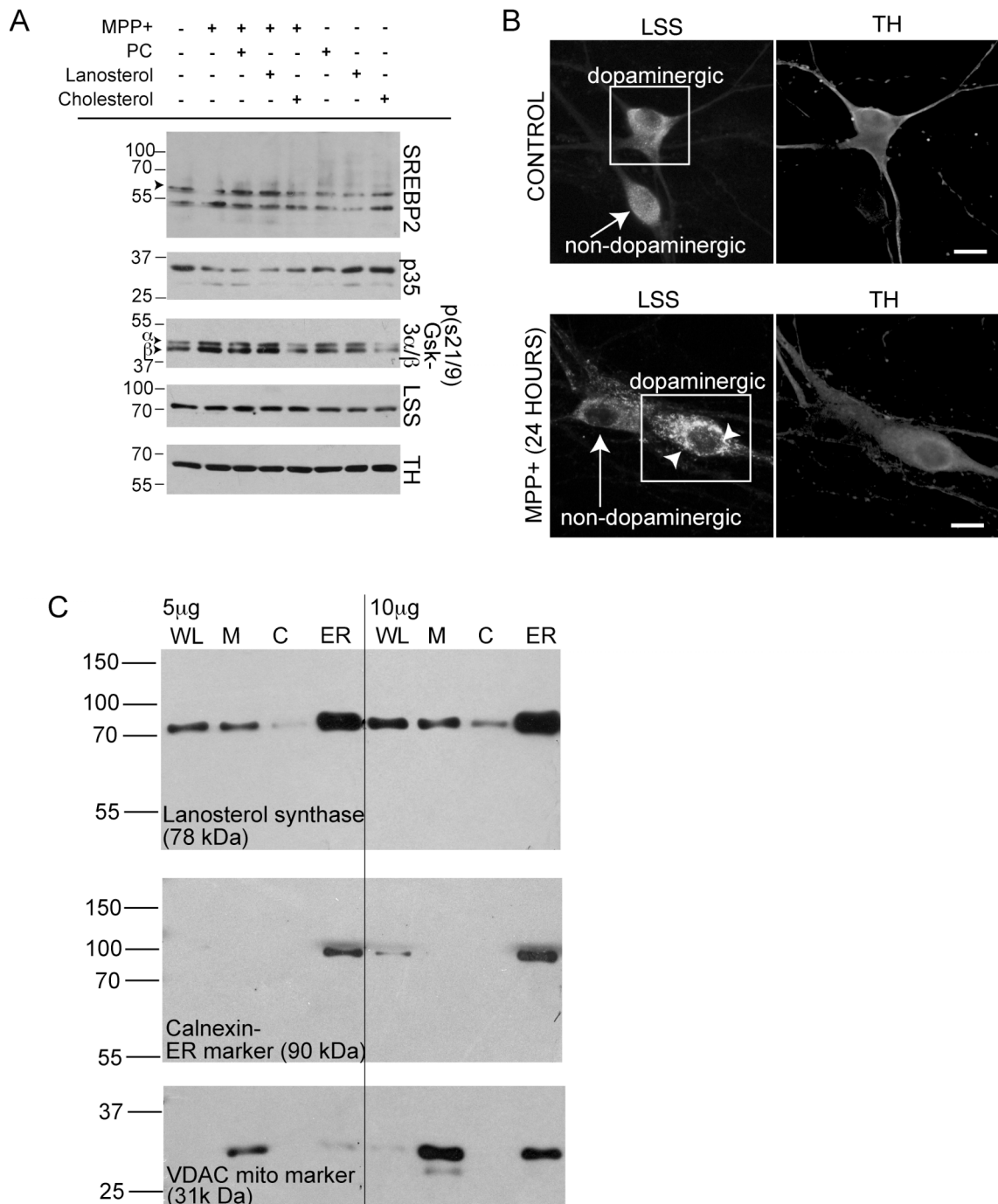


Figure 13: (A) Immunoblot analyses of several factors previously linked to neuroprotection in Parkinson's disease and/or MPTP treatment. (B) Immunofluorescence images of ventral midbrain neurons stained with LSS and TH, treated with or without MPP+. LSS appears more punctate in TH+ neurons upon MPP+ treatment. Scale bar represents 10 μm. (C) Subcellular fractionation of liver tissue. Mitochondrial – M, microsome/ER – ER, and cytosolic – C, fractions were purified from whole liver – WL. Immunoblot of calnexin (ER maker) and VDAC/porin (mitochondrial marker) were used to assess the purity of each fraction. LSS showed a clean single band at the expected weight of 78 kDa and is enriched in the ER fraction. A small amount of LSS is also detected in the mitochondrial fraction.

As reported by several groups, mammalian LSS is localized to the microsomal fraction (Bloch et al., 1957; Tchen and Bloch, 1957; Yamamoto and Bloch, 1969; Yamamoto et al., 1969). Rodent LSS has been purified, and the detected molecular weight is 78 kDa (Kusano et al., 1991). Crystal structure of human LSS reveals a putative membrane insertion domain in the ER (Thoma et al., 2004). By subcellular fractionation of whole rat liver tissues, we isolated mitochondria, microsomes, and cytosolic protein lysates and showed that the endogenous localization of LSS is enriched in the microsomal fraction (Fig 13C), consistent with the literature. However, I could also detect small amounts of LSS in the mitochondrial fraction (Fig 13C). This does not appear to be residual microsomal contamination in the mitochondria fraction because in the lanes loaded with 5 and 10 µg of mitochondrial protein, I do not detect the ER marker, calnexin (Fig 13C).

Consistent with our biochemical fractionation data, we found that LSS co-localized with an ER marker (KDEL) in both dopaminergic and non-dopaminergic neurons (Figure 14A). Extensive overlap between LSS and the ER marker was observed for both dopaminergic and non-dopaminergic neurons ($R^2$ = 0.83 ± 0.01 and 0.84 ± 0.01 respectively). Less overlap was found between LSS and TOMM20 (a mitochondrial marker) for both dopaminergic and non-dopaminergic neurons ($R^2$ = 0.70 ± 0.02 and 0.69 ± 0.02 respectively, Fig 14A, 2nd panel from the top). This pattern changed noticeably in dopaminergic neurons treated with MPP+. The co-localization of LSS with TOMM20 was markedly increased ($R^2$ = 0.856 ± 0.01, Fig 14A, bottom last panel), with concomitant reduction in the overlap of LSS with KDEL ($R^2$ = 0.69 ± 0.02, Fig 14A, 2nd panel from the bottom). Translocation

of LSS from the ER to mitochondria was also observed in dopaminergic neurons co-treated with MPP+ and lanosterol (Fig 14B). MPP+ did not, however, affect LSS localization in non-dopaminergic neurons (Fig 13B, 14B), consistent with the inability of these cells to take up MPP+. These data indicate that a significant fraction of LSS redistributes from the ER to mitochondria in dopaminergic neurons exposed to MPP+, suggesting that LSS (and its product lanosterol) may have a role in regulating mitochondrial function.

In addition, the translocation of LSS in dopaminergic neurons under toxic insult is also seen in mouse embryonic fibroblast (MEF) under serum starvation. As shown (Fig 15), LSS in MEF grown in normal 10% serum conditions co-localizes with the ER marker, KDEL (Fig 15A). After serum starvation for 12-16 hours, LSS localizes to the mitochondria, recapitulating the effects seen in dopaminergic neurons with MPP+ (Fig 14). We thus believe that the mitochondrial pools of LSS might have specific functions in connecting sterol metabolism to compromise cellular energetic.

*Figure 14: Lanosterol synthase (LSS) is redistributed from ER to mitochondria in dopaminergic neurons upon addition of MPP+.*
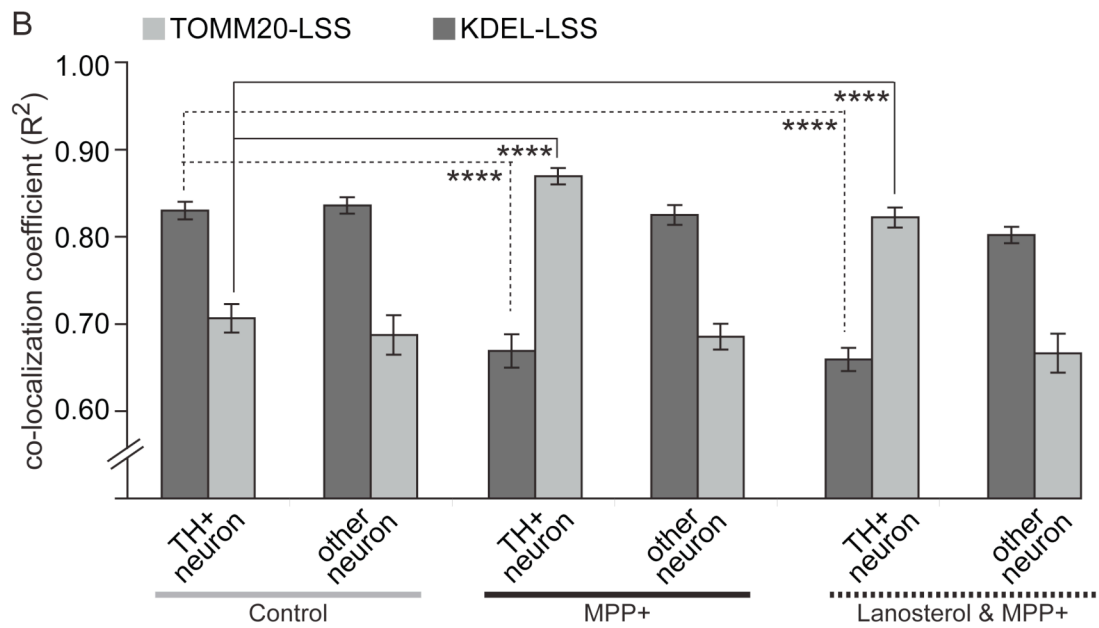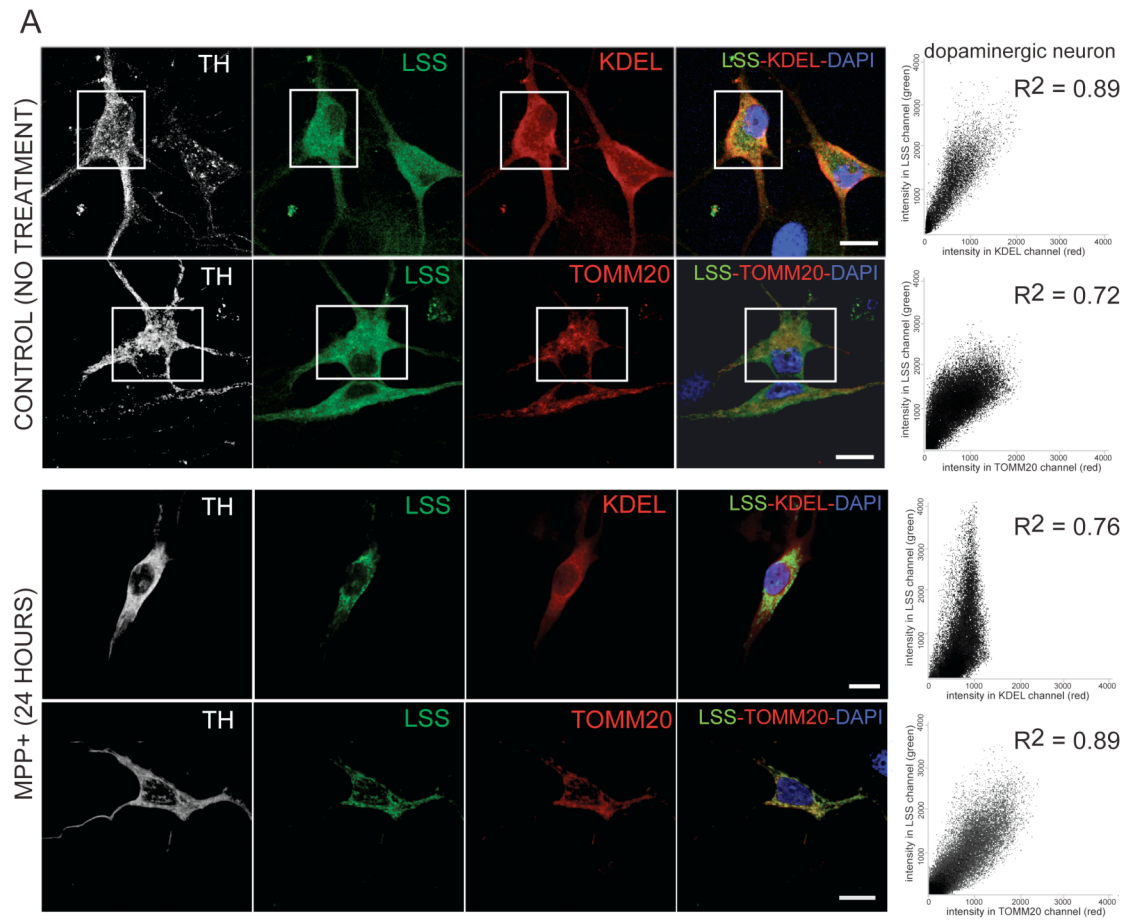
Figure 14: (A) Confocal images of ventral midbrain neurons stained with TH (white), LSS (green), either KDEL (red, 1st and 3rd panels from the top) or TOMM20 (red, 2nd and 4th panels from the top) in either control or with MPP+. White boxes show dopaminergic neurons as determined by TH+ staining. Right panels show pixel intensity correlation plots of LSS with either KDEL or TOMM20 in dopaminergic neurons. Scale bar represents 10 µm. (B) Average $R^2$ values (a measure of co-localization) of two classes of neurons in control and MPP+ treated conditions. In control, $R^2$ values from co-staining of KDEL-LSS, n = 26 and n = 27, TOMM20-LSS, n = 20 and n = 21, were assessed for dopaminergic and non-dopaminergic neurons respectively. In MPP+-treated cells, R2 values from co-staining of KDEL-LSS, n = 20 and n = 20, for TOMM20-LSS, n = 18 and n = 17, were assessed for dopaminergic and non-dopaminergic neurons respectively. In MPP+/lanosterol co-treated cells, R2 values from co-staining of KDEL-LSS, n = 18 and n = 23, for TOMM20-LSS, n = 19 and n = 18, were assessed for dopaminergic and non-dopaminergic neurons respectively. ****p < 0.00001 between control and MPP+ were calculated by two-tailed Student's t-test.

*Figure 15: LSS in MEF redistributes from ER to mitochondria upon serum starvation*

A. MEF cells with 10% serum
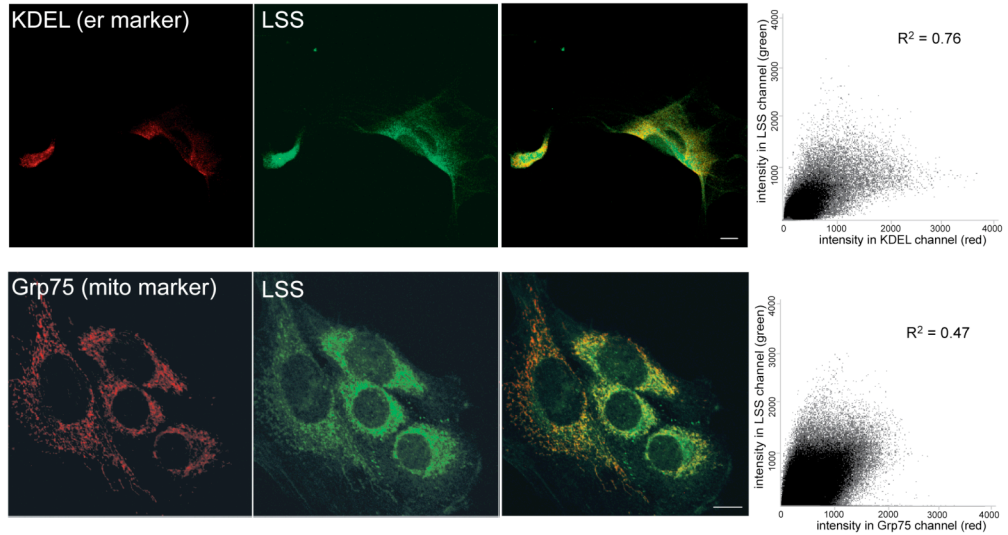


B. MEF cells serum starved overnight
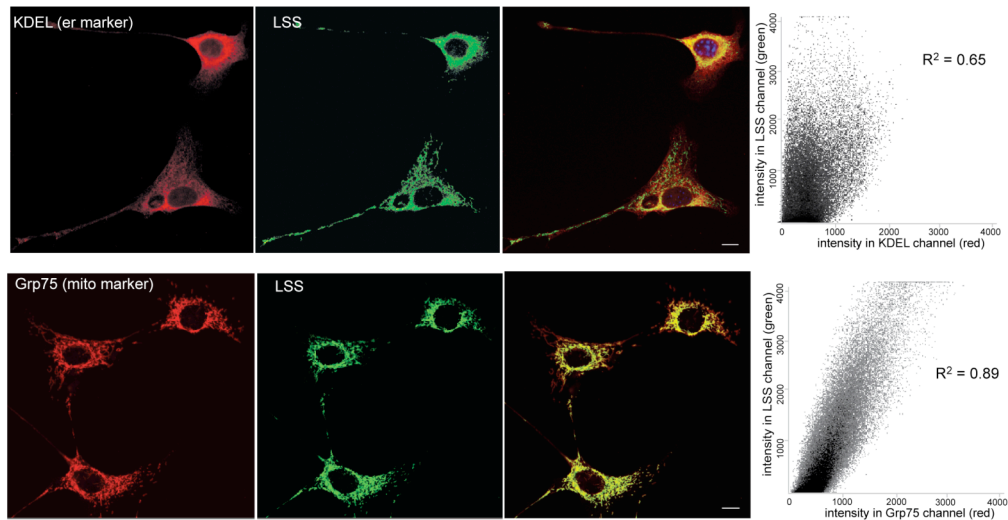


Figure 15: MEF grown in (A) Control – 10% serum or (B) serum starved for 12-16 hours were stained with LSS and ER-marker, KDEL, or mitochondrial marker, Grp75. Intensity of LSS versus KDEL or Grp75 were plotted on cross-correlation plots with linear regression fit ($R^2$) values. LSS in MEF grown in serum co-localizes with KDEL but upon serum starvation, LSS co-localizes with Grp75. Scale bar represent 10 µm.

There are a number of interpretations to the striking redistribution of LSS from ER to mitochondria in dopaminergic neurons upon MPP+ treatment. First, the enzyme is mis-localized and the mitochondrial form of LSS is non-functional. However, recently, lipidomic analysis of macrophages during stimulation with LipidA (a condition which can be expected to lead to oxidative bursts similar to MPP+ induced ROS stress) shows that generation of lanosterol is a pronounced response in several cellular compartments including mitochondria (Andreyev et al., 2010). Therefore, it is likely that mito-LSS is functional.

A second explanation is that LSS is re-organized as an immediate response to the MPP+ and that mito-LSS and ER-LSS have distinct roles. In ER, LSS generates lanosterol which will be further metabolized to cholesterol by the cholesterol synthetic machinery resident in that organelle. In mitochondria, the lanosterol might serve other purposes, as a mediator for mitochondrtial function or precursor of an unknown metabolite/membrane structure. Thus, lanosterol might be required in heightened amounts under such conditions, which in part could explain its lowered levels in mice after prolonged exposure to MPTP (chapter 1, Fig 6). Mitochondria are increasingly believed to be involved in autophagic responses to various extents (Hailey et al., 2010).  ER-mitochondrial connections could provide lipid for autophagic membrane formation (Hailey et al., 2010). This reasoning would argue for a more general relevance of our observations. Indeed, re-localization of LSS from ER to mitochondria is not limited to MPP+ stressed dopaminergic neurons. I observed similar re-localization in serum-starved fibroblast (Fig 15), again consistent with induction of the autophagic cell response.

Third, re-distribution of enzymes is commonly seen in cells during stress. For example, examination of > 800 yeast strains expressing various GFP coupled proteins revealed altered locations of certain proteins upon stress response (Narayanaswamy et al., 2009). The authors noted that these proteins are usually involved in intermediary metabolism. Movement of proteins or metabolites from ER to mitochondria is an important stress response, and impaired functions have been implicated in some neurodegenerative diseases. For example, Mitofusin-2, a protein that mediates ER-Mito trafficking, causes the inherited motor neuropathy disorder, Charcot-Marie-Tooth type IIa (de Brito and Scorrano, 2008). Disruption of mitofusion-2 dramatically impaired starvation-induced autophagy (Hailey et al., 2010). Two genes involved in familial PD, PINK1 and Parkin, accumulate and redistribute respectively to mitochondria upon mitochondrial uncoupling (Narendra et al., 2008), which is important for mitophagy (Geisler et al., 2010a). Importantly, translocation of Parkin to mitochondria has etiological significance as a number of pathologically associated Parkin mutants fail to translocate (Matsuda et al., 2010; Okatsu et al., 2010).

Taken together, if one were to assume that the translocation of LSS to the mitochondria has important function, it is likely that lanosterol has roles in regulating mitochondria physiology. To determine the roles of lanosterol in mitochondria and how lanosterol could be neuroprotective, we used a live-cell imaging approach to assess mitochondria function (Chapter 5).

## Chapter 5: Elucidating the mechanism of lanosterol's neuroprotection on dopaminergic neurons by imaging techniques.

*Introduction: Mitochondrial membrane potential and JC-1 dye*

One aspect of mitochondrial physiology can be assessed by measuring changes in mitochondrial membrane potential, $\Delta\Psi$. Mitochondrial membrane potential is a measurement of both electrical and chemical gradient which drive hydrogen ions across the inner membrane during the process of electron transport and oxidative phosphorylation, the mechanism behind ATP production. In the cell, this process is never completely coupled, allowing electron to be transported without ATP production. If, as we observed, LSS localization can be altered from ER to mitochondria upon toxin insult in neurons by MPP+, it is reasonable to expect that lanosterol could be of importance to mitochondrial function.

In neurons, induction of such "mild" uncoupling by lipids, such as CoQ, or proteins such as uncoupling proteins, UCPs, or brief exposure to artificial uncoupler such as FCCP (carbonyl-cyanide-4-(trifluoromethoxy)-phenylhydrazone) have been shown to be neuroprotective (Andrews et al., 2005; Conti et al., 2005; Horvath et al., 2003; Mattiasson et al., 2003; Stout et al., 1998). If "mild" uncoupling were to occur upon lanosterol addition, the measurement of $\Delta\Psi$ would decrease and this could be a mechanism of neuroprotection. Futhermore, alteration in mitochondrial membrane potential in mammalian cells can cause PINK1's recruitment of Parkin. And since PD-associated Parkin mutations cause a decrease in mitophagy in (Geisler et al., 2010b), we thus asked if lanosterol could also mediate autophagosome formation in dopaminergic neurons.

To investigate whether $\Delta\Psi$ is altered in neurons upon addition of lanosterol, we employed the lipophilic cationic dye, JC-1. The dye can be loaded in live cells and selectively enters into mitochondria. In cells with high membrane potential, the dye would form aggregates, resulting in a red shift in emission spectrum. However, in cells with low potential, the dye will be in monomeric structure and emits in green. Using, the change in red/green ratio, we can assess the change in mitochondrial membrane potential.

In this final chapter, I first set up the live-imaging assay in neurons to measure changes in mitochondrial membrane potential. Upon validating this assay with known uncouplers, I tested the effects of various lipids. Since mitochondria uncoupling has been associated with mitophagy, I also determined if lanosterol has a role in autophagy. Using LC3 as a marker for autophagy, I quantified both the size and number of autophagic vacuoles (AVs) in primary ventral midbrain neurons upon MPP+/lanosterol treatment.

*Materials and Method: Assessing mitochondrial membrane potential and autophagy*

**Live-cell confocal imaging and measurement of mitochondrial membrane potential**

Mitochondrial membrane potential was assessed using 5,5',6,6'-tetrachloro-1,1',3,3'-tetraethylbenzimidazolocarbocyanine iodide (JC-1) as described (White and Reynolds, 1996) with slight modifications. All live-imaging experiments were conducted in cell medium, (37°C & 5% $CO_2$) with a spinning disk confocal microscope, equipped with a Cool SNAP HQ2 CCD camera (Photometrics), a fully automated stage and built in autofocusing system (PFS, Nikon), and driven by Metamorph 7.6 (Universal Imaging). JC-1 is excited at 488-nm, and its fluorescence emission was collected at 530 ± 10

nm (green) and 590 ± 17 nm (red), corresponding to peak fluorescence from the monomer and aggregate signals, respectively. Mitochondrial membrane potential was measured by taking the red to green emission ratio.

For ventral midbrain cultures (DIV7), cells were seeded at 50 cells/mm$^2$ in a glass-bottom labtek well. Cells were loaded with 1 μg/ml JC-1 (Invitrogen) in culture medium, and were incubated for 30 min at 37°C, washed twice with HBSS, and imaged in conditioned culture medium. Multi-position time-lapse imaging of 10-15 randomly chosen fields was performed at 2-minute intervals over 40 minutes. At the end of the experiment, ventral midbrain cells were fixed on stage for 20 minutes with 4% PFA and stained for TH with a secondary antibody coupled to Alexafluro-568 (red) and DAPI. The retrospective staining of TH allowed for the identification of dopaminergic neurons, which were the only ones included in the analyses. Hippocampal cultures were plated at a higher density (300cells/mm$^2$), and multi-position time-lapse imaging of 3-4 fields was performed at 30-seconds intervals for 20 minutes.

For both types of cultures, the intensity of the JC-1 red-to-green ratio was measured in each frame, and the change in mitochondrial membrane potential was plotted as $\Delta f/f_0$, where $f_0$ is the average JC-1 red-to-green ratio over the first 10 frames before treatment. Decay curves were fitted to a mono-exponential function, $y = x_0 e^{-t/\tau}$, using IGOR Pro 6.1.

### *ATP extraction and measurement*

Two to three million hippocampal neurons were cultured for seven days and treated with various types of liposome (PC, Cholesterol, and lanosterol) for 24 hours. For each independent experiment, 2 technical

replicates were performed. Cells were washed three times with ice-cold PBS, then placed immediately with 200 μL of ice-cold 10% trichloroacetic acid (TCA) and kept on ice for 15 minutes. TCA supernatant were kept in -80°C for 1 week before measurement of ATP by luciferase assay. ATP Bioluminesence Assay Kit (Roche) was used to determine concentration of ATP.

### Quantification of autophagosome vacuoles (AV)

Ventral midbrain cultures plated on 12-mm coverslips were treated for 24 h with 10 μM MPP+ with or without 5 μM PC, 5 μM cholesterol, or 5 μM lanosterol. Cells were washed three times with PBS, then fixed with 4% paraformaldehyde for 20 min and permeabilized with 100μg/ml of digitonin for 10 minutes. Following permeabilization, cells were washed 3 times with PBS and stained with anti-TH (secondary: Alexa-fluor 488, green) and anti-LC3 (1:100, mouse monoclonal, MBL cat no: 152-3A, secondary: Alexa-fluor 555, red). To quantify AV in dopaminergic neurons, TH+ cell soma were imaged with a laser-scanning confocal microscope (LSM510, Carl Zeiss) with excitation and emission filters meeting the secondary Alexa-fluor antibody dye specifications. Images were taken using a 63X objective with the same laser power and gain. The 12-bit images were quantified using ImageJ (analyze particle drop-in). For each image, detected LC3 puncta were intensity thresholded (<1000) and gated for size (<15 pixel). For each condition, 40-60 TH+ cells were assessed from three independent experiments.

As a positive control for our method of evaluating AV, mouse embryonic fibroblast (MEFs) grown in serum or serum deprived were stained with LC3 and quantified according to the same parameters. As expected and

shown below (Fig 16), there is approximately a 25-fold increase in AV upon serum starvation.

### *Quantification of mitophagy in axons*

E18.5 hippocampal neurons were electroporated using the Amaxa poration system (Lonza) with MitoRed construct (Clonetech, cat no: PT-3633-5). Cells were then plated in microfluidic chambers (Xona microfluidics), which allowed for physical separation of axons and cell somas. At DIV7, neurons were treated with 5 µM PC, 5 µM cholesterol, 5 µM lanosterol, or 200 nM of rapamycin (positive control) for 24 hours. Cells were then fixed with 4% paraformaldehyde for 20 min and permeabilized with 100µg/ml of digitonin for 10 minutes. Following permeabilization, cells were washed 3 times with PBS, and stained with anti-LC3 (secondary: Alexa-fluor 488, green). To quantify mitophagy, the percentage of MitoRed and LC3 positive mitochondria were plotted as a percentage to total MitoRed positive mitochondria using the Metamorph 7.6 colocalization drop-in. For each condition, images of 40-50 axons were taken from three independent experiments.

*Figure 16: Endogenous detection of LC3 in MEFs*

A

MEF- control endogenous LC3          4 hours serum starvation



B
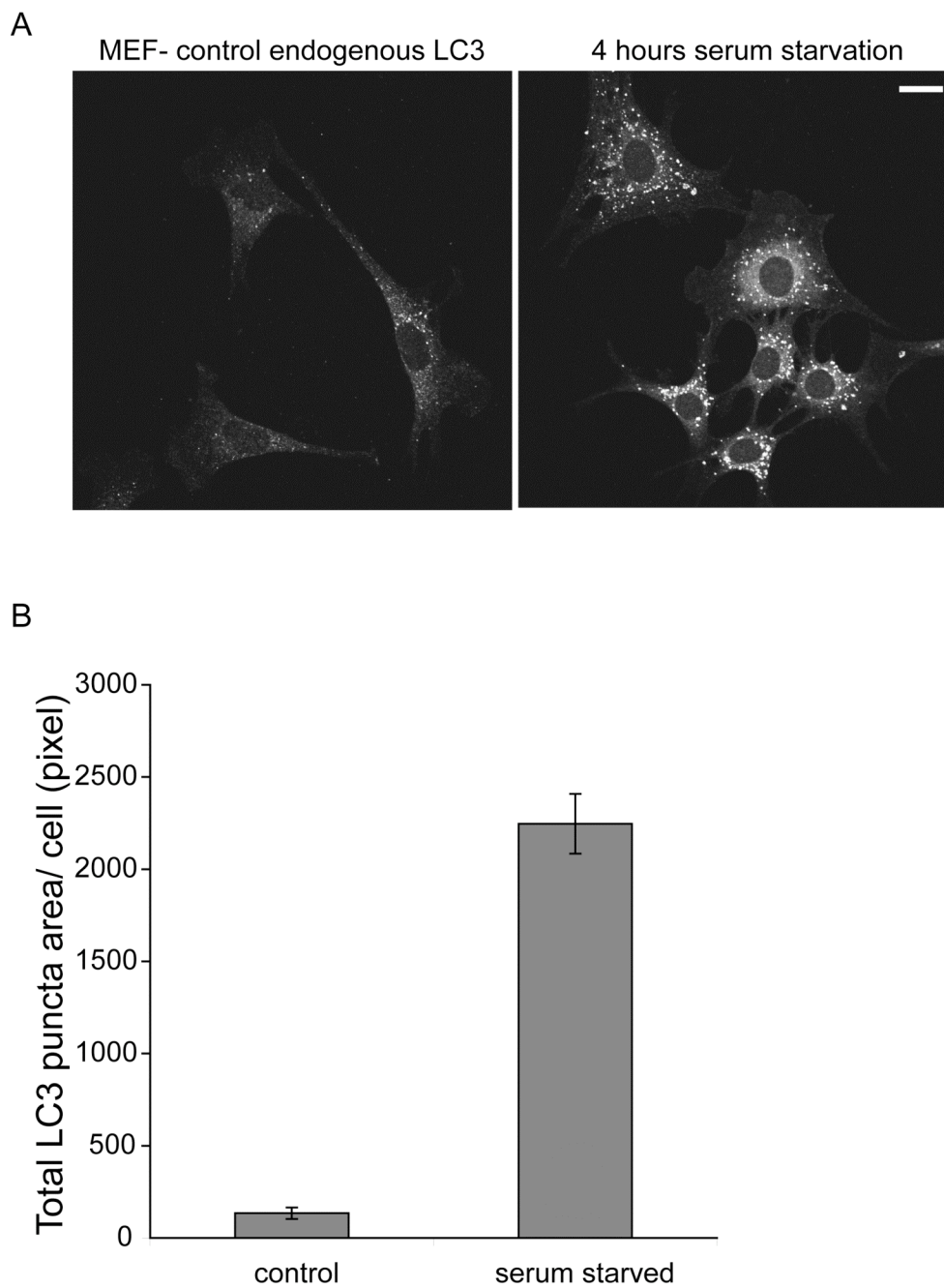


Figure 16: (A) Confocal images of mouse embryonic fibroblast (MEF) stained with LC3. Left panel corresponds to cells grown in 10% FBS, right panel corresponds to cells serum starved for 4 hours. Scale bar represents 10 μm. (B) Quantification of autophagosome vacuoles total area (size * number of AV) of n > 20 MEFs from 3 independent experiments. Error bars represent SEM.

*Results: Live-imaging analysis of neuronal mitochondrial membrane potential*

Even though JC-1 is well-established dye in the literature, the concentration used for each cell type differs. The amount loaded in neurons was published to be 2 μg/ml. However, in our study, we found that this concentration is too high, causing most of the dye to appear in aggregate forms. The final concentration used in our study is 0.5 μg/ml. As a positive control to our live imaging assay, we treated neurons stained with JC-1 with protonophore m-chlorophenylhydrazone (CCCP), an uncoupler of mitochondrial oxidative phosphorylation (Fig 17A). As expected, treatment of neurons with 200 nM of CCCP induced a sharp and immediate drop of mitochondrial membrane potential. As shown, $\Delta\Psi$ was altered by 25% while there is no change in $\Delta\Psi$ for control, non-treated neurons (Fig 17B). Under these same experimental conditions, exogenous lanosterol reduced the $\Delta\Psi$ by ~20% over 15 min, whereas PC and cholesterol had no significant effect (Fig 18).

These experiments were repeated again in ventral midbrain cultures. As these cultures were grown at a lower density than the hippocampal culture, we were only able to image at 2 minutes per frame over 40 minutes in order to capture multiple fields. At the end of the experiments, dopaminergic neurons were identified by posteriori staining for TH. Similar to results shown in hippocamapal neurons, lanosterol induces a similar (~20%) reduction in membrane potential in dopaminergic neurons (Fig 19).

Since MPP+ uptake depends on ATP levels (Ramsay and Singer, 1986), it is possible that the addition of lanosterol causes mitochondrial depolarization, and subsequently ATP depletion. This would inhibit MPP+

uptake in the mitochondria. To determine if lanosterol alters ATP levels, we measured levels of ATP in neurons treated with PC, cholesterol, or lanosterol. We did not see any significant changes in the levels of ATP across all treatment conditions (Fig 20), indicating that lanosterol is unlikely to inhibit MPP+ uptake. Thus, one mechanism by which lanosterol could mediate neuroprotection is through the uncoupling of mitochondria.

*Figure 17: Mitochondrial membrane potential assay*
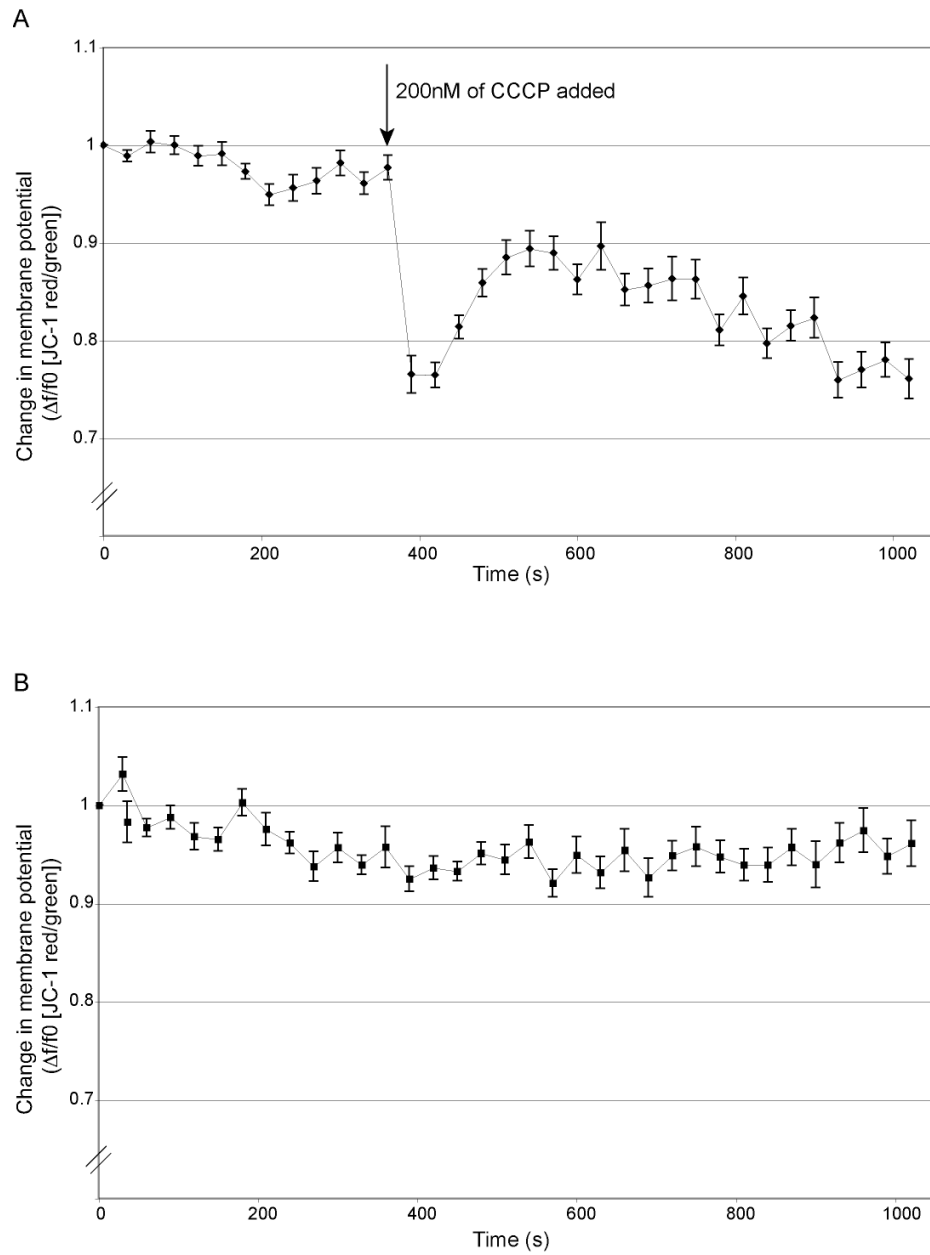


Figure 17: Graphical representations of the change in mitochondrial membrane potential versus time in (A) the positive control using 200 nM CCCP and (B) the negative control, which received no treatment. Error bars represent SEM ($n > 30$) from more than three independent experiments.

*Figure 18: Lanosterol induces mild uncoupling in neuronal mitochondria*
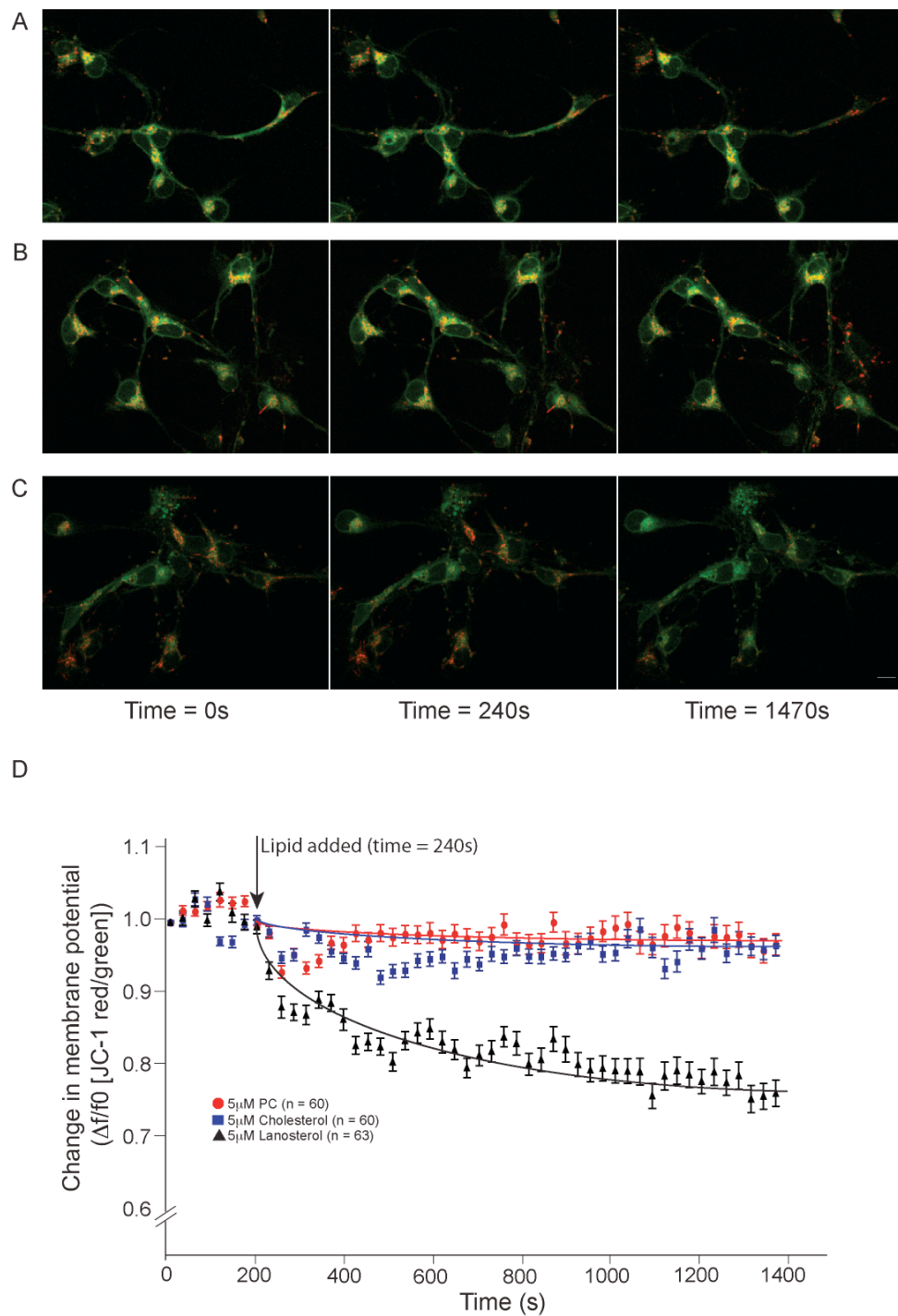


Figure 18: Live imaging of hippocampal neurons was performed after cells were loaded with JC-1. The change in mitochondrial membrane potential is measured as the ratio of intensity in the emissions channel at 594 (red) to 510 nm (green). Images shown are at the start of the experiment (time = 0 s), immediately before lipid addition (time = 240 s), and at the end of the experiment (time = 1470 s). Scale bar represents 10 μm. Neurons were treated with (A) 5 μM PC, (B) 5 μM cholesterol, or (C) 5 μM lanosterol. (D) Plot of JC-1 red to green ratio, Δf/f0, versus time for each condition.

*Figure 19: Lanosterol induces mild uncoupling of dopaminergic neurons*
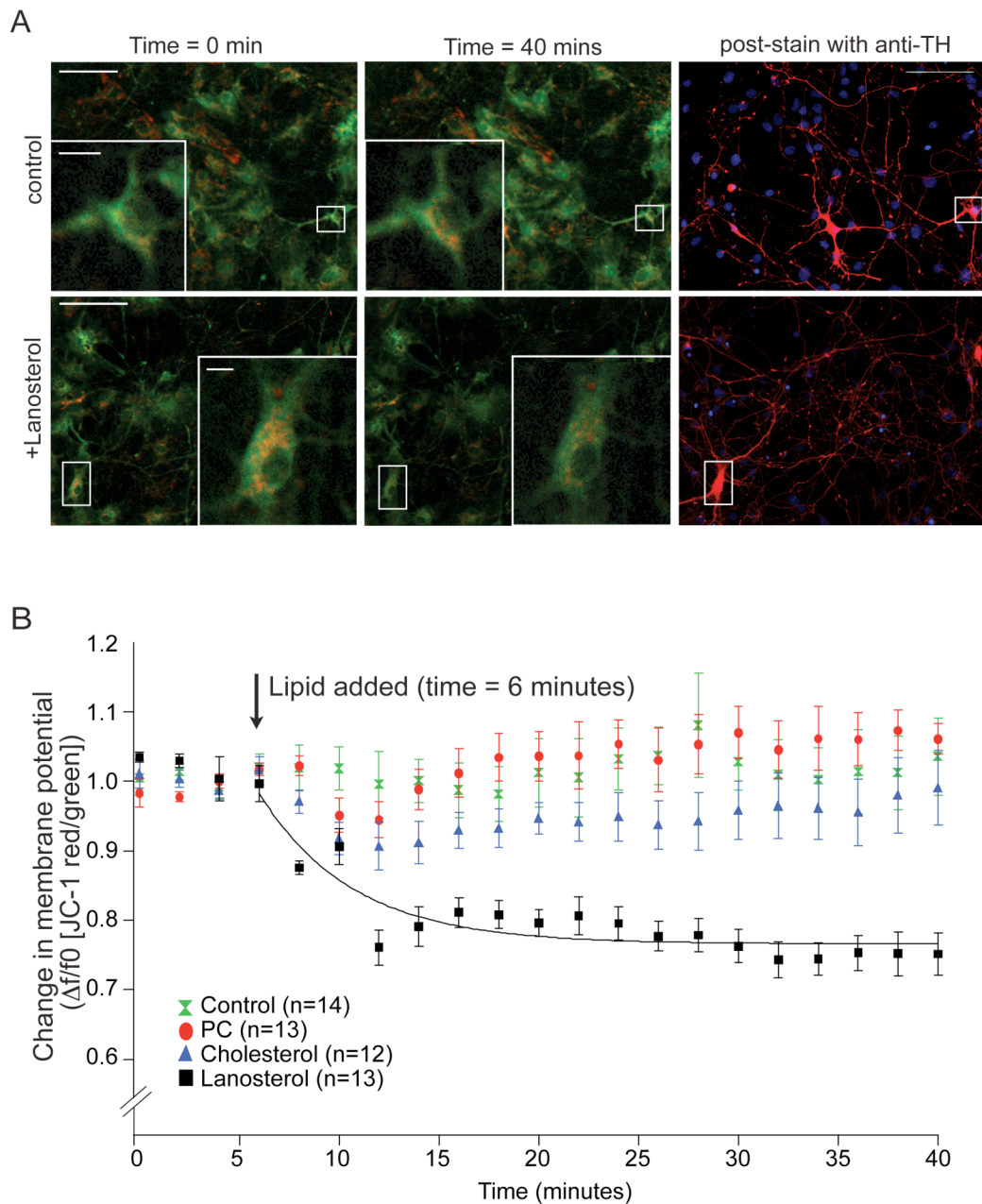


Figure 19: Live imaging of JC-1 loaded neuronal cultures. (A) Images of control and lanosterol-treated ventral midbrain cultures at the start of the experiment (time = 0 min, left panel) and the end of the experiment (time = 40 mins, middle panel). Right panels represent posteriori staining of TH for identification of dopaminergic neurons. White boxes represent magnified TH+ neurons. Scale bar represents 100 µm in main figure and 10 µm in magnified box. (B) Plot of $\Delta f/f0$ versus time for dopaminergic neurons, n > 10 for each condition from three independent experiments. In both types of cultures, lanosterol induces about 20% decrease in mitochondrial membrane potential.

*Figure 20: Analysis of ATP in hippocampal cultures treated with various lipids*

A



B
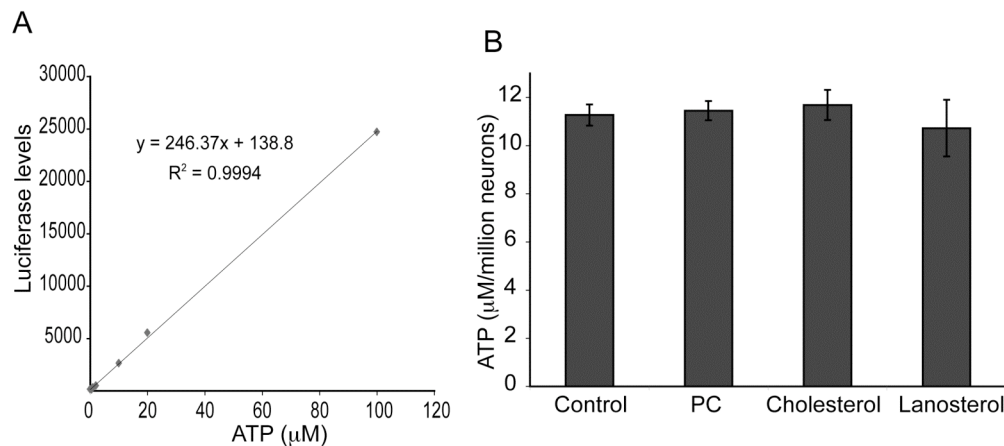


Figure 20: (A) Bio–luminescence intensities for known ATP levels were fitted to a linear equation to obtain a standard curve. (B) ATP levels measure in neurons treated with various lipids conditions showed no significant changes in all four conditions. Error bars represent SEM over three independent experiments.

### *Lanosterol increases autophagy in dopaminergic neurons.*

Previous studies have shown that the loss of mitochondrial membrane potential can initiate the autophagic degradation of damaged mitochondria (Matsuda et al., 2010; Narendra et al., 2008). Gene linked to familial forms of PD, such as PINK and Parkin are thought to regulate this process, and PD-associated Parkin mutations cause a decrease in mitophagy in mammalian cell lines (Geisler et al., 2010b). We thus asked if lanosterol mediates autophagosome formation in dopaminergic neurons. Using LC3 as a marker for autophagy, we quantified both the size and number of autophagic vacuoles (AVs) in primary ventral midbrain neurons upon MPP+/lanosterol treatment. Similar to other studies (Cherra et al., 2010), we found that addition of MPP+ in primary dopaminergic neurons increased the number of AVs by about 2.5 folds (Fig 21). There is also about a 75% increase in the average size of AVs with MPP+ treatment. Remarkably, when neurons were exposed to lanosterol

alone, we observed a similar increase in AV size and number. Co-treatment of MPP+ and lanosterol led to an additive effect on autophagy, with significant increase in both the numbers and size of AVs, compared to MPP+ or lanosterol alone (Fig 21).

Next, we addressed whether lanosterol has a specific effect on axonal mitophagy. In PD, axons of dopaminergic neurons progressively degenerate and "die back", in a process which may be accelerated by mitochondrial dysfunction and involve mitophagy. For this, we grew hippocampal neurons in microfluidic chambers to segregate axons from neuronal cell bodies and dendrites (Park et al., 2009). Mitochondria were visualized by expression of the fluorescent reporter MitoRed and neurons were immunostained for endogeneous LC3. We found a small but significant increase in co-localization of MitoRed with LC3 (Fig 22) upon lanosterol treatment, suggesting an increase of axonal mitophagy. Taken together, these results suggest that the protective effects of lanosterol are mediated by mitochondria uncoupling, and subsequent clearance of damaged mitochondria.

*Figure 21: Lanosterol and MPP+ increase the number of autophagosome vacuoles in dopaminergic neurons*
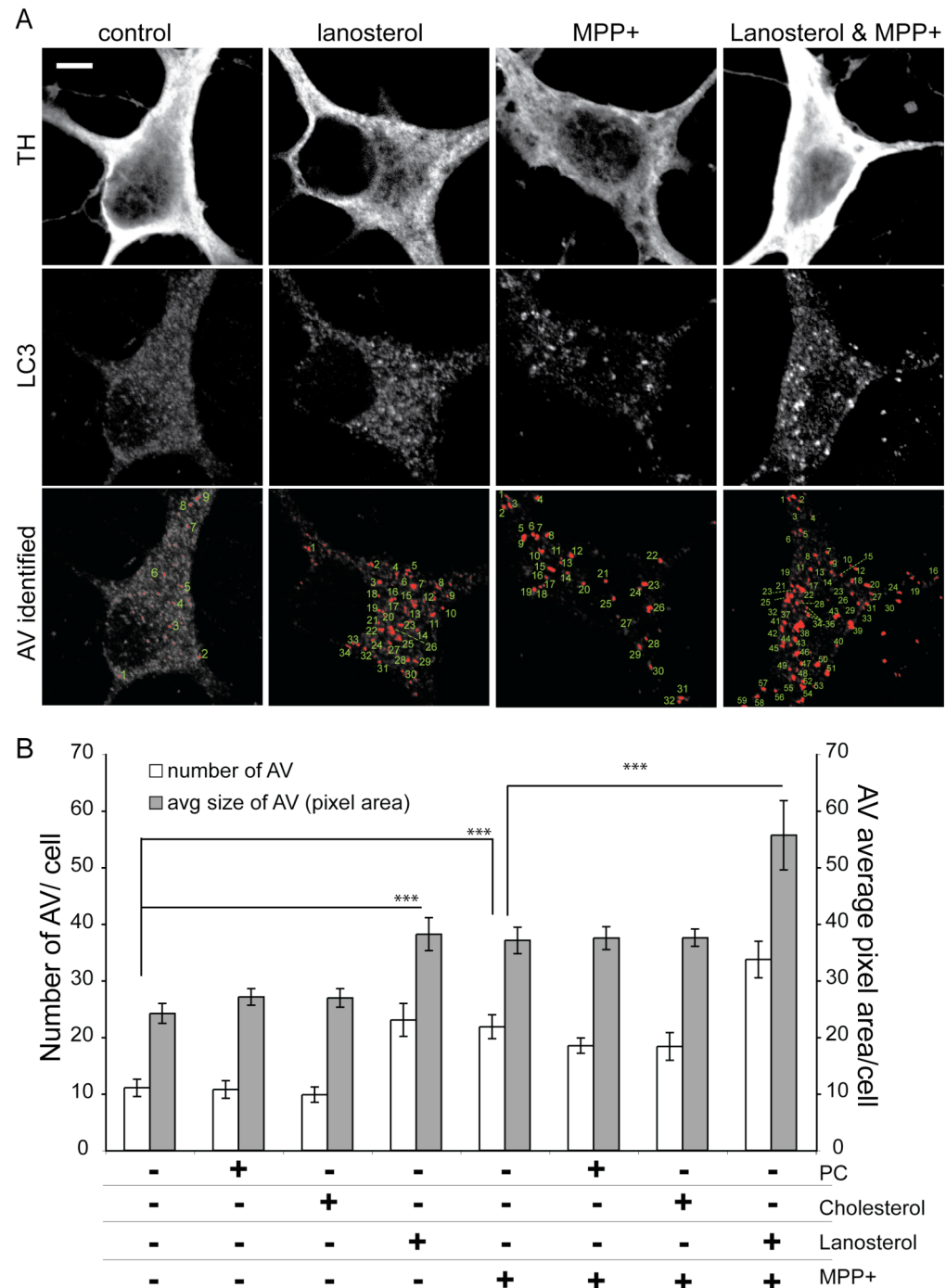


Figure 21: (A) Confocal images of ventral midbrain neurons stained with TH (top panels), LC3 (middle panels) and AV quantification (ImageJ software output, bottom panels) with various treatment conditions indicated on the top.  Scale bar represents 10 µm. (B) Graphical plot showing the average number of AV identified per TH+ cells and the average size of AV in pixel area during treatment with various lipids and MPP+ co-treatment. For each condition, n > 40 TH+ cells from 3 independent experiments. Error bars represent SEM. ***p < 0.001

*Figure 22: Lanosterol increases mitophagy in axons*



Figure 22: (A) Confocal images of hippocamal axons stained with LC3 (top panels, green) and electroporated with MitoRed (middle panels, red). Bottom panel showing overlay of LC3 and MitoRed. White arrow represents co-localization of the two channels. Scale bar represents 20 μm. (B) Graphical plot of average percentage of mitochondria with LC3 positive stains. Error bars represent SEM. For each condition, n > 40 axons were assessed from 3 independent experiments. *p < 0.05

## Conclusion and perspectives

In this thesis, I have first used an *in silico* approach to map out possible pathways that could be of importance to dopaminergic neurons. Secondly, I performed a thorough characterization of sterol metabolites in the affected brain regions of an established animal model for PD, MPTP-treated mice, and found specific and substantial reductions of lanosterol. I cannot rule out the possibility that lanosterol is oxidized or metabolized to di-hydrolanosterol or other products in MPTP treated animals because I was unable to measure these oxidized metabolites.

Other than this work, only a few other studies have biochemically addressed sterol biosynthesis and metabolism in neurons. For neurodegeneration models, in rats treated with 3-nitropropionic acid, lathosterol levels were lower in the striatum but higher in serum (Teunissen et al., 2001). Studies by Nieweg et al. (2009) showed that lanosterol levels are substantially higher in neurons than in astrocytes or oligodendrocytes (Nieweg et al., 2009), further suggesting that lanosterol plays an important role in neurons.

Consistent with a role of lanosterol in PD pathogenesis, we observed an improved survival of MPP+-treated dopaminergic neurons upon exogenous addition of lanosterol (Chapter 2). Much of the subsequent work attempted to elucidate the mechanism by which lanosterol protects dopaminergic neurons. As such, one important observation is the striking relocalization of LSS from the ER to mitochondria in dopaminergic neurons following MPP+ treatment (Chapter 4), suggesting an increase of lanosterol synthesis in the mitochondria. Interestingly, recent lipidomic analysis of macrophages

stimulated with LipidA (a condition that leads to oxidative bursts) showed a pronounced increase in lanosterol levels in several intracellular compartments, including mitochondria (Andreyev et al., 2010), implicating that modulation of lanosterol metabolism may be part of a global cellular response to stress.

If upregulation of lanosterol synthesis is part of a cellular defense mechanism, it is not clear why lanosterol levels drop in response to MPTP treatment. In this regard, it is interesting to note that two recent papers reported lowered lanosterol levels in the serum of patients with Alzheimer's disease (Kolsch et al., 2011), and in fibroblasts challenged by virus infection (Blanc et al., 2011). One possible explanation for these seemingly contradicting results is that distinct types of stress differentially impact lanosterol metabolism. Perhaps, in some cases, the substantial decrease in lanosterol levels cannot be compensated by upregulation of lanosterol synthesis as part of the cell's protective response. Alternatively, I cannot exclude the possibility that translocation of LSS to mitochondria in response to MPP+ is an epiphenomenon, which is not indicative of a cellular response to stress.

These results, however, demonstrate that exogenous addition of lanosterol leads to mild uncoupling of mitochondria in dopaminergic and glutamatergic neurons, with no detectable impact on ATP levels (Chapter 5). The mitochondria uncoupling and protective effects of lanosterol are strikingly similar to those observed with low dose of the uncoupler, FCCP, which improves cellular survival in ischaemic preconditioning but has no significant impact on ATP levels (Brennan et al., 2006). In the context of PD, the mitochondrial uncoupling effect of lanosterol has important implications. For

example, Parkin is recruited to mitochondria via PINK1 upon membrane depolarization (Narendra et al., 2008), and regulates the clearance of damaged mitochondria by mitophagy in mammalian cell lines (Geisler et al., 2010a). In addition, the translocation of Parkin to mitochondria has etiological significance, as a number of disease-associated Parkin mutant proteins fail to translocate (Matsuda et al., 2010; Okatsu et al., 2010). Together, these data point to a role of mitochondrial uncoupling and autophagy in PD pathogenesis. In line with this model, our results reveal that lanosterol induces mitochondrial uncoupling (Fig 18, 19) and promotes autophagy (Fig 21, 22).

To date, the evidence linking PD to impaired mitochondrial function is substantial, including (1) identification of (rare) PD-associated mutations that affect mitochondrial function, e.g., the putative kinase PINK1 (PARK6), which is targeted to mitochondria, the E3 ligase Parkin (PARK2), and DJ-1 (PARK7); (2) similarities between PD and clinical symptoms that arise upon exposure to the neurotoxin MPTP, a complex I inhibitor; and (3) a significant decrease in complex I/II activity in platelets of patients with PD (Haas et al., 1995). But exactly what aspects of mitochondria functions are impaired in PD has been an evolving answer throughout the last few decades for neurobiologists.

While mitochondria are classically seen as the powerhouse of the cell by generation of ATP through the respiratory chain/oxidative phosphorylation (mitochondria bioenergetics), there are many other functions that are equally as important though less mentioned such as calcium buffering through ER-Mito communication, quality control of mitochondria (mitophagy), and mitochondria trafficking (Schon and Przedborski, 2011). In the earlier days of

PD research, bioenergetics defects in PD and oxidative stress, caused by impaired electron chain transport, were the two most popular hypotheses and thought to be the cause of the disease. But the data supporting these has been refuted throughout years and currently, the role of mitochondria bioenergetic compromises are seen as a consequence rather than the cause of the disease (see recent review, (Schon and Przedborski, 2011). Thus, the present view is to focus on mitochondria biology in the context of PD as an integrative subcellular system, encompassing four major aspects: (1) mitochondria bioenergetics, (2) mito-ER interactions, (3) mitochondria quality control by mitophagy, fusion, of fission, and (4) mitochondria trafficking in a highly polarized cell (such as neurons). Under such a view, any alteration in mitochondria dynamics (aspects 2-4: interaction with ER, mitophagy, or trafficking) instead of bioenergetics, would have a greater importance in neurons due to their high morphological polarity compared to myocytes.

Our results showed that a sterol biosynthetic enzyme, LSS, upon cellular stress, translocates from the ER to mitochondria, which could provide key connection between lipid and mitochondria dynamics of a dopaminergic neuron. Furthermore, exogenous addition of lanosterol leads to mild uncoupling. As shown in other studies, mitochondrial uncoupling is neuroprotective in various models, including MPTP-induced neurodegeneration (Andrews et al., 2005; Conti et al., 2005; Horvath et al., 2003). While the mechanisms involved are still unclear, some studies have suggested that uncoupling reduces superoxide species, offering an explanation for improved neuronal survival in the MPTP model, since oxidative stress is thought to be the primary cause of cell death (Andrews et al., 2005; Conti et

al., 2005). In other studies, transient mitochondrial uncoupling is neuroprotective in glutamate-induced neurotoxicity, as it prevents uptake of calcium from the cytosol to mitochondria (Stout et al., 1998). Finally, a recent study showed that DJ-1, a gene involved in early onset PD, regulates the expression of two uncoupling proteins (UCP4 and UCP5) and controls oxidative stress in mitochondria of dopaminergic neurons in the substantia nigra (Guzman et al., 2010). While these studies cited above have identified different modulators by which a cell/neuron alters mitochondria membrane potential, they are in good agreement with my findings, whereby uncoupling mechanism proves to be a central regulator of cellular response to stress.

Taking these concepts together and the data presented here, I thus propose the following model (Fig 23). It has been well known that dopaminergic neurons in the SNpc have high pacemaking activities in absence of any excitatory inputs (Grace and Onn, 1989). This is achieved at a high expense by increasing cytoslic $Ca^{2+}$ levels via L-type $Ca^{2+}$ channels. This high $Ca^{2+}$ cytosolic flux also increases superoxides species in the mitochondria (Beal, 1998). To compensate for this, in SNpc dopaminergic neurons, there are a number of "buffering" mechanisms. For example, there are elevated levels of the cytosolic $Ca^{2+}$ binding protein, Calbindin, compared to the dopaminergic neurons of VTA (Liang et al., 1996). Uncoupling mechanisms specifically in these neurons appear to be important to buffer oxidative stress generated by high $Ca^{2+}$(Guzman et al., 2010). Thus in a disease or stress state, another way to increase a neuron's buffering capacity could be by uncoupling via translocation of LSS from ER to mitochondria, allowing for a local increase of lanosterol. At the same time or as a consequence, there is also an

increase in autophagosome formation as mitophagy is highly linked to the mitochondrial membrane potential.

In a theoretical pathogenic scenario like PD, if there is a compromise in this pathway, by either (1) lack of $Ca^{2+}$ buffer, (2) lack of superoxide quencher, (3) lack of uncoupling ability,  (4) defects in autophagic initiation, (5) impaired mitophagy, or any the above combinations, one could speculate that a cell type with a higher basal "burden" of oxidative stress or cytoslic calcium would tend to be most vulnerable. This model, if correct, appears to be an attractive one as it integrates many main lines of evidence and hypotheses published in the PD literature, including oxidative stress, autophagy/ protein quality control, and mitochodria dysfunction.  However, clearly, this might very well be only a partial model as it does not address all the risk factors associated with PD. For example, there is no explanation to how ER stress or misfolded proteins could result in PD pathogensis. There are also genes involved in PD that appear to have no link to this model such as UCHL1 (Table 1).

*Figure 23: Proposed mechanism of lanosterol's neuroprotection*
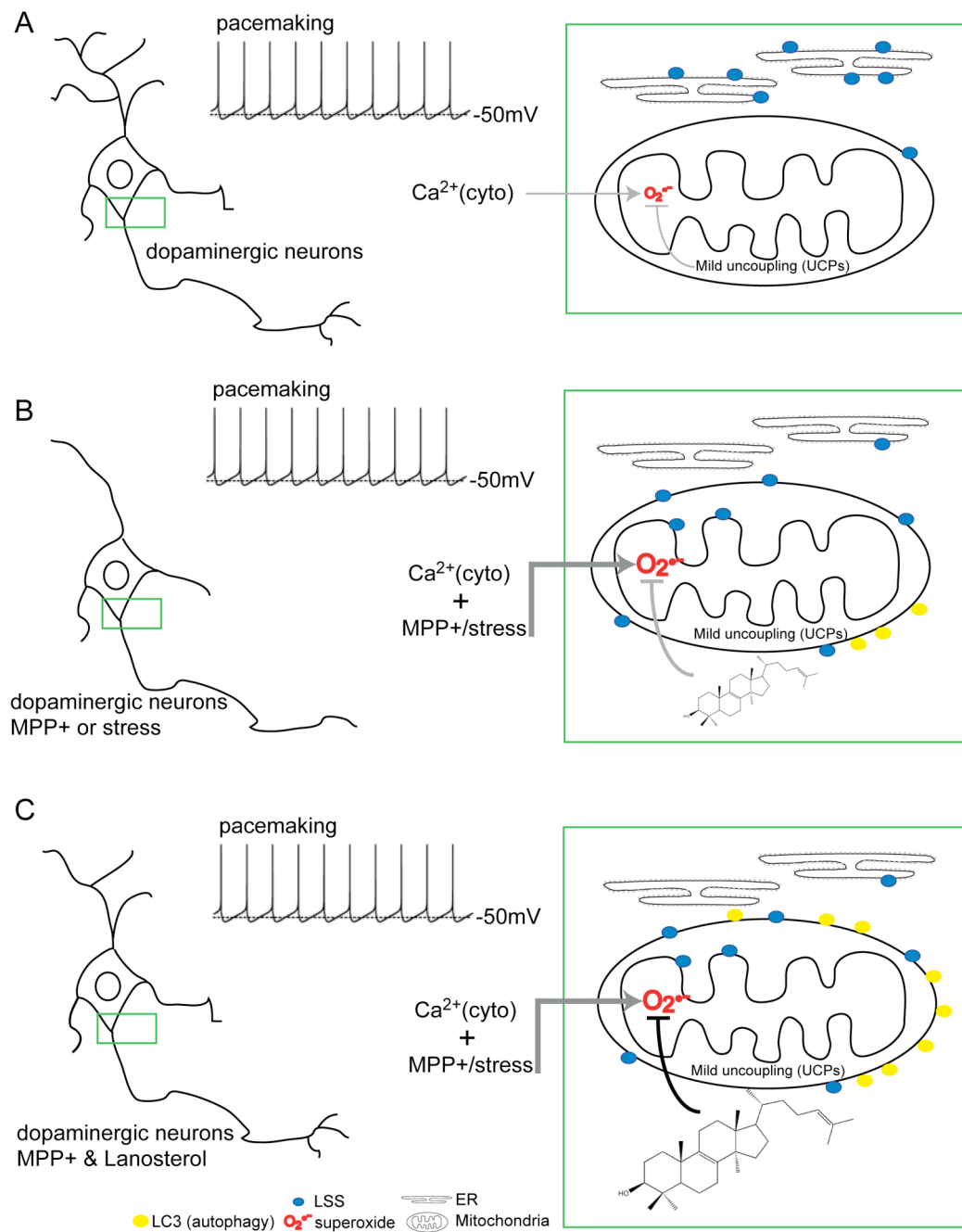


Figure 23: (A) In a healthy state, pacemaking activities of SNpc dopaminergic neurons result in high cytosolic $Ca^{2+}$ and superoxide. This can be ameliorated by endogenous uncoupling defense system. (B) Under cellular stress, where there is additional burden of superoxide species, LSS translocates from ER to mitochondria to increase local lanosterol level. Autophagy is also increased in this process. However, this might not be sufficient to prevent cell death. (C) In MPP+ and lanosterol treatment, exogenous lanosterol could increase uncoupling capacity as well as induce autophagy. This allows for additional cellular defense upon pathogenesis.

However, the proposed model is conceptually important. In considering PD, which is a multifactorial, adult on-set degenerative disease, one ought to evaluate the evidence in terms of an integrative pathway and identify associated risks factors. We ought to see misregulation in $Ca^{2+}$ or autophagy not as individual causes but as collective components of risks in a disease state. Because in sporadic cases, where one could find no known mutations in these identified pathways, where do these risks factors come from?

Perhaps, this is where lipid analysis (or lipidomics) could provide additional insights. For example, in any given disease state, the protein along with environmental risks could lead to a change in metabolites inventory of cells or tissues. This misregulation could thus be a key to the disease state. Among cellular metabolites, lipids in the brain represent one of the highest yet poorly understood classes. Thus, as shown in this work, by examining the sterol metabolism pathway, I have uncovered an additional component of this multi-factorial aetiology.

In conclusion, this thesis reports that lanosterol is not only a precursor for cholesterol synthesis, but acts as a cellular survival factor. These findings provide a novel mechanism for lanosterol-mediated cellular survival by regulating the mitochondrial membrane potential. These results also tie in well with the current literature to elucidate PD pathogenesis. Finally, these findings have important relevance for lanosterol-mediated mitochondrial function, and they bring sterol lipid metabolism to the forefront of neurobiology and neurodegeneration research.

## **Bibliography**

Aharon-Peretz, J., Rosenbaum, H. and Gershoni-Baruch, R. (2004) Mutations in the glucocerebrosidase gene and Parkinson's disease in Ashkenazi Jews. *N Engl J Med*, **351**, 1972-1977.

Andrews, Z.B., Horvath, B., Barnstable, C.J., Elsworth, J., Yang, L., Beal, M.F., Roth, R.H., Matthews, R.T. and Horvath, T.L. (2005) Uncoupling protein-2 is critical for nigral dopamine cell survival in a mouse model of Parkinson's disease. *J Neurosci*, **25**, 184-191.

Andreyev, A.Y., Fahy, E., Guan, Z., Kelly, S., Li, X., McDonald, J.G., Milne, S., Myers, D., Park, H., Ryan, A., Thompson, B.M., Wang, E., Zhao, Y., Brown, H.A., Merrill, A.H., Raetz, C.R., Russell, D.W., Subramaniam, S. and Dennis, E.A. (2010) Subcellular organelle lipidomics in TLR-4-activated macrophages. *J Lipid Res*, **51**, 2785-2797.

Beal, M.F. (1998) Excitotoxicity and nitric oxide in Parkinson's disease pathogenesis. *Ann Neurol*, **44**, S110-114.

Beal, M.F., Matthews, R.T., Tieleman, A. and Shults, C.W. (1998) Coenzyme Q10 attenuates the 1-methyl-4-phenyl-1,2,3,tetrahydropyridine (MPTP) induced loss of striatal dopamine and dopaminergic axons in aged mice. *Brain Res*, **783**, 109-114.

Becker, C. and Meier, C.R. (2009) Statins and the risk of Parkinson disease: an update on the controversy. *Expert Opin Drug Saf*, **8**, 261-271.

Bergman, H., Wichmann, T. and DeLong, M.R. (1990) Reversal of experimental parkinsonism by lesions of the subthalamic nucleus. *Science*, **249**, 1436-1438.

Blanc, M., Hsieh, W.Y., Robertson, K.A., Watterson, S., Shui, G., Lacaze, P., Khondoker, M., Dickinson, P., Sing, G., Rodriguez-Martin, S., Phelan, P., Forster, T., Strobl, B., Muller, M., Riemersma, R., Osborne, T., Wenk, M.R., Angulo, A. and Ghazal, P. (2011) Host defense against viral infection involves interferon mediated down-regulation of sterol biosynthesis. *PLoS Biol*, **9**, e1000598.

Bligh, E.G. and Dyer, W.J. (1959) A rapid method of total lipid extraction and purification. *Can J Biochem Physiol*, **37**, 911-917.

Bloch, K., Clayton, R.B. and Schneider, P.B. (1957) Synthesis of lanosterol in vivo. *J Biol Chem*, **224**, 175-183.

Bonnet, D., Garcia, M., Vecino, E., Lorentz, J.G., Sahel, J. and Hicks, D. (2004) Brain-derived neurotrophic factor signalling in adult pig retinal ganglion cell neurite regeneration in vitro. *Brain Res*, **1007**, 142-151.

Braak, H., Del Tredici, K., Rub, U., de Vos, R.A., Jansen Steur, E.N. and Braak, E. (2003) Staging of brain pathology related to sporadic Parkinson's disease. *Neurobiol Aging*, **24**, 197-211.

Brennan, J.P., Southworth, R., Medina, R.A., Davidson, S.M., Duchen, M.R. and Shattock, M.J. (2006) Mitochondrial uncoupling, with low concentration FCCP, induces ROS-dependent cardioprotection independent of KATP channel activation. *Cardiovasc Res*, **72**, 313-321.

Buccoliero, R. and Futerman, A.H. (2003) The roles of ceramide and complex sphingolipids in neuronal cell function. *Pharmacol Res*, **47**, 409-419.

Chaudhary, L.R. and Hruska, K.A. (2001) The cell survival signal Akt is differentially activated by PDGF-BB, EGF, and FGF-2 in osteoblastic cells. *J Cell Biochem*, **81**, 304-311.

Cherra, S.J., 3rd, Kulich, S.M., Uechi, G., Balasubramani, M., Mountzouris, J., Day, B.W. and Chu, C.T. (2010) Regulation of the autophagy protein LC3 by phosphorylation. *J Cell Biol*, **190**, 533-539.

Chia, W.J., Jenner, A.M., Farooqui, A.A. and Ong, W.Y. (2008) Changes in cytochrome P450 side chain cleavage expression in the rat hippocampus after kainate injury. *Exp Brain Res*, **186**, 143-149.

Chung, C.Y., Seo, H., Sonntag, K.C., Brooks, A., Lin, L. and Isacson, O. (2005) Cell type-specific gene expression of midbrain dopaminergic neurons reveals molecules involved in their vulnerability and protection. *Hum Mol Genet*, **14**, 1709-1725.

Cleren, C., Yang, L., Lorenzo, B., Calingasan, N.Y., Schomer, A., Sireci, A., Wille, E.J. and Beal, M.F. (2008) Therapeutic effects of coenzyme Q10 (CoQ10) and reduced CoQ10 in the MPTP model of Parkinsonism. *J Neurochem*, **104**, 1613-1621.

Conti, B., Sugama, S., Lucero, J., Winsky-Sommerer, R., Wirz, S.A., Maher, P., Andrews, Z., Barr, A.M., Morale, M.C., Paneda, C., Pemberton, J., Gaidarova, S., Behrens, M.M., Beal, F., Sanna, P.P., Horvath, T. and Bartfai, T. (2005) Uncoupling protein 2 protects dopaminergic neurons from acute 1,2,3,6-methyl-phenyl-tetrahydropyridine toxicity. *J Neurochem*, **93**, 493-501.

Cookson, M.R. (2010) DJ-1, PINK1, and their effects on mitochondrial pathways. *Mov Disord*, **25 Suppl 1**, S44-48.

da Silva, T.M., Munhoz, R.P., Alvarez, C., Naliwaiko, K., Kiss, A., Andreatini, R. and Ferraz, A.C. (2008) Depression in Parkinson's disease: a double-blind, randomized, placebo-controlled pilot study of omega-3 fatty-acid supplementation. *J Affect Disord*, **111**, 351-359.

Dauer, W. and Przedborski, S. (2003) Parkinson's disease: mechanisms and models. *Neuron*, **39**, 889-909.

de Brito, O.M. and Scorrano, L. (2008) Mitofusin 2 tethers endoplasmic reticulum to mitochondria. *Nature*, **456**, 605-610.

de Chaves, E.I., Rusinol, A.E., Vance, D.E., Campenot, R.B. and Vance, J.E. (1997) Role of lipoproteins in the delivery of lipids to axons during axonal regeneration. *J Biol Chem*, **272**, 30766-30773.

de Lau, L.M. and Breteler, M.M. (2006) Epidemiology of Parkinson's disease. *Lancet Neurol*, **5**, 525-535.

de Lau, L.M., Koudstaal, P.J., Hofman, A. and Breteler, M.M. (2006) Serum cholesterol levels and the risk of Parkinson's disease. *Am J Epidemiol*, **164**, 998-1002.

Desbarats, J., Birge, R.B., Mimouni-Rongy, M., Weinstein, D.E., Palerme, J.S. and Newell, M.K. (2003) Fas engagement induces neurite growth through ERK activation and p35 upregulation. *Nat Cell Biol*, **5**, 118-125.

Di Paolo, G. and De Camilli, P. (2006) Phosphoinositides in cell regulation and membrane dynamics. *Nature*, **443**, 651-657.

Dietschy, J.M. (2009) Central nervous system: cholesterol turnover, brain development and neurodegeneration. *Biol Chem*, **390**, 287-293.

Elbaz, A. and Moisan, F. (2008) Update in the epidemiology of Parkinson's disease. *Curr Opin Neurol*, **21**, 454-460.

Fahy, E., Sud, M., Cotter, D. and Subramaniam, S. (2007) LIPID MAPS online tools for lipid research. *Nucleic Acids Res*, **35**, W606-612.

Fernandez, A., Llacuna, L., Fernandez-Checa, J.C. and Colell, A. (2009) Mitochondrial cholesterol loading exacerbates amyloid beta peptide-induced inflammation and neurotoxicity. *J Neurosci*, **29**, 6394-6405.

Frank-Cannon, T.C., Tran, T., Ruhn, K.A., Martinez, T.N., Hong, J., Marvin, M., Hartley, M., Trevino, I., O'Brien, D.E., Casey, B., Goldberg, M.S. and Tansey, M.G. (2008) Parkin deficiency increases vulnerability to inflammation-related nigral degeneration. *J Neurosci*, **28**, 10825-10834.

Galpern, W.R. and Cudkowicz, M.E. (2007) Coenzyme Q treatment of neurodegenerative diseases of aging. *Mitochondrion*, **7 Suppl**, S146-153.

Garcia-Gorostiaga, I., Sanchez-Juan, P., Mateo, I., Rodriguez-Rodriguez, E., Sanchez-Quintana, C., del Olmo, S.C., Vazquez-Higuera, J.L., Berciano, J., Combarros, O. and Infante, J. (2009) Glycogen synthase kinase-3 beta and tau genes interact in Parkinson's and Alzheimer's diseases. *Ann Neurol*, **65**, 759-761; author reply 761-752.

Geisler, S., Holmstrom, K.M., Skujat, D., Fiesel, F.C., Rothfuss, O.C., Kahle, P.J. and Springer, W. (2010a) PINK1/Parkin-mediated mitophagy is dependent on VDAC1 and p62/SQSTM1. *Nat Cell Biol*, **12**, 119-131.

Geisler, S., Holmstrom, K.M., Treis, A., Skujat, D., Weber, S.S., Fiesel, F.C., Kahle, P.J. and Springer, W. (2010b) The PINK1/Parkin-mediated mitophagy is compromised by PD-associated mutations. *Autophagy*, **6**, 871-878.

Giovannone, B., Tsiaras, W.G., de la Monte, S., Klysik, J., Lautier, C., Karashchuk, G., Goldwurm, S. and Smith, R.J. (2009) GIGYF2 gene disruption in mice results in neurodegeneration and altered insulin-like growth factor signaling. *Hum Mol Genet*, **18**, 4629-4639.

Grace, A.A. and Onn, S.P. (1989) Morphology and electrophysiological properties of immunocytochemically identified rat dopamine neurons recorded in vitro. *J Neurosci*, **9**, 3463-3481.

Greene, J.G., Dingledine, R. and Greenamyre, J.T. (2005) Gene expression profiling of rat midbrain dopamine neurons: implications for selective vulnerability in parkinsonism. *Neurobiol Dis*, **18**, 19-31.

Guzman, J.N., Sanchez-Padilla, J., Wokosin, D., Kondapalli, J., Ilijic, E., Schumacker, P.T. and Surmeier, D.J. (2010) Oxidant stress evoked by pacemaking in dopaminergic neurons is attenuated by DJ-1. *Nature*, **468**, 696-700.

Haas, R.H., Nasirian, F., Nakano, K., Ward, D., Pay, M., Hill, R. and Shults, C.W. (1995) Low platelet mitochondrial complex I and complex II/III activity in early untreated Parkinson's disease. *Ann Neurol*, **37**, 714-722.

Hahn, C.M., Kleinholz, H., Koester, M.P., Grieser, S., Thelen, K. and Pollerberg, G.E. (2005) Role of cyclin-dependent kinase 5 and its activator P35 in local axon and growth cone stabilization. *Neuroscience*, **134**, 449-465.

Hailey, D.W., Rambold, A.S., Satpute-Krishnan, P., Mitra, K., Sougrat, R., Kim, P.K. and Lippincott-Schwartz, J. (2010) Mitochondria supply membranes for autophagosome biogenesis during starvation. *Cell*, **141**, 656-667.

Han, X. (2004) The role of apolipoprotein E in lipid metabolism in the central nervous system. *Cell Mol Life Sci*, **61**, 1896-1906.

He, X., Jenner, A.M., Ong, W.Y., Farooqui, A.A. and Patel, S.C. (2006) Lovastatin modulates increased cholesterol and oxysterol levels and has a neuroprotective effect on rat hippocampal neurons after kainate injury. *J Neuropathol Exp Neurol*, **65**, 652-663.

Heacock, A.M., Klinger, P.D., Seguin, E.B. and Agranoff, B.W. (1984) Cholesterol synthesis and nerve regeneration. *J Neurochem*, **42**, 987-993.

Holmstrom, T.E., Mattsson, C.L., Falting, J.M. and Nedergaard, J. (2008) Differential signalling pathways for EGF versus PDGF activation of Erk1/2 MAP kinase and cell proliferation in brown pre-adipocytes. *Exp Cell Res*, **314**, 3581-3592.

Horvath, T.L., Diano, S., Leranth, C., Garcia-Segura, L.M., Cowley, M.A., Shanabrough, M., Elsworth, J.D., Sotonyi, P., Roth, R.H., Dietrich, E.H., Matthews, R.T., Barnstable, C.J. and Redmond, D.E., Jr. (2003) Coenzyme Q induces nigral mitochondrial uncoupling and prevents dopamine cell loss in a primate model of Parkinson's disease. *Endocrinology*, **144**, 2757-2760.

Hu, G., Antikainen, R., Jousilahti, P., Kivipelto, M. and Tuomilehto, J. (2008) Total cholesterol and the risk of Parkinson disease. *Neurology*.

Huang, X., Abbott, R.D., Petrovitch, H., Mailman, R.B. and Ross, G.W. (2008) Low LDL cholesterol and increased risk of Parkinson's disease: prospective results from Honolulu-Asia Aging Study. *Mov Disord*, **23**, 1013-1018.

Huang, X., Chen, H., Miller, W.C., Mailman, R.B., Woodard, J.L., Chen, P.C., Xiang, D., Murrow, R.W., Wang, Y.Z. and Poole, C. (2007) Lower low-density lipoprotein cholesterol levels are associated with Parkinson's disease. *Mov Disord*, **22**, 377-381.

Jackson-Lewis, V., Jakowec, M., Burke, R.E. and Przedborski, S. (1995) Time course and morphology of dopaminergic neuronal death caused by the neurotoxin 1-methyl-4-phenyl-1,2,3,6-tetrahydropyridine. *Neurodegeneration*, **4**, 257-269.

Jackson-Lewis, V. and Przedborski, S. (2007) Protocol for the MPTP mouse model of Parkinson's disease. *Nat Protoc*, **2**, 141-151.

Jones, J.M., Albin, R.L., Feldman, E.L., Simin, K., Schuster, T.G., Dunnick, W.A., Collins, J.T., Chrisp, C.E., Taylor, B.A. and Meisler, M.H. (1993) mnd2: a new mouse model of inherited motor neuron disease. *Genomics*, **16**, 669-677.

Julien, C., Berthiaume, L., Hadj-Tahar, A., Rajput, A.H., Bedard, P.J., Di Paolo, T., Julien, P. and Calon, F. (2006) Postmortem brain fatty acid profile of levodopa-treated Parkinson disease patients and parkinsonian monkeys. *Neurochem Int*, **48**, 404-414.

Kaech, S. and Banker, G. (2006) Culturing hippocampal neurons. *Nat Protoc*, **1**, 2406-2415.

Keeney, P.M., Xie, J., Capaldi, R.A. and Bennett, J.P., Jr. (2006) Parkinson's disease brain mitochondrial complex I has oxidatively damaged subunits and is functionally impaired and misassembled. *J Neurosci*, **26**, 5256-5264.

Kolsch, H., Heun, R., Jessen, F., Popp, J., Hentschel, F., Maier, W. and Lutjohann, D. (2011) Alterations of cholesterol precursor levels in Alzheimer's disease. *Biochim Biophys Acta*, **1801**, 945-950.

Koob, A.O., Ubhi, K., Paulsson, J.F., Kelly, J., Rockenstein, E., Mante, M., Adame, A. and Masliah, E. (2010) Lovastatin ameliorates alpha-synuclein accumulation and oxidation in transgenic mouse models of alpha-synucleinopathies. *Exp Neurol*, **221**, 267-274.

Kravitz, A.V., Freeze, B.S., Parker, P.R., Kay, K., Thwin, M.T., Deisseroth, K. and Kreitzer, A.C. (2010) Regulation of parkinsonian motor behaviours by optogenetic control of basal ganglia circuitry. *Nature*, **466**, 622-626.

Kusano, M., Abe, I., Sankawa, U. and Ebizuka, Y. (1991) Purification and some properties of squalene-2,3-epoxide: lanosterol cyclase from rat liver. *Chem Pharm Bull (Tokyo)*, **39**, 239-241.

Larsen, K., Hedegaard, C., Bertelsen, M.F. and Bendixen, C. (2009) Threonine 53 in alpha-synuclein is conserved in long-living non-primate animals. *Biochem Biophys Res Commun*, **387**, 602-605.

Lein, E.S., Hawrylycz, M.J., Ao, N., Ayres, M., Bensinger, A., Bernard, A., Boe, A.F., Boguski, M.S., Brockway, K.S., Byrnes, E.J., Chen, L., Chen, L., Chen, T.M., Chin, M.C., Chong, J., Crook, B.E., Czaplinska, A., Dang, C.N., Datta, S., Dee, N.R., Desaki, A.L., Desta, T., Diep, E., Dolbeare, T.A., Donelan, M.J., Dong, H.W., Dougherty, J.G., Duncan, B.J., Ebbert, A.J., Eichele, G., Estin, L.K., Faber, C., Facer, B.A., Fields, R., Fischer, S.R., Fliss, T.P., Frensley, C., Gates, S.N., Glattfelder, K.J., Halverson, K.R., Hart, M.R., Hohmann, J.G., Howell, M.P., Jeung, D.P., Johnson, R.A., Karr, P.T., Kawal, R., Kidney, J.M., Knapik, R.H., Kuan, C.L., Lake, J.H., Laramee, A.R., Larsen, K.D., Lau, C., Lemon, T.A., Liang, A.J., Liu, Y., Luong, L.T., Michaels, J., Morgan, J.J., Morgan, R.J., Mortrud, M.T., Mosqueda, N.F., Ng, L.L., Ng, R., Orta, G.J., Overly, C.C., Pak, T.H., Parry, S.E., Pathak, S.D., Pearson, O.C., Puchalski, R.B., Riley, Z.L., Rockett, H.R., Rowland, S.A., Royall, J.J., Ruiz, M.J., Sarno, N.R., Schaffnit, K., Shapovalova, N.V., Sivisay, T., Slaughterbeck, C.R., Smith, S.C., Smith, K.A., Smith, B.I., Sodt, A.J., Stewart, N.N., Stumpf, K.R., Sunkin, S.M., Sutram, M., Tam, A., Teemer, C.D., Thaller, C., Thompson, C.L., Varnam, L.R., Visel, A., Whitlock, R.M., Wohnoutka, P.E., Wolkey, C.K., Wong, V.Y., Wood, M., Yaylaoglu, M.B., Young, R.C., Youngstrom, B.L., Yuan, X.F., Zhang, B., Zwingman, T.A. and Jones, A.R. (2007) Genome-wide atlas of gene expression in the adult mouse brain. *Nature*, **445**, 168-176.

Lesage, S. and Brice, A. (2009) Parkinson's disease: from monogenic forms to genetic susceptibility factors. *Hum Mol Genet*, **18**, R48-59.

Li, Y., Liu, W., Oo, T.F., Wang, L., Tang, Y., Jackson-Lewis, V., Zhou, C., Geghman, K., Bogdanov, M., Przedborski, S., Beal, M.F., Burke, R.E. and Li, C. (2009) Mutant LRRK2(R1441G) BAC transgenic mice

recapitulate cardinal features of Parkinson's disease. *Nat Neurosci*, **12**, 826-828.

Liang, C.L., Sinton, C.M., Sonsalla, P.K. and German, D.C. (1996) Midbrain dopaminergic neurons in the mouse that contain calbindin-D28k exhibit reduced vulnerability to MPTP-induced neurodegeneration. *Neurodegeneration*, **5**, 313-318.

Lim, A., Tsuang, D., Kukull, W., Nochlin, D., Leverenz, J., McCormick, W., Bowen, J., Teri, L., Thompson, J., Peskind, E.R., Raskind, M. and Larson, E.B. (1999) Clinico-neuropathological correlation of Alzheimer's disease in a community-based case series. *J Am Geriatr Soc*, **47**, 564-569.

Liu, J.P., Tang, Y., Zhou, S., Toh, B.H., McLean, C. and Li, H. (2010) Cholesterol involvement in the pathogenesis of neurodegenerative diseases. *Mol Cell Neurosci*, **43**, 33-42.

Lo Bianco, C., Ridet, J.L., Schneider, B.L., Deglon, N. and Aebischer, P. (2002) alpha -Synucleinopathy and selective dopaminergic neuron loss in a rat lentiviral-based model of Parkinson's disease. *Proc Natl Acad Sci U S A*, **99**, 10813-10818.

Lu, X.H., Fleming, S.M., Meurers, B., Ackerson, L.C., Mortazavi, F., Lo, V., Hernandez, D., Sulzer, D., Jackson, G.R., Maidment, N.T., Chesselet, M.F. and Yang, X.W. (2009) Bacterial artificial chromosome transgenic mice expressing a truncated mutant parkin exhibit age-dependent hypokinetic motor deficits, dopaminergic neuron degeneration, and accumulation of proteinase K-resistant alpha-synuclein. *J Neurosci*, **29**, 1962-1976.

Luthi-Carter, R., Taylor, D.M., Pallos, J., Lambert, E., Amore, A., Parker, A., Moffitt, H., Smith, D.L., Runne, H., Gokce, O., Kuhn, A., Xiang, Z., Maxwell, M.M., Reeves, S.A., Bates, G.P., Neri, C., Thompson, L.M., Marsh, J.L. and Kazantsev, A.G. (2010) SIRT2 inhibition achieves neuroprotection by decreasing sterol biosynthesis. *Proc Natl Acad Sci U S A*, **107**, 7927-7932.

Ma, C.H., Bampton, E.T., Evans, M.J. and Taylor, J.S. (2009) Synergistic effects of osteonectin and brain-derived neurotrophic factor on axotomized retinal ganglion cells neurite outgrowth via the mitogen-activated protein kinase-extracellular signal-regulated kinase1/2 pathways. *Neuroscience*.

Matsuda, N., Sato, S., Shiba, K., Okatsu, K., Saisho, K., Gautier, C.A., Sou, Y.S., Saiki, S., Kawajiri, S., Sato, F., Kimura, M., Komatsu, M., Hattori, N. and Tanaka, K. (2010) PINK1 stabilized by mitochondrial depolarization recruits Parkin to damaged mitochondria and activates latent Parkin for mitophagy. *J Cell Biol*, **189**, 211-221.

Mattiasson, G., Shamloo, M., Gido, G., Mathi, K., Tomasevic, G., Yi, S., Warden, C.H., Castilho, R.F., Melcher, T., Gonzalez-Zulueta, M., Nikolich, K. and Wieloch, T. (2003) Uncoupling protein-2 prevents neuronal death and diminishes brain dysfunction after stroke and brain trauma. *Nat Med*, **9**, 1062-1068.

Mori, M., Sawashita, J. and Higuchi, K. (2007) Functional polymorphisms of the Lss and Fdft1 genes in laboratory rats. *Exp Anim*, **56**, 93-101.

Muller, T., Buttner, T., Gholipour, A.F. and Kuhn, W. (2003) Coenzyme Q10 supplementation provides mild symptomatic benefit in patients with Parkinson's disease. *Neurosci Lett*, **341**, 201-204.

Namgung, U., Choi, B.H., Park, S., Lee, J.U., Seo, H.S., Suh, B.C. and Kim, K.T. (2004) Activation of cyclin-dependent kinase 5 is involved in axonal regeneration. *Mol Cell Neurosci*, **25**, 422-432.

Narayanaswamy, R., Levy, M., Tsechansky, M., Stovall, G.M., O'Connell, J.D., Mirrielees, J., Ellington, A.D. and Marcotte, E.M. (2009) Widespread reorganization of metabolic enzymes into reversible assemblies upon nutrient starvation. *Proc Natl Acad Sci U S A*, **106**, 10147-10152.

Narendra, D., Tanaka, A., Suen, D.F. and Youle, R.J. (2008) Parkin is recruited selectively to impaired mitochondria and promotes their autophagy. *J Cell Biol*, **183**, 795-803.

Narendra, D.P., Jin, S.M., Tanaka, A., Suen, D.F., Gautier, C.A., Shen, J., Cookson, M.R. and Youle, R.J. (2010) PINK1 is selectively stabilized on impaired mitochondria to activate Parkin. *PLoS Biol*, **8**, e1000298.

Neystat, M., Rzhetskaya, M., Oo, T.F., Kholodilov, N., Yarygina, O., Wilson, A., El-Khodor, B.F. and Burke, R.E. (2001) Expression of cyclin-dependent kinase 5 and its activator p35 in models of induced apoptotic death in neurons of the substantia nigra in vivo. *J Neurochem*, **77**, 1611-1625.

Nieweg, K., Schaller, H. and Pfrieger, F.W. (2009) Marked differences in cholesterol synthesis between neurons and glial cells from postnatal rats. *J Neurochem*, **109**, 125-134.

Okatsu, K., Saisho, K., Shimanuki, M., Nakada, K., Shitara, H., Sou, Y.S., Kimura, M., Sato, S., Hattori, N., Komatsu, M., Tanaka, K. and Matsuda, N. (2010) p62/SQSTM1 cooperates with Parkin for perinuclear clustering of depolarized mitochondria. *Genes Cells*, **15**, 887-900.

Park, J.W., Kim, H.J., Byun, J.H., Ryu, H.R. and Jeon, N.L. (2009) Novel microfluidic platform for culturing neurons: culturing and biochemical analysis of neuronal components. *Biotechnol J*, **4**, 1573-1577.

Pfrieger, F.W. (2003) Cholesterol homeostasis and function in neurons of the central nervous system. *Cell Mol Life Sci*, **60**, 1158-1171.

Piomelli, D., Astarita, G. and Rapaka, R. (2007) A neuroscientist's guide to lipidomics. *Nat Rev Neurosci*, **8**, 743-754.

Ramonet, D., Daher, J.P., Lin, B.M., Stafa, K., Kim, J., Banerjee, R., Westerlund, M., Pletnikova, O., Glauser, L., Yang, L., Liu, Y., Swing, D.A., Beal, M.F., Troncoso, J.C., McCaffery, J.M., Jenkins, N.A., Copeland, N.G., Galter, D., Thomas, B., Lee, M.K., Dawson, T.M., Dawson, V.L. and Moore, D.J. (2011) Dopaminergic neuronal loss, reduced neurite complexity and autophagic abnormalities in transgenic mice expressing G2019S mutant LRRK2. *PLoS One*, **6**, e18568.

Ramsay, R.R. and Singer, T.P. (1986) Energy-dependent uptake of N-methyl-4-phenylpyridinium, the neurotoxic metabolite of 1-methyl-4-phenyl-1,2,3,6-tetrahydropyridine, by mitochondria. *J Biol Chem*, **261**, 7585-7587.

Rantham Prabhakara, J.P., Feist, G., Thomasson, S., Thompson, A., Schommer, E. and Ghribi, O. (2008) Differential effects of 24-

hydroxycholesterol and 27-hydroxycholesterol on tyrosine hydroxylase and alpha-synuclein in human neuroblastoma SH-SY5Y cells. *J Neurochem*, **107**, 1722-1729.

Rayport, S., Sulzer, D., Shi, W.X., Sawasdikosol, S., Monaco, J., Batson, D. and Rajendran, G. (1992) Identified postnatal mesolimbic dopamine neurons in culture: morphology and electrophysiology. *J Neurosci*, **12**, 4264-4280.

Ross, C.A. and Smith, W.W. (2007) Gene-environment interactions in Parkinson's disease. *Parkinsonism Relat Disord*, **13 Suppl 3**, S309-315.

Schapira, A.H. (2008) Mitochondria in the aetiology and pathogenesis of Parkinson's disease. *Lancet Neurol*, **7**, 97-109.

Schapira, A.H. (2010) Complex I: inhibitors, inhibition and neurodegeneration. *Exp Neurol*, **224**, 331-335.

Schon, E.A. and Przedborski, S. (2011) Mitochondria: the next (neurode)generation. *Neuron*, **70**, 1033-1053.

Sharon, R., Bar-Joseph, I., Mirick, G.E., Serhan, C.N. and Selkoe, D.J. (2003) Altered fatty acid composition of dopaminergic neurons expressing alpha-synuclein and human brains with alpha-synucleinopathies. *J Biol Chem*, **278**, 49874-49881.

Shin, J.H., Ko, H.S., Kang, H., Lee, Y., Lee, Y.I., Pletinkova, O., Troconso, J.C., Dawson, V.L. and Dawson, T.M. (2011) PARIS (ZNF746) repression of PGC-1alpha contributes to neurodegeneration in Parkinson's disease. *Cell*, **144**, 689-702.

Shults, C.W., Oakes, D., Kieburtz, K., Beal, M.F., Haas, R., Plumb, S., Juncos, J.L., Nutt, J., Shoulson, I., Carter, J., Kompoliti, K., Perlmutter, J.S., Reich, S., Stern, M., Watts, R.L., Kurlan, R., Molho, E., Harrison, M. and Lew, M. (2002) Effects of coenzyme Q10 in early Parkinson disease: evidence of slowing of the functional decline. *Arch Neurol*, **59**, 1541-1550.

Song, J.H., Wang, C.X., Song, D.K., Wang, P., Shuaib, A. and Hao, C. (2005) Interferon gamma induces neurite outgrowth by up-regulation of p35 neuron-specific cyclin-dependent kinase 5 activator via activation of ERK1/2 pathway. *J Biol Chem*, **280**, 12896-12901.

Spindler, M., Beal, M.F. and Henchcliffe, C. (2009) Coenzyme Q10 effects in neurodegenerative disease. *Neuropsychiatr Dis Treat*, **5**, 597-610.

Stout, A.K., Raphael, H.M., Kanterewicz, B.I., Klann, E. and Reynolds, I.J. (1998) Glutamate-induced neuron death requires mitochondrial calcium uptake. *Nat Neurosci*, **1**, 366-373.

Sugino, K., Hempel, C.M., Miller, M.N., Hattox, A.M., Shapiro, P., Wu, C., Huang, Z.J. and Nelson, S.B. (2006) Molecular taxonomy of major neuronal classes in the adult mouse forebrain. *Nat Neurosci*, **9**, 99-107.

Tchen, T.T. and Bloch, K. (1957) On the conversion of squalene to lanosterol in vitro. *J Biol Chem*, **226**, 921-930.

Thoma, R., Schulz-Gasch, T., D'Arcy, B., Benz, J., Aebi, J., Dehmlow, H., Hennig, M., Stihle, M. and Ruf, A. (2004) Insight into steroid scaffold formation from the structure of human oxidosqualene cyclase. *Nature*, **432**, 118-122.

Vance, J.E., Karten, B. and Hayashi, H. (2006) Lipid dynamics in neurons. *Biochem Soc Trans*, **34**, 399-403.

Virmani, A., Gaetani, F. and Binienda, Z. (2005) Effects of metabolic modifiers such as carnitines, coenzyme Q10, and PUFAs against different forms of neurotoxic insults: metabolic inhibitors, MPTP, and methamphetamine. *Ann N Y Acad Sci*, **1053**, 183-191.

Wada, H., Yasuda, T., Miura, I., Watabe, K., Sawa, C., Kamijuku, H., Kojo, S., Taniguchi, M., Nishino, I., Wakana, S., Yoshida, H. and Seino, K. (2009) Establishment of an improved mouse model for infantile neuroaxonal dystrophy that shows early disease onset and bears a point mutation in Pla2g6. *Am J Pathol*, **175**, 2257-2263.

Watanabe, Y., Himeda, T. and Araki, T. (2005) Mechanisms of MPTP toxicity and their implications for therapy of Parkinson's disease. *Med Sci Monit*, **11**, RA17-23.

White, R.J. and Reynolds, I.J. (1996) Mitochondrial depolarization in glutamate-stimulated neurons: an early signal specific to excitotoxin exposure. *J Neurosci*, **16**, 5688-5697.

Yamamoto, S. and Bloch, K. (1969) On the enzymes catalysing the transformation of squalene to lanosterol. *Biochem J*, **113**, 19P-20P.

Yamamoto, S., Lin, K. and Bloch, K. (1969) Some properties of the microsomal 2,3-oxidosqualene sterol cyclase. *Proc Natl Acad Sci U S A*, **63**, 110-117.

Yang, L., Calingasan, N.Y., Wille, E.J., Cormier, K., Smith, K., Ferrante, R.J. and Beal, M.F. (2009) Combination therapy with coenzyme Q10 and creatine produces additive neuroprotective effects in models of Parkinson's and Huntington's diseases. *J Neurochem*, **109**, 1427-1439.

Yao, F., Yu, F., Gong, L., Taube, D., Rao, D.D. and MacKenzie, R.G. (2005) Microarray analysis of fluoro-gold labeled rat dopamine neurons harvested by laser capture microdissection. *J Neurosci Methods*, **143**, 95-106.

Zhao, T., De Graaff, E., Breedveld, G.J., Loda, A., Severijnen, L.A., Wouters, C.H., Verheijen, F.W., Dekker, M.C., Montagna, P., Willemsen, R., Oostra, B.A. and Bonifati, V. (2011) Loss of nuclear activity of the FBXO7 protein in patients with parkinsonian-pyramidal syndrome (PARK15). *PLoS One*, **6**, e16983.

Zhou, H., Falkenburger, B.H., Schulz, J.B., Tieu, K., Xu, Z. and Xia, X.G. (2007) Silencing of the Pink1 gene expression by conditional RNAi does not induce dopaminergic neuron death in mice. *Int J Biol Sci*, **3**, 242-250.

Zimran, A., Neudorfer, O. and Elstein, D. (2005) The glucocerebrosidase gene and Parkinson's disease in Ashkenazi Jews. *N Engl J Med*, **352**, 728-731; author reply 728-731.